Research Infrastructure Quality Assurance

GAW Report No. 280

Fifth WMO Filter Radiometer Comparison (FRC-V)

27 September to 25 October 2021
Davos, Switzerland

WEATHER CLIMATE WATER

WORLD METEOROLOGICAL ORGANIZATION

GLOBAL ATMOSPHERE WATCH

Research Infrastructure Quality Assurance

GAW Report No. 280

Fifth WMO Filter Radiometer Comparison (FRC-V)

27 September to 25 October 2021

Davos, Switzerland

Prepared by

Stelios Kazadzis, Natalia Kouremeti, Julian Gröbner
Physikalisch-Meteorologisches Observatorium Davos, World Radiation Center

Chair, Publications Board
World Meteorological Organization (WMO)
7 bis, avenue de la Paix
P.O. Box 2300
CH-1211 Geneva 2, Switzerland

Tel.: +41 (0) 22 730 84 03
Email: publications@wmo.int

CONTENTS

1. INTRODUCTION

Aerosol optical depth (AOD) is a quantitative measure of the extinction of solar radiation by aerosol scattering and absorption between an observation point and the top of the atmosphere. Therefore, it is a measure of the integrated columnar aerosol load, and the most important parameter for direct radiative forcing studies. AOD is not directly measurable but is rather retrieved from observations of the spectral transmission of the atmosphere. Multi-wavelength AOD has been defined as an essential climate variable by various global bodies and agencies, such as the Global Climate Observing System (GCOS), the WMO Global Atmosphere Watch (GAW) Programme, the European Space Agency Climate Change Initiative, as well as calibration/validation-related initiatives and others.

AOD measurements are performed by measuring the direct beam with sun-pointing instruments, or estimated from the difference of simultaneous global and diffuse irradiance measurements. WMO recommends measuring (at least) at three of the following centre wavelengths: 368, 412, 500, 675, 778 and 862 nm, with a bandwidth of 5 nm (*Recent Progress in Sun Photometry: Determination of the Aerosol Optical Depth* (WMO/TD-No. 143)). The field-of-view geometry for direct-beam radiometers varies for different instrument types. WMO recommends the specifications of a full opening angle of 2.5° and a slope angle of 1° (*Recent Progress in Sun Photometry: Determination of the Aerosol Optical Depth* (WMO/TD-No. 143)).

AOD can be derived from the ground, with measurements of the spectral transmission of direct solar radiation, by sun photometers. There are various types of such instruments: sun-pointing or rotating shadow-band filter radiometers, as well as spectroradiometers. Surface-based global networks of AOD observations measure spectral AOD at numerous locations worldwide. Such networks include the Aerosol Robotic Network (AERONET) (Holben et al., 1998; Gilles et al., 2019), the Global Atmospheric Watch Precision Filter Radiometer network (GAW-PFR) (Kazadzis et al., 2018b), the sky radiometer network (SKYNET) (Nakajima et al., 2020) (the latter two also contribute to the WMO World Data Centre for Aerosols), the Bureau of Meteorology (BOM) Radiation Network and CSIRO/AeroSpan (Mitchell et al., 2017), and the National Oceanic and Atmospheric Administration/Earth System Research Laboratory's (NOAA/ESRL) SURFRAD network. Several AOD intercomparison campaigns, with the participation of reference instruments that belong to the above networks, have taken place as short-term intensive field campaigns (for example, the FRC-IV: see Kazadzis et al., 2018a) or long-term campaigns (for example, Cuevas et al., 2019) and have proven a successful method of relating the methodologies of standards from one network to another in deriving AOD. Recently, sun photometer calibration has been linked to the SI units (International System of Units) through the absolute calibration of a Precision Filter Radiometer (PFR) at the German national metrology institute (Physikalisch-Technische Bundesanstalt) (Kouremeti et al., 2022).

In 2006, WMO, through the former Commission for Instruments and Methods of Observations, recognized "the need for establishing a primary reference AOD Centre to satisfy the need for traceability of Optical Depth (OD) measurements, conducting international intercomparisons guaranteeing data quality needed in climate studies" (*Commission for Instruments and Methods of Observation (CIMO) – Fourteenth session: Abridged Final Report with Resolutions and Recommendations* (WMO-No. 1019)). It was recommended that the World Optical Depth Research and Calibration Centre (WORCC) at the Physikalisch-Meteorologisches Observatorium Davos, World Radiation Centre (PMOD/WRC) be designated as the primary WMO reference centre for AOD measurements as part of the WRC activities (*Commission for Instruments and Methods of Observation (CIMO) – Fourteenth session: Abridged Final Report with Resolutions and Recommendations* (WMO-No. 1019)).

The quality of AOD data from intercomparisons can be evaluated by applying the WMO criteria discussed in GAW Report No. 162 (*WMO/GAW Experts Workshop on a Global Surface-based Network for Long-Term Observations of Column Aerosol Optical Properties* (WMO/TD-No. 1287)). According to these criteria, seeing as the ability to trace the calibration to a primary reference "is not currently possible based on physical measurement systems, the initial form of traceability will be based on difference criteria". That is, at an intercomparison or co-location, traceability is established if the AOD difference between networks is within specified limits. The definition of these limits depends on the method of

measurement used. For finite field-of-view instruments, the limit ("U95") is defined as follows for air mass (m):

$$U95 < \pm (0.005 + 0.010/m) \quad (1)$$

where the first term of the formula (0.005) accounts for instrumental and algorithmic (post-processing) uncertainties, while the second term represents the uncertainty related to the calibration of each instrument. The latter corresponds to a requirement for the relative uncertainty in the instrument calibration to be equal to or less than 1%.

The Fifth Filter Radiometer Comparison (FRC-V) was held, with one year delay due to the COVID-19 pandemic and related restrictions, concurrently with the Thirteenth International Pyrheliometer Comparison in Davos, Switzerland. Instrumentation belonging to various AOD global networks were invited to participate, including three reference instruments from the Centre for Aerosol Remote Sensing (CARS) of the pan-European research infrastructure ACTRIS (Aerosol, Clouds and Trace Gases Research Infrastructure) facility. The comparison took place at the premises of PMOD/WRC from 27 September to 25 October 2021. In total, 31 filter radiometers and spectroradiometers from 12 participating countries participated in this campaign, while 28 of them provided AOD data, presented here.

The objective of the FRC-V campaign was to compare aerosol optical depth and Ångström exponents (AE) derived from different instruments belonging to different global, regional or national networks, in order to quantify the main factors that are responsible for possible deviations. The aim of the whole activity was to initiate action towards homogenization of the AOD measurements on a global scale. The comparison protocol was formulated according to WMO recommendations. Measurements of each instrument were compared to measurements taken by the WORCC Precision Filter Radiometer (PFR) reference triad (hereafter referred to as the "WORCC PFR reference triad").

2. SET UP AND MEASUREMENTS

2.1 Location and conditions

The PMOD/WRC is situated at the edge of the small town of Davos in the eastern part of Switzerland (46° 49'N, 9° 51'E, at 1 590 m above sea level). The valley of Davos extends east to west, and in autumn the horizon limits solar observations to zenith angles smaller than about 78° (from about 0650 to 1520 hours UTC). The monthly average sunshine duration in September and October is 173 and 156 hours respectively, and the average AOD is 0.053 for 500 nm.

The FRC-V comparison lasted for 29 days from 27 September to 25 October 2021. During this period, there were 11 days (see Figure 1) with at least 4 hours of sunshine. Measurements from these days have been used for comparing the participating instruments. During the intercomparison days, AOD at 500 nm varied from 0.02 up to 0.1, which can be considered normal values for the area. Figure 1 shows the AOD variability during the intercomparison days.

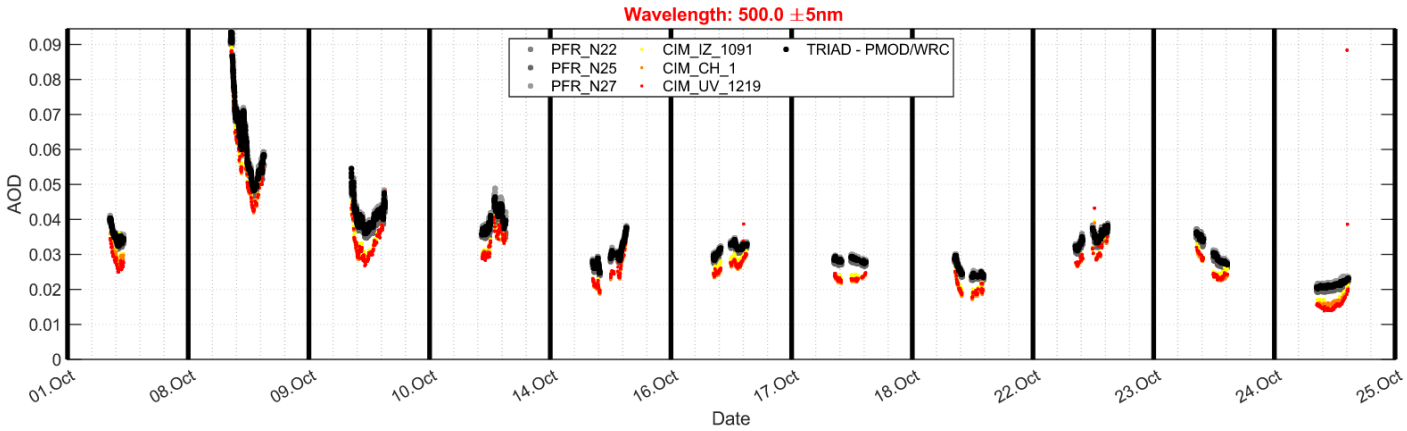

Figure 1. Average AOD at 500 nm measured by the WORCC PFR reference triad and the three CIMEL CARS/ACTRIS reference instruments

2.2 Instrumentation

The participating filter radiometers were only of the direct-pointing type, such as classic sun photometers, including sky-scanning radiometers used in direct sun mode. The hemispherical rotating shadow-band radiometer, which is the primary instrument for NOAA (GAW Report No. 231) did not take part in the present campaign. In addition, spectroradiometers able to measure with high spectral resolution participated. Details of the 28 participating instruments are as follows:

a. Thirteen (13) instruments (including the three constituting the WORCC PFR reference triad) were of the Precision Filter Radiometer (PFR) type, that is used in the GAW AOD network (*WMO/GAW Experts Workshop on a Global Surface-based Network for Long-term Observations of Column Aerosol Optical Properties* (WMO/TD-No. 1287); Kazadzis et al., 2018b). The PFR is a classic sun photometer with four independent channels, a field of view (FOV) of ± 1.25° and is equipped with 3 nm to 5 nm bandwidth interference filters. The detector unit is held at a constant temperature of 20° C by an active Peltier system.
b. One (1) radiometer was of the Carter-Scott SP02 type (Mitchell and Forgan, 2003), which is similar to the PFR, but has a wider field of view of ± 2.5° and no temperature controlling system.
c. Four (4) were CIMEL CE318 sun and sky-scanning radiometers, as used by AERONET (Giles et al., 2019). These instruments have a narrow FOV of 1.2° and measure the sun with eight channels sequentially within a few seconds.

d. Five (5) were Precision Solar Radiometers (PSR) that are direct sun-pointing spectroradiometers manufactured at PMOD/WRC. They are able to measure the spectrum from 320 nm up to 1 030 nm, with a variable step of an average value of 0.7 nm (Gröbner and Kouremeti, 2019).
e. Two (2) were direct sun-pointing POM-2 sky radiometers belonging to the SKYNET network (Nakajima et al., 2020), manufactured by Prede Co., Ltd.
f. One (1) was a sun and sky filter radiometer (CW193) belonging to CARSNET (China Aerosol Remote Sensing Network) (Che et al., 2019). The CW193 is equipped with a direct solar tracking system, able to measure in nine channels sequentially from 340 nm up to 1 640 nm (Zheng et al., 2022).
g. Two (2) were scanning spectroradiometers (QASUME). The QASUME, which is the European reference for solar ultraviolet (UV) measurements (Gröbner et al., 2005), is equipped with a direct sun input and solar tracking system. It is able to measure spectrally from 300 nm up to 500 nm and the newly developed infrared version IR-QASUME covers the range from 550 nm to 1 700 nm.

Details about the instrument types and participating institutes can be found in Table 1. In addition, a summary of the basic characteristics of each instrument type is provided in Table 2. The calibration of the sun photometers is based on a Langley calibration or the transfer of the Langley calibration though the reference instrument of each network. The spectroradiometers typically are calibrated in the laboratory using an irradiance standard (for example, the field emission-type lamp). The top-of-the-atmosphere (TOA) spectrum, necessary for the AOD retrievals, is acquired from an independent ground-based or satellite TOA solar irradiance high resolution spectrum (for example, QASUMEFTS: see Gröbner et al., 2017) and TSIS-1 Hybrid Solar Reference Spectrum (Coddington et al., 2021). Detailed information about the calibration of each instrument is provided in Appendix 2. Some of the instruments have two separate calibrations (as indicated in Table 1) and therefore yielded two data sets (instrument numbers 7 and 10–13 in Table 1)

Table 1. List of participants and instrument types

Instrument number (hardware)	*AOD data set number*	*Country*	*Institute*	*Type of radiometer*	*Network*	*Calibration type and analysis (analysis by Institute unless stated otherwise)*	*Acronym*
1	1	Switzerland	PMOD/WRC	PFR-N	GAW-PFR	WORCC-PMOD/WRC Reference triad #1	PFR_N22
2	2	Switzerland	PMOD/WRC	PFR-N	GAW-PFR	WORCC-PMOD/WRC Reference triad #2	PFR_N25
3	3	Switzerland	PMOD/WRC	PFR-N	GAW-PFR	WORCC-PMOD/WRC Reference triad #3	PFR_N27
4	4	Switzerland	PMOD/WRC	PFR-N	GAW-PFR	WORCC-PMOD/WRC Langley at Mauna Loa, USA	PFR_ML_07

Instrument number (hardware)	*AOD data set number*	*Country*	*Institute*	*Type of radiometer*	*Network*	*Calibration type and analysis (analysis by Institute unless stated otherwise)*	*Acronym*
5	5	Switzerland	PMOD/WRC	PFR-N	GAW-PFR	WORCC-PMOD/WRC Langley at Izaña, Spain	PFR_CH_24
6	6	Switzerland	PMOD/WRC	PFR-N	GAW-PFR	WORCC-PMOD/WRC	PFR_CH_21
7	7	Switzerland	PMOD/WRC	PFR-N	GAW-PFR	WORCC-PMOD/WRC	PFR_CH_01
	8					PTB SI-traceable calibration	PFR_IR_01
8	9	Switzerland	PMOD/WRC	PFR-N	GAW-PFR	WORCC-PMOD/WRC	PFR_NS_101
9	10	Switzerland	PMOD/WRC	PFR-N	GAW-PFR	WORCC-PMOD/WRC	PFR_NS_105
10	11	Sweden	SMHI	PFR-N	GAW-PFR, Associate Station	WORCC-PMOD/WRC	PFR_SE_N35
	12					WORCC-PMOD/WRC during FRC-V PMOD/WRC analysis	PFR-CA-35
11	13	Germany	DWD-MOL	PFR-N	GAW-PFR, Associate Station	WORCC-PMOD/WRC	PFR_DE_N57
	14					WORCC-PMOD/WRC during FRC-V PMOD/WRC analysis	PFR_CA_57
12	15	Austria	University of Innsbruck	PFR-N	National	WORCC-PMOD/WRC	PFR_AT_N08
	16					WORCC-PMOD/WRC during FRC-V PMOD/WRC analysis	PFR_CA_08
13	17	Republic of Korea	NIMS-KMA	PFR-N	GAW-PFR	WORCC-PMOD/WRC during FRC-V	PFR_KO_N58
	18					WORCC-PMOD/WRC during FRC-V PMOD/WRC analysis	PFR_CA_58
14	19	France	LOA, Université de Lille	CIMEL	AERONET-Europe – ACTRIS	CARS-ACTRIS	CIM_CH_1

Instrument number (hardware)	*AOD data set number*	*Country*	*Institute*	*Type of radiometer*	*Network*	*Calibration type and analysis (analysis by Institute unless stated otherwise)*	*Acronym*
15	20	France/ Switzerland	LOA, Université de Lille – PMOD/WRC	CIMEL	AERONET -Europe– ACTRIS	CARS-ACTRIS Langley at Mauna Loa, USA	CIM_UL_1270
16	21	Spain	Universidad de Valladolid	CIMEL	AERONET -Europe – ACTRIS	CARS-ACTRIS Langley at Izaña, Spain	CIM_UV_1219
17	22	Spain	AEMET (Izaña Atmospheric Research Centre)	CIMEL	AERONET -Europe – ACTRIS	CARS-ACTRIS Langley at Izaña, Spain	CIM_IZ_1091
18	23	Italy	ARPA Valle d'Aosta	POM-2	SKYNET-Europe	SKYNET	POM_IT_1
19	24	Germany	DWD-MOL	POM-2	National	SKYNET	POM_DE_1
20	25	Australia	Bureau of Meteorology (BOM)	SPO2	National	BOM	SPO_AU_2
21	26	China	Academy of Science	CW Photom	National		CW_193_CN
22	27	Germany	DWD-MOL	PSR	National	PMOD/WRC – SI-traceable PMOD/WRC analysis	PSR_DE_4
23	28	Germany	DWD-MOL	PSR	National	PMOD/WRC – SI-traceable PMOD/WRC analysis	PSR_DE_6
24	29	Switzerland	PMOD/WRC	PSR	PMOD/ WRC	PMOD/WRC – SI-traceable	PSR_CH_0
25	30	Switzerland	PMOD/WRC	PSR	PMOD/ WRC	PMOD/WRC – SI-traceable	PSR_CH_8
26	31	Switzerland	PMOD/WRC	PSR	PMOD/ WRC	PMOD/WRC – SI-traceable	PSR_CH_9
27	32	Switzerland	PMOD/WRC	QASUME	PMOD/ WRC	PMOD/WRC – SI-traceable	QASUME
28	33	Switzerland	PMOD/WRC	IR-QASUME	PMOD/ WRC	PMOD/WRC – SI-traceable	IR-QASUME
29*		Saudi Arabia	King Abdullah City for Atomic and Renewable Energy	POM-2	National		

Instrument number (hardware)	*AOD data set number*	*Country*	*Institute*	*Type of radiometer*	*Network*	*Calibration type and analysis (analysis by Institute unless stated otherwise)*	*Acronym*
30*		China	Academy of Science	CIMEL	National		
31*		Spain	Universidad de Granada	CIMEL	National	CARS-ACTRIS	

*Did not submit data

Notes: SMHI = Swedish Meteorological and Hydrological Institute; DWD-MOL = German Weather Service-Meteorological Observatory Lindenberg; NIMS-KMA = National Institute of Meteorological Sciences-Korea Meteorological Administration; LOA = Laboratory for Atmospheric Optics; AEMET = Spanish State Meteorological Agency; ARPA = Regional Environmental Protection Agency; PTB = German National Metrology Institute.

Table 2. Summary of basic characteristics of each instrument type

	Instrument type	*Measuring wavelengths (nm)*	*Field of view at FWHM (°)*	*FWHM (nm)*	*Measurement principle*
1	PFR-N	368, 412, 500, 863	2.5	3.8–5.4	Sun pointing on tracker
2	CIMEL	340, 379, 440, 500, 670, 870, 1 020, 1 640	1.2	2 (340 nm), 4 (380 nm), 10 (440 nm to 1 020 nm)	Sun pointing on tracker
3	CW193	340, 379, 440, 500, 670, 870, 1 021, 1 640	1.3	2–4(UV), 10 (visible) up to 25 (infrared)	Sun pointing on tracker
4	POM-2	315, 340, 380, 400, 500, 675, 870, 940, 1 020, 1 627, 2 200	1	3 (UV), 10 (visible) up to 20 (infrared)	Sun pointing on tracker
5	PSR	320–1 030, step of 0.7	1.5	1.5–6	Sun pointing on tracker
6	SPO2	368, 500, 812, 868	2.4	5	Sun pointing on tracker
7	QASUME	250–550, step of 0.5	2	0.78	Sun pointing on tracker
8	IR-QASUMER	500–1 700, step of 0.5	2	~1.4 (<1 000 nm) ~2.1 (>1 000 nm)	Sun pointing on tracker

Note: FWHM = Full width at half maximum

2.3 Data acquisition and aerosol optical depth retrieval

Measurements of direct solar irradiance were nominally taken at each full minute by the participants' data acquisition systems, yielding typically 500 observations per cloudless day. Actual sampling/averaging rates ranged from 15 seconds to 1 minute, depending on the instrument. "Full minute" time registration is defined as the time (minute) at the start of the sampling. The raw measurements were evaluated by each participant according to their preferred algorithms, including cloud-screening, and submitted for comparison.

The set of measurements covered wavelengths between 368 nm and 1 020 nm. As the WORCC PFR reference triad instruments were measuring at 368 nm, 412 nm, 500 nm and 862 nm, the AODs and the Ångström exponents (AEs) calculated from all four PFR AODs were used to derive AODs at wavelengths measured by other instruments. The AOD intercomparison wavelengths are shown in Table 3.

Table 3. AOD intercomparison wavelengths

Wavelength (nm)	*Instrument (Table 2)*	*Wavelength (nm)*	*Instrument*
368	1, 5–8	500	All
380*	2–8	675*	2–8
400*	4	863/870	All
412	1, 5–8	1 020*	2–8
440*	2, 3		

*using PFR Ångström exponents

In order to compare Ångström exponents, they were derived from all available aerosol optical depths from 368 nm up to 870 nm, depending on the instrument. Atmospheric pressure, precipitable water, relative humidity and temperature readings (every 10 minutes) from the MeteoSwiss weather station located at the comparison site were provided to all participants. In addition, the atmospheric pressure was measured every 1 minute by a SETRA barometer calibrated at the Swiss Federal Institute of Metrology (METAS) in August 2021. Total ozone column content, measured with a double-monochromator Brewer spectroradiometer at PMOD/WRC, was available as well. In order to avoid AOD-related discrepancies introduced by uncertainties linked to the above-mentioned auxiliary data, all participants used the provided data set. Several of the participating radiometers were calibrated at various sites within a few months prior to the FRC-V. Their performance during this comparison can be used to estimate the homogeneity of AOD observations across weather services or networks. Details about each instrument's calibration history can be found in Appendix 2.

2.4 Comparison basics and WORCC reference triad

During the FRC-V, measurements from participating radiometers were evaluated using a uniform comparison software. FRC-V was based on AOD retrievals derived from measurements processed by different algorithms that are used in the normal operation of the radiometers. Recommendations for the comparisons were formulated during a WMO/GAW experts workshop held in 2004 in Davos (*WMO/GAW Experts Workshop on a Global Surface-based Network for Long-term Observations of Column Aerosol Optical Properties* (WMO/TD-No. 1287)), which called for:

- More than 1 000 data points with AOD at 500 nm between 0.04 and 0.20;
- A minimum duration of 5 days;
- Traceability requiring 95% uncertainty within ± (0.005 + 0.01/m) optical depths.

During FRC-V, weather conditions allowed for over 1 000 measurements on 11 days (for example, PFRs ~2 500, CIMELs ~1 500, POMs ~1 050, PSRs ~1 700) permitting the above-mentioned recommendations to be accomplished. During the campaign, AOD data retrieved from direct solar irradiance measurements of participating instruments were compared with the WORCC PFR reference triad. Before the start of the campaign, the WORCC PFR reference triad instruments were intercompared with three PFR instruments that had performed measurements at Izaña, Tenerife, Spain and Mauna Loa, Hawaii, United States of America, for nearly one year. Using the Langley calibration, results of these three instruments' top-of-atmosphere (TOA) voltages were determined. During ten cloudless days in August and September 2021, the three above-mentioned instruments, together with the three WORCC PFR reference triad instruments, were intercompared. The differences in the calibration factors derived from the three (Izaña and Mauna Loa) instruments were less than 0.5% for all four PFR wavelengths.

3. RESULTS

3.1 Aerosol optical depth comparison

Concerning the AOD results, each single AOD measurement of the participating instrument was compared with the synchronous measurement that was derived from the mean of the three PFRs forming the WORCC PFR reference triad. As mentioned, each participant used its own cloud-screening procedure. Since all measurements were compared with the WORCC PFR reference triad, the number of compared observations has an upper limit related to the number of the cloud-screened WORCC PFR reference triad measurements/minutes per day. The overview of the intercomparison in all wavelengths is presented in Figure 2, while the results of the comparison for six wavelengths are shown in Figure 3(a)–(f).

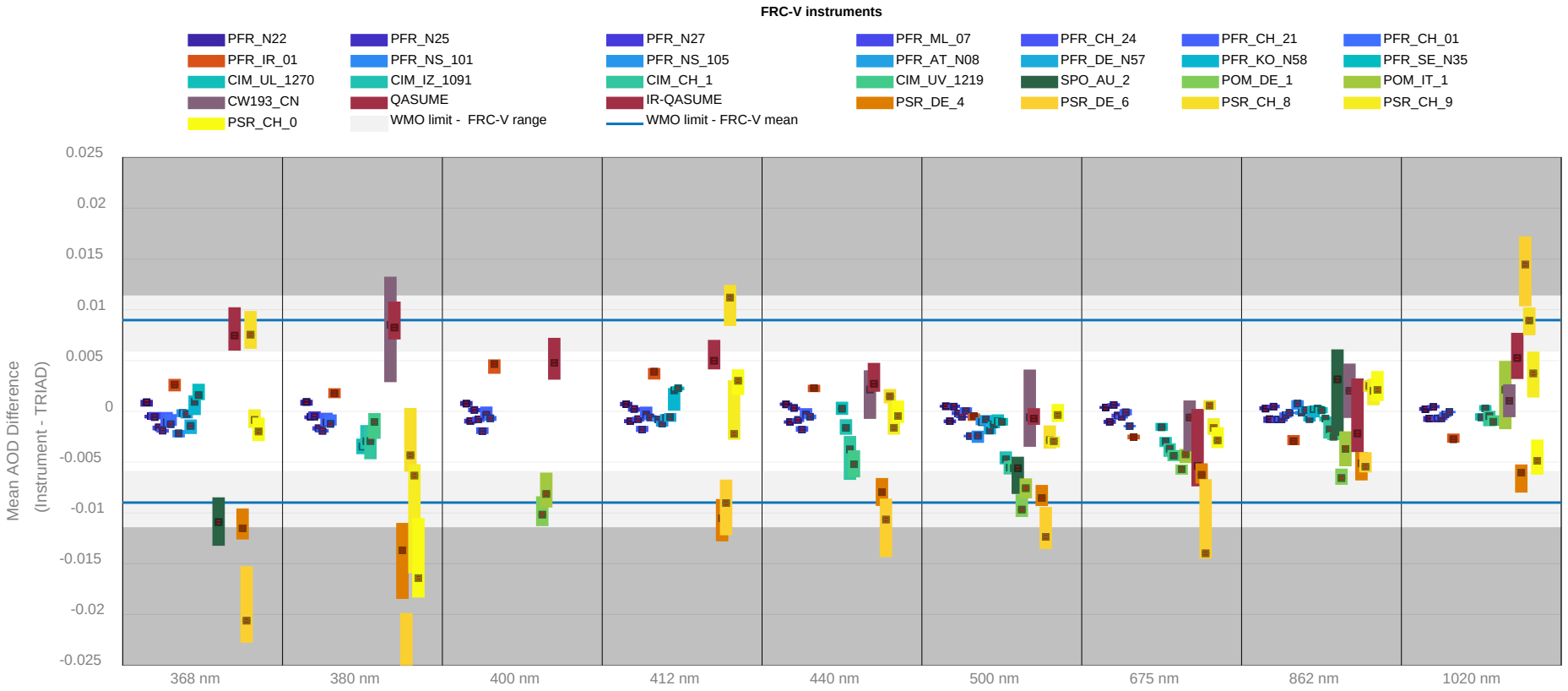

Figure 2. Average difference of each instrument compared with the WORCC PFR reference triad. All wavelengths not matching the four PFR wavelengths have been retrieved for the PFRs, based on the AODs and AEs calculated from the PFRs. The 10th and 90th percentiles are also shown as coloured vertical bars. WMO limits (averages based on the relative air masses during the measurement period) are shown as blue horizontal lines.

(a) 368/380 nm

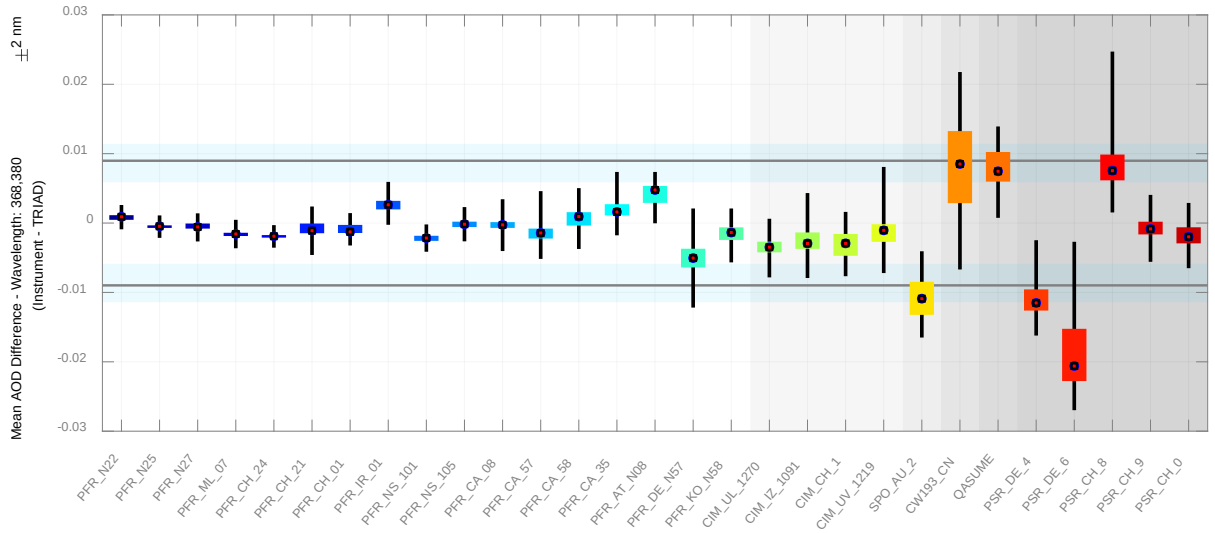

(b) 400/412/440 nm

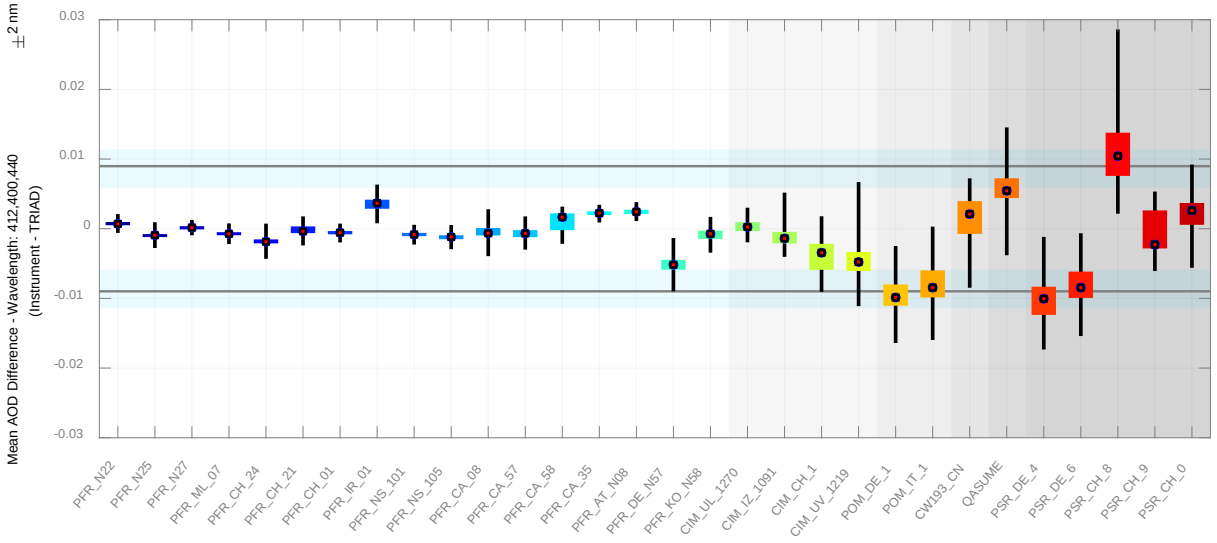

(c) 500 nm

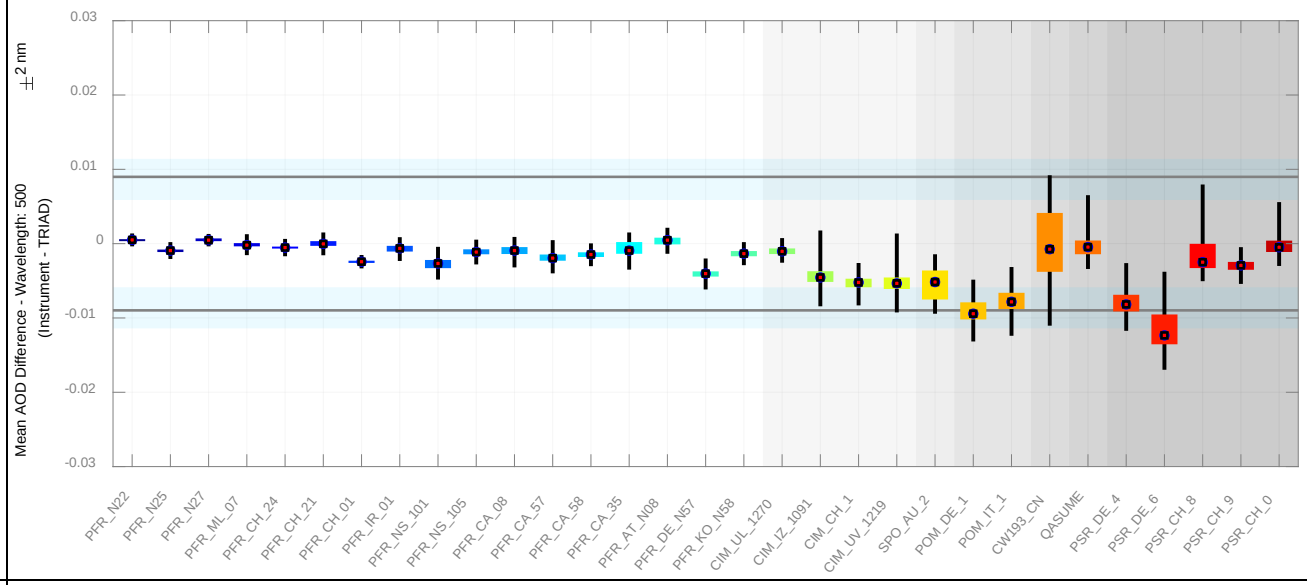

(d) 675 nm

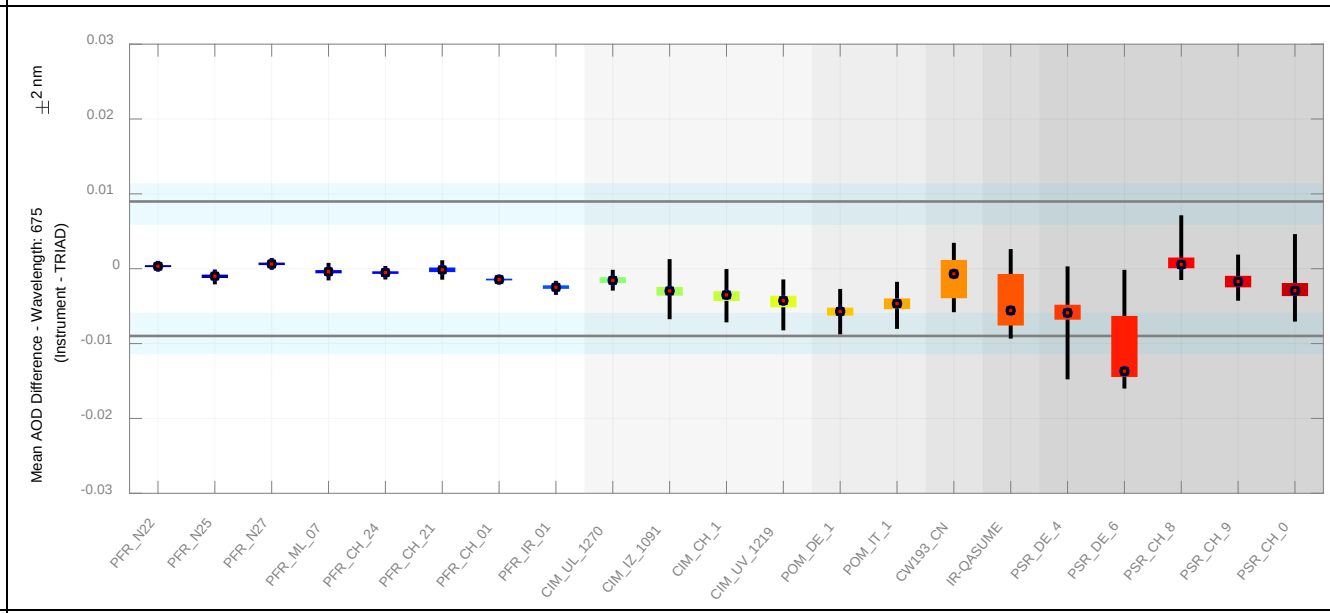

(e) 862/870 nm

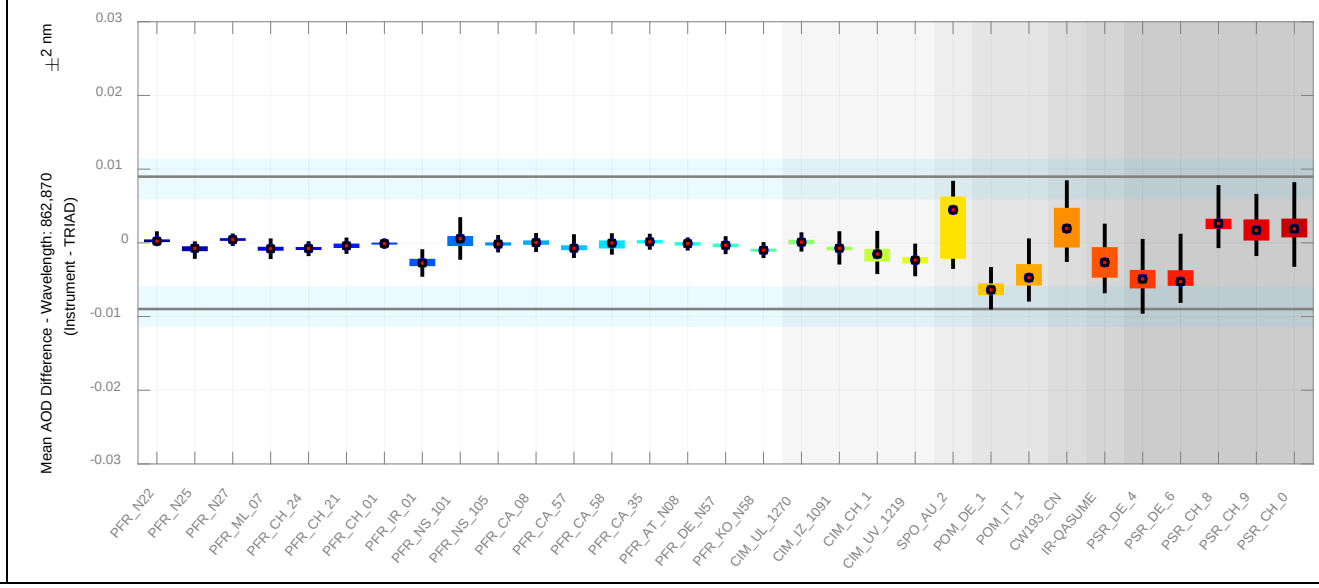

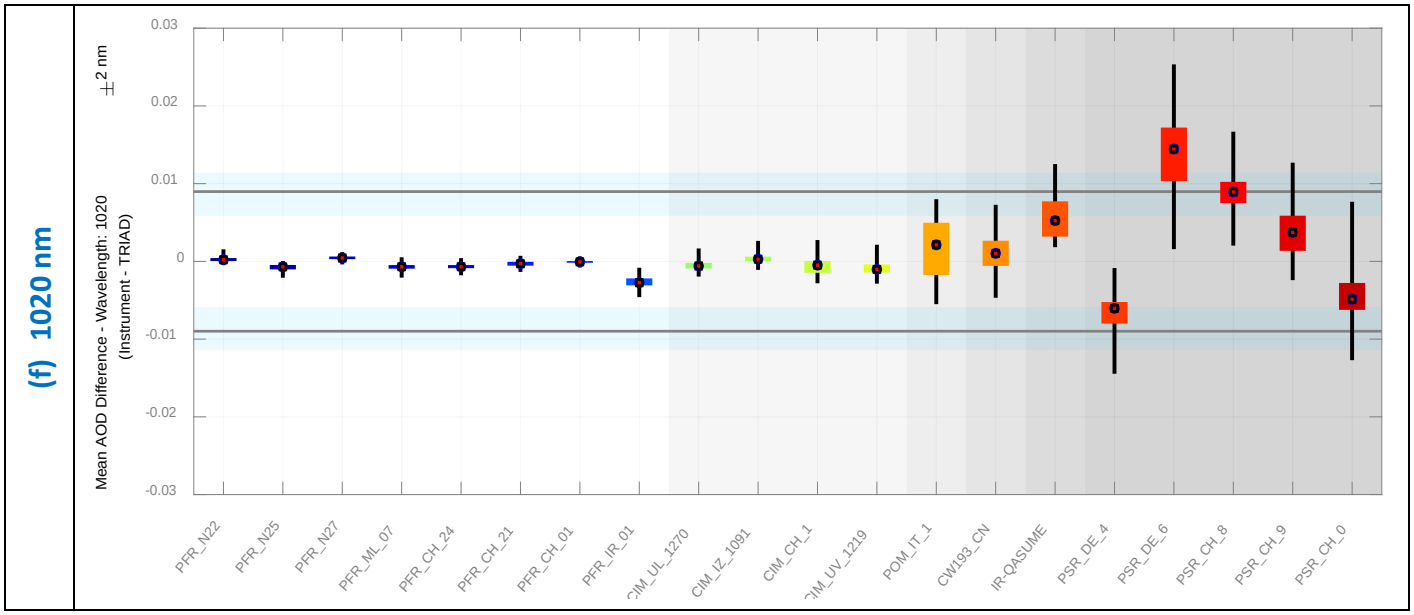

Figure 3. AOD comparison results at: (a) 368/380 nm;(b) 400/412/440 nm; (c) 500 nm; (d) 675 nm; (e) 862/870 nm; and (f) 1 020 nm. The open circles represent the median difference of each instrument from the PFR reference triad at each wavelength over the 11 FRC-V selected days. The size of the coloured boxes represents the 10th and 90th percentiles, while the black vertical lines represent the minimum and maximum values of the distribution, excluding outliers. Black horizontal lines represent the average WMO limits, with light blue representing the range of these limits, based on the air mass change during each day.

Statistics and graphical representations of the performance of each individual instrument for each wavelength can be found in Appendices 3 and 4, respectively. A synopsis of the comparison statistics for the four PFR wavelengths with instruments grouped by type, is shown in Table 4. In addition, the percentage of instruments that lie within the WMO criterion of 0.005 + 0.01/m optical depths for each of the 9 compared wavelengths is shown in Figure 4 and Table 5.

Table 4. Statistics of AOD difference to the WORCC PFR reference triad at four wavelengths (ranges)

Instrument type (number of instruments)	368 nm or 380 nm		400 nm or 412 nm or 440 nm		500 ± 3 nm		865 ± 5 nm	
	AOD difference Median ± 1σ *(10^{-3})	Correlation coefficient [min, max]	AOD Difference Median ± 1σ * (10^{-3})	Correlation coefficient [min, max]	AOD difference Median ± 1σ *(10^{-3})	Correlation coefficient [min, max]	AOD difference Median ± 1σ * (10^{-3})	Correlation coefficient [min, max]
PFR (14)	–0.5 ± 3.1	[0.992, 1.000]	–0.6 ± 2.1	[0.998, 1.000]	–0.9 ± 1.5	[0.995, 1.000]	–0.2 ± 0.8	[0.982, 0.999]
CIM (4)	–2.9 ± 1.1	[0.994, 0.998]	–2.7 ± 2.4	[0.985, 0.999]	–5.1 ± 2.2	[0.997, 0.999]	–1.2 ± 1.1	[0.973, 0.998]
POM (2)			–9.2 ± 1.4	[0.993, 0.994]	–8.6 ± 1.5	[0.995, 0.996]	–5.1 ± 2.0	[0.935, 0.978]
PSR (5)	–2.0 ± 10.8	[0.982, 0.998]	–2.2 ± 8.9	[0.983, 0.995]	–2.9 ± 4.9	[0.987, 0.998]	+2.0 ± 4.1	[0.910, 0.990]
QASUME (1)	+7.5	[0.900,	+5.0	[0.937,	–0.7	[0.977,	–2.2	[0.735,

(UV to IR)		0.900]		0.937]		0.977]		0.735]
SPO2	–10.9	[0.990, 0.990]			–5.6	[0.990, 0.990]	+3.2	[0.975, 0.975]
CW193	+8.5	[0.928, 0.928]	+2.1	[0.991, 0.991]	–0.6	[0.932, 0.932]	+2.0	[0.788, 0.788]
All	–1.3	[0.900, 1.000]	–1.4	[0.937, 1.000]	–2.9	[0.932, 1.000]	–0.2	[0.735, 0.999]

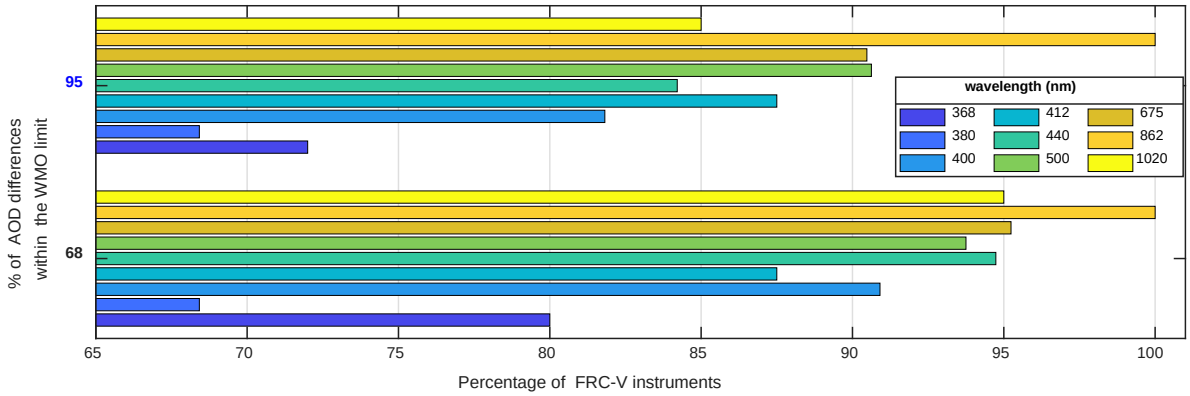

Figure 4. Percentage of instruments that lie within the WMO criterion of 0.005 + 0.01/m optical depths for each of the 9 compared wavelengths. The vertical axis shows minimum level of agreement, 68% and 95%, with 95% to be the WMO traceability criterion.

Table 5. Percentage of instruments with 95% and 68% agreement within the WMO limits

Level of agreement	*368 nm % of inst.*	*380 nm % of inst.*	*400 nm % of inst.*	*412 nm % of inst.*	*440 nm % of inst.*	*500 nm % of inst.*	*675 nm % of inst.*	*862 nm % of inst.*	*1020 nm % of inst.*
68%	80	68	91	88	95	94	95	100	95
95%	72	68	82	88	84	91	90	100	85

3.2 Ångström exponents

The Ångström empirical law $\tau(\lambda) = \beta\lambda^{-a}$ is often used to describe the AOD spectral distribution and in modelling of the atmospheric radiative transfer, or for interpolating AOD between disparate wavelengths. The value of the AE(α) is also a qualitative indicator of the aerosol particle size distribution, and allows for discrimination between coarse mode aerosols (α < 1) (typical for dust and sea salt) and fine mode aerosols (α > 2) (associated with pollution and biomass burning). The curvature of the AOD spectrum is often approximated by a second-order polynomial of the form:

$$\ln\tau(\lambda) = a + b\ln(\lambda) + c(\ln(\lambda))^2 \quad (2)$$

(Eck et al., 1999; O'Neill et al., 2001). Cachorro et al. (2001) demonstrated the necessity of defining a standard spectral range where the Ångström parameters should be determined. AEs from each instrument were calculated with a polynomial fitting, using a common range, limited from 368 nm up to 870 nm (for example, PFRs and the SPO from 368 nm to 862 nm and all others from 380 nm to 870 nm). Major AE deviations are linked to instruments showing spectrally variable AOD differences from the PFR reference triad. Results are presented in Figure 5.

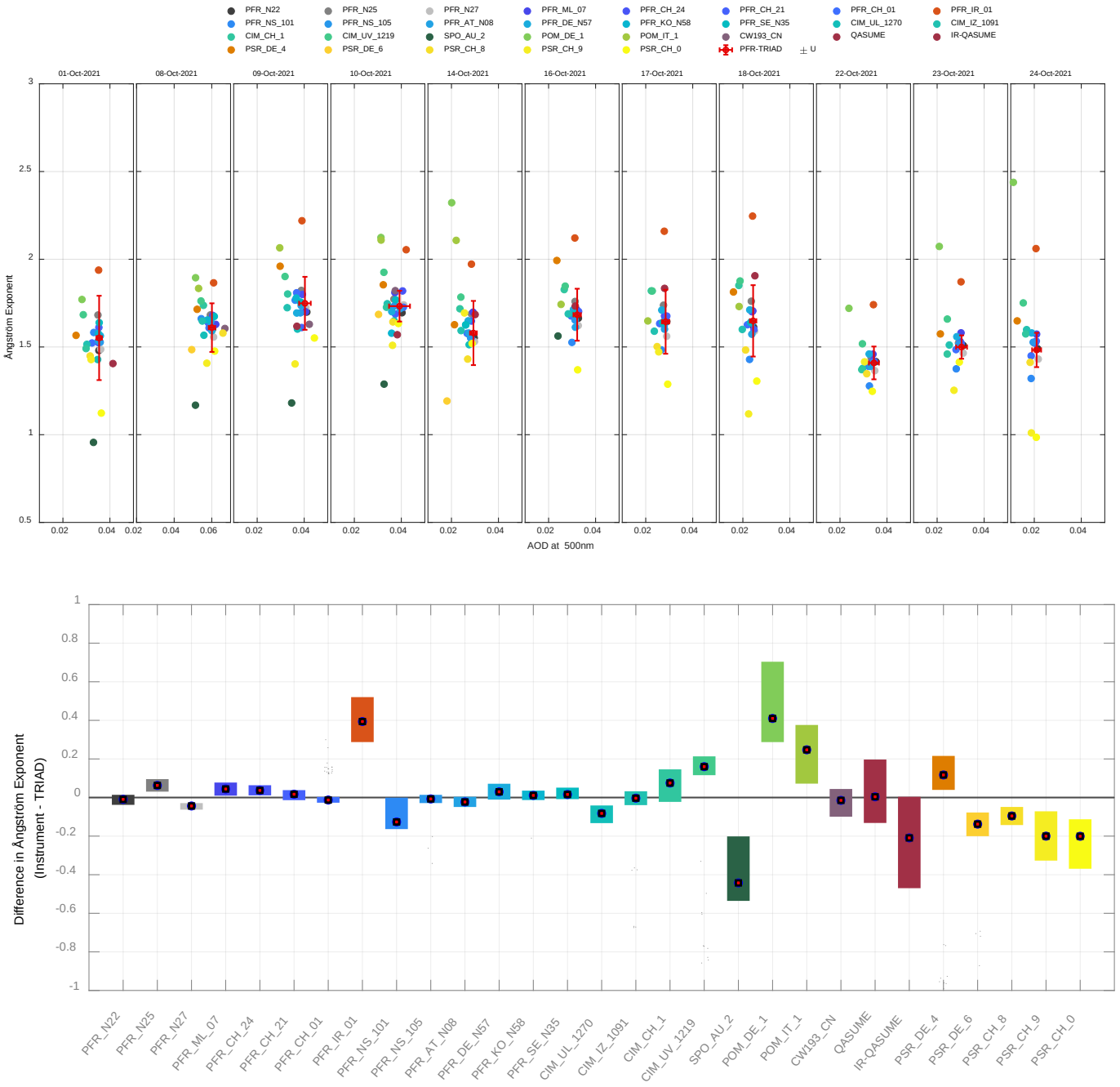

Figure 5. Upper panel: AEs as derived by all instruments for each day of the campaign as a function of AOD at 500 nm. Error bars represent the daily variability of AOD (horizontal red bars) and AE (vertical red bars) from the WORCC PFR reference triad. Lower panel: Difference in the AE between each instrument and the WORCC PFR reference triad. The size of the coloured boxes represents the 10th and 90th percentiles.

4. CONCLUSIONS AND RECOMMENDATIONS

A total number of 31 instruments were invited to participate in the FRC-V. Three of the instruments were unable to participate in the campaign, mainly due to technical (solar tracking) problems. The intercomparison fulfilled the WMO recommendations concerning the number of days and measurements performed.

For the overview statistics of FRC-V, the 28 instruments, with their initial calibration and participant analysis, have been considered. In addition, the SI-traceable AOD retrieval of the PFR_CH_01(PFR_IR_01) and four instruments also calibrated at PMOD/WRC (according to Table 1) were included, bringing the maximum possible total number of available AOD data sets to 33.

Concerning the comparison of the instruments/data sets with the WORCC PFR reference triad: case A is defined as the case where at least 68%, and case B as the case where at least 95% of the data comparing each of the instruments/data sets with the WORCC PFR triad at a certain wavelength, are within the WMO limits. Based on Table 5 for the UV range, at least 68% of total instruments can be attributed to cases A and B. For AODs from 400 nm up to 1 020 nm, 82% and 88% of instruments achieved the A and B cases respectively. Of the 32 instruments/data sets for AOD at 500 nm, 29 can be attributed to case B; of the 32 instruments/data sets for AOD at 862 nm, 32 can be attributed to case B.

It is suggested that the following are the main factors that could lead to an improvement of the reported agreement: calibration homogenization, improvements in pointing, homogenization of inputs used in the AOD retrieval algorithm (common set of ozone cross-sections, nitrogen dioxide (NO_2) optical depth determination, air mass calculation and Rayleigh scattering formulas), and improvement in each instrument characterization.

Table 6 presents a comparison of the FRC-V statistics with those obtained at the FRC-IV (GAW Report No. 231).

Table 6. Comparison of results from FRC-IV and FRC-V: number of instruments (AOD data sets submitted) out of the total number of instruments satisfying the U95 limit (case B)

Wavelength (nm)	*368/380*	*402/412/440*	*500*	*675*	*862/870*	*1024*
FRC-IV	16/24	16/24	27/29		25/29	
FRC-V*	22/30	26/31	29/32	19/21	32/32	17/20

*Appendix 4 results

Concerning the determination of the Ångström exponent comparisons, most (24/29) of the instruments agreed, within AE of ±0.2, compared with the WORCC reference triad (taking into account only initial calibrations and not instruments/data sets re-calibrated in Davos (see Table 1 and Appendix 3)). This was despite the fact that AEs in some instruments had been calculated using a different number of wavelengths and, in some cases, different spectral ranges (see Table 2).

The results of the FRC-V, which included a large variety of AOD measuring instrumentation, via the participation of reference instruments from AERONET-Europe/ACTRIS, SKYNET, GAW-PFR, CARSNET and the Australian aerosol network, can be considered as an important step for global AOD homogeneity initiatives. The ultimate aim is a unified AOD product to be used for long-term aerosol and radiative forcing studies, case studies involving accurate AOD retrievals, and satellite validation-related activities, thereby enhancing the WMO and GCOS essential climate variable multiwavelength AOD.

5. REFERENCES

Cachorro, V. E.; Vergaz, R.; de Frutos, A. M. A Quantitative Comparison of Alpha Ångström Turbidity Parameter Retrieved in Different Spectral Ranges Based on Spectroradiometer Solar Radiation Measurements. *Atmospheric Environment* **2001**, *35* (30), 5117–5124. https://doi.org/10.1016/S1352-2310(01)00321-1.

Che, H.; Xia, X.; Zhao, H. et al. Spatial Distribution of Aerosol Microphysical and Optical Properties and Direct Radiative Effect from the China Aerosol Remote Sensing Network. *Atmospheric Chemistry and Physics* **2019**, *19* (18), 11843–11864. https://doi.org/10.5194/acp-19-11843-2019.

Coddington, O. M.; Richard, E. C.; Harber, D. et al. The TSIS-1 Hybrid Solar Reference Spectrum. *Geophysical Research Letters* **2021**, *48* (12). https://doi.org/10.1029/2020GL091709.

Cuevas, E.; Romero-Campos, P. M.; Kouremeti, N. et al. Aerosol Optical Depth Comparison between GAW-PFR and AERONET-Cimel Radiometers from Long-term (2005–2015) 1-min Synchronous Measurements. *Atmospheric Measurement Techniques* **2019**, *12* (8), 4309–4337. https://doi.org/10.5194/amt-12-4309-2019.

Eck, T. F.; Holben, B. N.; Reid, J. S. et al. Wavelength Dependence of the Optical Depth of Biomass Burning, Urban, and Desert Dust Aerosols. *Journal of Geophysical Research* **1999**, *104* (D24), 31333–31349. https://doi.org/10.1029/1999JD900923.

Giles, D. M.; Sinyuk, A.; Sorokin, M. G. et al. Advancements in the Aerosol Robotic Network (AERONET) Version 3 Database – Automated Near-real-time Quality Control Algorithm with Improved Cloud Screening for Sun Photometer Aerosol Optical Depth (AOD) Measurements. *Atmospheric Measurement Techniques* **2019**, *12*, 169–209. https://doi.org/10.5194/amt-12-169-2019.

Global Atmosphere Watch (GAW). *Fourth WMO Filter Radiometer Comparison (FRC-IV)* (GAW Report No. 231); World Meteorological Organization: Geneva, 2016.

Gröbner, J.; Kouremeti, N. The Precision Solar Spectroradiometer (PSR) for Direct Solar Irradiance Measurements. *Solar Energy* **2019**, *185*, 199–210. https://doi.org/10.1016/j.solener.2019.04.060.

Gröbner, J.; Schreder, J.; Kazadzis, S. et al. Traveling Reference Spectroradiometer for Routine Quality Assurance of Spectral Solar Ultraviolet Irradiance Measurements. *Applied Optics* **2005**, *44* (25), 5321–5331. https://doi.org/10.1364/AO.44.005321.

Gröbner, J.; Kröger, I.; Egli, L. et al. The High-resolution Extraterrestrial Solar Spectrum (QASUMEFTS) Determined from Ground-based Solar Irradiance Measurements. *Atmospheric Measurement Techniques* **2017**, *10* (9), 3375–3383. https://doi.org/10.5194/amt-10-3375-2017.

Holben., B. N.; Eck, T. F.; Slutsker, I. et al. AERONET—A Federated Instrument Network and Data Archive for Aerosol Characterization. *Remote Sensing of Environment* **1998**, *66* (1), 1–16. https://doi.org/10.1016/S0034-4257(98)00031-5.

Kazadzis, S.; Kouremeti, N.; Diémoz, H. et al. Results from the Fourth WMO Filter Radiometer Comparison for Aerosol Optical Depth Measurements. *Atmospheric Chemistry and Physics* **2018a**, *18* (5), 3185–3201. https://doi.org/10.5194/acp-18-3185-2018.

Kazadzis, S.; Kouremeti, N.; Nyeki, S. et al. The World Optical Depth Research and Calibration Center (WORCC) Quality Assurance and Quality Control of GAW-PFR AOD Measurements. *Geoscientific Instrumentation, Methods And Data Systems* **2018b**, *7* (1), 39–53. https://doi.org/10.5194/gi-7-39-2018.

Kouremeti, N.; Nevas, S.; Kazadzis, S. et al. SI-traceable Solar Irradiance Measurements for Aerosol Optical Depth Retrieval. *Metrologia* **2022**, *5US9* (4). https://doi.org/10.1088/1681-7575/ac6cbb.

Mitchell, R. M.; Forgan, B. W. Aerosol Measurement in the Australian Outback: Intercomparison of Sun Photometers. *Journal of Atmospheric and Oceanic Technology* **2003**, *20* (1), 54–66. https://doi.org/10.1175/1520-0426(2003)020<0054:AMITAO>2.0.CO;2.

Mitchell, R. M.; Forgan, B. W.; Campbell, S. K. The Climatology of Australian Aerosol. *Atmospheric Chemistry and Physics* **2017**, *17* (8), 5131–5154. https://doi.org/10.5194/acp-17-5131-2017.

Nakajima, T.; Campanelli, M.; Che, H. et al. An Overview of and Issues with Sky Radiometer Technology and SKYNET. *Atmospheric Measurement Techniques* **2020**, *13*, 4195–4218. https://doi.org/10.5194/amt-13-4195-2020.

O'Neill, N. T.; Eck, T. F.; Holben, B. N. et al. Bimodal Size Distribution Influences on the Variation of Ångström Derivatives in Spectral and Optical Depth Space. *Journal of Geophysical Research* **2001**, *106* (D9), 9787–9806. https://doi.org/10.1029/2000JD900245.

World Meteorological Organization (WMO). *Recent Progress in Sun Photometry: Determination of the Aerosol Optical Depth* (WMO/TD-No. 143). GAW Report No. 43. Geneva, 1986.

World Meteorological Organization (WMO) *WMO/GAW Experts Workshop on a Global Surface-based Network for Long-term Observations of Column Aerosol Optical Properties* (WMO/TD-No. 1287). GAW Report No. 162. Geneva, 2005.

World Meteorological Organization (WMO). *Commission for Instruments and Methods of Observation (CIMO) - Fourteenth session: Abridged Final Report with Resolutions and Recommendations* (WMO-No. 1019). WMO: Geneva, 2007.

Zheng, Y.; Che, H.; Wang, Y. et al. Evaluation of Aerosol Microphysical, Optical and Radiative Properties Measured with a Multiwavelength Photometer. *Atmospheric Measurement Techniques* **2022**, *15* (7), 2139–2158. https://doi.org/10.5194/amt-15-2139-2022.

6. APPENDICES

Appendix 1: List of participants

Stelios Kazadzis Physikalisch-Meteorologisches Observatorium Davos, World Radiation Center (PMOD/WRC) Dorfstrasse 33, CH-7260 Davos Dorf Switzerland stelios.kazadzis@pmodwrc.ch	Bruce W. Forgan Bureau of Meteorology PO Box 1289, Melbourne 3001 Victoria Australia b.forgan@bom.gov.au
Natalia Kouremeti Physikalisch-Meteorologisches Observatorium Davos, World Radiation Center (PMOD/WRC) Dorfstrasse 33, CH-7260 Davos Dorf Switzerland Natalia.kouremeti@pmodwrc.ch	Michael Milner Standards and Metrology Bureau of Meteorology 700 Collins St, Docklands, Vic, 3008, Australia m.milner@bom.gov.au
Julian Gröbner Physikalisch-Meteorologisches Observatorium Davos, World Radiation Center (PMOD/WRC) Dorfstrasse 33, CH-7260 Davos Dorf Switzerland julian.groebner@pmodwrc.ch	Philippe Goloub Laboratoire d'Optique Atmosphérique, Université des Sciences et Technologies de Lille 1, Bât. P5, 59655, Villeneuve d'Ascq France goloub@loa.univ-lille1.fr
Luc Blarel Laboratoire d'Optique Atmosphérique, Université des Sciences et Technologies de Lille 1, Bât. P5, 59655, Villeneuve d'Ascq France luc.blarel@univ-lille.fr	Gael Dubois Laboratoire d'Optique Atmosphérique, Université des Sciences et Technologies de Lille 1, Bât. P5, 59655, Villeneuve d'Ascq France gael.dubois@univ-lille.fr
Ralf Becker Deutscher Wetterdienst Meteorologisches Observatorium Lindenberg – Richard Assmann Observatorium Am Observatorium 12, 15848 Tauche, OT: Lindenberg Germany Ralf.Becker@dwd.de	Lionel Doppler Deutscher Wetterdienst Meteorologisches Observatorium Lindenberg – Richard Assmann Observatorium Am Observatorium 12, 15848 Tauche, OT: Lindenberg Germany lionel.doppler@dwd.de
Stefan Wacker Deutscher Wetterdienst Meteorologisches Observatorium Lindenberg – Richard Assmann Observatorium Am Observatorium 12, 15848 Tauche, OT: Lindenberg Germany stefan.wacker@dwd.de	Thomas Carlund Swedish Meteorological and Hydrological Institute 601 76 Norrköping Sweden Thomas.Carlund@smhi.se

Africa Barreto Izaña Atmospheric Research Centre (AEMET) State Meteorological Agency Santa Cruz de Tenerife Spain abarretov@aemet.es	Emilio Cuevas Izaña Atmospheric Research Centre (AEMET) State Meteorological Agency Santa Cruz de Tenerife Spain ecuevasa@aemet.es
Carlos Toledano Atmospheric Optics Group (GOA), University of Valladolid, 47071, Valladolid Spain toledano@goa.uva.es	Victor Estelles Department of Earth Physics and Thermodynamics University of Valencia Spain vestelle@uv.es
Henri Diémoz Aria e Atmosfera – Radiazione solare e atmosfera ARPA Valle d'Aosta loc. Grande Charrière 44 Saint-Christophe (11020) Italy h.diemoz@arpa.vda.it	Monica Campanelli Institute of Atmospheric Sciences and Climate (ISAC), National Research Council, ISAC-CNR Via Fosso del Cavaliere 100, 00133, Rome Italy m.campanelli@isac.cnr.it
Huizheng Che Key Laboratory of Atmospheric Chemistry Chinese Academy of Meteorological Sciences China Meteorological Administration 46 Zhong-Guan-Cun S. Ave., Beijing 100081 China chehz@cma.gov.cn, chehuizheng@gmail.com	Yu Zheng Key Laboratory of Atmospheric Chemistry Chinese Academy of Meteorological Sciences China Meteorological Administration 46 Zhong-Guan-Cun S. Ave., Beijing 100081 China yuzheng@cma.gov.cn
Kim Sumin Innovative Meteorological Research Department 393–17, Haeangwangwang-ro Anmyeon-eup Taean-gun, Chungnam 32164 Republic of Korea	Jeong Won-Seok Climate Research Department, National Institute of Meteorological Sciences Jeju Republic of Korea
Axel Kreuter Division of Biomedical Physics (BMP), Medical University Innsbruck Müllerstraße 44, A 6020, Innsbruck Austria axel.kreuter@i-med.ac.at	Francisco Navas Guzmán Atmospheric Physics Group (GFAT) University of Granada, 18071, Granada Spain fguzman@ugr.es
Kyriaki Papachristopoulou National Observatory of Athens Athens Greece kpapachr@noa.gr	Angelos Karanikolas Physikalisch-Meteorologisches Observatorium Davos, World Radiation Center (PMOD/WRC) Dorfstrasse 33, CH-7260 Davos Dorf Switzerland angelos.Karanikolas@pmodwrc.ch

Panagiotis Raptis National Observatory of Athens Athens Greece piraptis@noa.gr	Franz Zeilinger Physikalisch-Meteorologisches Observatorium Davos, World Radiation Center (PMOD/WRC) Dorfstrasse 33, CH-7260 Davos Dorf Switzerland franz.zeilinger@pmodwrc.ch
Jakob Föller Physikalisch-Meteorologisches Observatorium Davos, World Radiation Center (PMOD/WRC) Dorfstrasse 33, CH-7260 Davos Dorf Switzerland Jakob.Foeller@pmodwrc.ch	Christian Thomann Physikalisch-Meteorologisches Observatorium Davos, World Radiation Center (PMOD/WRC) Dorfstrasse 33, CH-7260 Davos Dorf Switzerland Christian.thomann@pmodwrc.ch
Abdullah Al-Adwani National Renewable Energy Data Center King Abdullah City for Atomic and Renewable Energy Tel. +966 11 8085641 Saudi Arabia a.adwani@energy.gov.sa	Aktiri Masoom Physikalisch-Meteorologisches Observatorium Davos, World Radiation Center (PMOD/WRC) Dorfstrasse 33, CH-7260 Davos Dorf Switzerland akriti.masoom@pmodwrc.ch

Appendix 2. Instrument calibrations report

Instrument	Calibration
PFR_ML_07	WORCC-PMOD/WRC Langley calibration at the high mountain station, Mauna Loa, December 2020 to August 2021
PFR_CH_24	WORCC-PMOD/WRC calibration transfer based on PFR_ML_07, Davos, August 2021
PFR_CH_21	WORCC-PMOD/WRC Langley calibration at the high mountain station, Izaña, 09 January 2019 to 01 September 2020
PFR_CH_01	WORCC-PMOD/WRC, calibration transfer from WORCC PFR reference triad, Davos, May 2021
PFR_IR_01	SI-traceable irradiance calibration at Physikalisch-Technische Bundesanstalt (PTB – German national metrology institute) Top-of-atmosphere spectrum QASUME (Quality Assurance of Spectral Ultraviolet Measurements in Europe) FTS (Fourier transform spectroradiometer) (λ<400 nm) and TSIS-1 (Total and Spectral Solar Irradiance Sensor-1) (λ>400 nm)
PFR_NS_101	WORCC-PMOD/WRC calibration transfer from WORCC PFR reference triad, Davos, May 2021
PFR_NS_105	WORCC-PMOD/WRC calibration transfer from WORCC PFR reference triad, Davos, May 2021
PFR_CA_N08	WORCC-PMOD/WRC calibration transfer from WORCC PFR reference triad, Davos, FRC-V
PFR_CA_N57	WORCC-PMOD/WRC calibration transfer from WORCC PFR reference triad, Davos, FRC-V
PFR_KO_58	WORCC-PMOD/WRC calibration transfer from WORCC PFR reference triad, Davos, FRC-V
PFR_SE_35	WORCC-PMOD/WRC calibration transfer from WORCC PFR reference triad, Davos, FRC-V
PFR_AT_N08	WORCC-PMOD/WRC calibration transfer from WORCC PFR reference triad, Davos, October 2017
PFR_DE_N57	WORCC-PMOD/WRC calibration transfer from WORCC PFR reference triad, Davos, March 2021
PFR_KO_N58	WORCC-PMOD/WRC calibration transfer from WORCC PFR reference triad, Davos, FRC-V (new filters)
-PFR_SE_N35	WORCC-PMOD/WRC calibration transfer from WORCC PFR reference triad, Davos, December 2019
CIM_UL_1270	LOA-ACTRIS/CARS Langley calibration at the high mountain station, Mauna Loa
CIM_IZ_1091	AEMET-ACTRIS/CARS Langley Calibration at the high mountain station, Izaña, May 2021
CIM_CH_1	LOA-ACTRIS/CARS, OHP (Observatoire de Haute-Provence), August 2021
CIM_UV_1219	University Valladolid-ACTRIS/CARS Langley calibration at the high mountain station, Izaña, 2021
SPO_AU_2	BOM calibration transfer from reference instrument of the network
POM_DE_1	SKYNET adapted Langley method
POM_IT_1	SKYNET adapted Langley method
CW193_CN	Intercomparison calibration with CARSNET reference instruments at Chinese Academy of Meteorological Sciences (CAMS) station, May 2021
QASUME	PMOD/WRC Laboratory calibration – Irradiance standard: field emission lamp (FEL) calibrated at PTB, top-of-atmosphere spectrum: QASUMEFTS and TSIS-1 Hybrid Solar Reference Spectrum (HSRS)

Instrument	Calibration
IR-QASUME	PMOD/WRC Laboratory calibration – Irradiance standard: FEL calibrated at PTB, top-of-atmosphere spectrum: TSIS-1 HSRS
PSR_DE_4	PMOD/WRC Laboratory calibration – Irradiance standard: FEL calibrated at PTB, top-of-atmosphere spectrum: QASUMEFTS and TSIS-1 HSRS
PSR_DE_6	PMOD/WRC Laboratory calibration – Irradiance standard: FEL calibrated at PTB, top-of-atmosphere spectrum: QASUMEFTS and TSIS-1 HSRS
PSR_CH_8	PMOD/WRC Laboratory calibration – Irradiance standard: FEL calibrated at PTB, top-of-atmosphere spectrum: QASUMEFTS and TSIS-1 HSRS
PSR_CH_9	PMOD/WRC Laboratory calibration – Irradiance standard: FEL calibrated at PTB, top-of-atmosphere spectrum: QASUMEFTS and TSIS-1 HSRS
PSR_CH_0	PMOD/WRC Laboratory calibration – Irradiance standard: FEL calibrated at PTB, top-of-atmosphere spectrum: QASUMEFTS and TSIS-1 HSRS

Appendix 3. Comparison statistics for each instrument and for each measured wavelength

Wavelength: 368 / 380 nm

Instrument	Median ± 1σ	Percentiles [5, 95]	Correlation coefficient	Linear fit (slope, intercept)	Number of data points	% within WMO limits
PFR_N22	+0.001 ± 0.001	[–0.000, +0.001]	1.000	(0.995, 0.001)	3 204	100
PFR_N25	–0.000 ± 0.001	[–0.001, +0.001]	1.000	(1.003, –0.001)	3 160	100
PFR_N27	–0.001 ± 0.001	[–0.001, +0.001]	0.999	(0.991, –0.000)	3 183	100
PFR_ML_07	–0.002 ± 0.001	[–0.002, +0.000]	1.000	(1.019, –0.002)	3 152	100
PFR_CH_24	–0.002 ± 0.001	[–0.003, –0.000]	1.000	(1.008, –0.002)	3 129	100
PFR_CH_21	–0.001 ± 0.001	[–0.002, +0.001]	0.999	(1.018, –0.002)	2 913	100
PFR_CH_01	–0.001 ± 0.001	[–0.002, +0.000]	0.999	(1.023, –0.002)	3 160	100
PFR_IR_01	+0.003 ± 0.001	[+0.001, +0.005]	0.999	(1.030, 0.001)	3 217	100
PFR_NS_101	–0.002 ± 0.001	[–0.003, –0.001]	1.000	(0.992, –0.002)	3 030	100
PFR_NS_105	–0.000 ± 0.001	[–0.001, +0.001]	1.000	(1.002, –0.000)	3 091	100
PFR_CA_08	–0.000 ± 0.001	[–0.002, +0.001]	0.999	(0.995, –0.000)	2 292	100
PFR_CA_57	–0.001 ± 0.002	[–0.003, +0.003]	0.998	(1.063, –0.004)	3 073	100
PFR_CA_58	+0.001 ± 0.001	[–0.002, +0.002]	0.999	(0.960, 0.003)	1 693	100
PFR_CA_35	+0.002 ± 0.002	[+0.000, +0.006]	0.999	(1.070, –0.002)	1 596	100
PFR_AT_N08	+0.005 ± 0.002	[+0.001, +0.006]	0.999	(1.059, –0.000)	456	100
PFR_DE_N57	–0.005 ± 0.002	[–0.009, –0.002]	0.997	(1.049, –0.008)	1 877	94
PFR_KO_N58	–0.001 ± 0.001	[–0.004, +0.000]	0.997	(1.011, –0.002)	2 851	100
PFR_SE_N35	+0.009 ± 0.004	[+0.002, +0.014]	0.992	(1.057, 0.005)	917	64
CIM_UL_1270	–0.003 ± 0.001	[–0.005, –0.001]	0.998	(1.025, –0.005)	417	100
CIM_IZ_1091	–0.003 ± 0.002	[–0.005, +0.002]	0.995	(1.004, –0.003)	2 336	100
CIM_CH_1	–0.003 ± 0.002	[–0.006, –0.001]	0.994	(1.008, –0.003)	1 506	100
CIM_UV_1219	–0.001 ± 0.006	[–0.005, +0.002]	0.998	(1.017, –0.002)	2 256	100
SPO_AU_2	–0.011 ± 0.003	[–0.015, –0.005]	0.990	(1.068, –0.015)	989	48
CW193_CN	+0.009 ± 0.007	[–0.001, +0.020]	0.928	(0.917, 0.016)	192	62
QASUME	+0.007 ± 0.003	[+0.001, +0.014]	0.900	(0.867, 0.014)	112	64
PSR_DE_4	–0.012 ± 0.002	[–0.014, –0.006]	0.994	(0.983, –0.010)	2 301	18
PSR_DE_6	–0.021 ± 0.005	[–0.025, –0.008]	0.982	(0.974, –0.018)	634	5
PSR_CH_8	+0.008 ± 0.006	[+0.004, +0.025]	0.993	(1.262, –0.004)	2 058	77
PSR_CH_9	–0.001 ± 0.001	[–0.003, +0.002]	0.998	(0.979, 0.000)	2 702	100
PSR_CH_0	–0.002 ± 0.001	[–0.004, +0.000]	0.997	(0.987, –0.001)	3 108	100

Wavelength: 400 / 412 / 440 nm

Instrument	Median ± 1σ	Percentiles [5, 95]	Correlation coefficient	Linear fit (slope, intercept)	Number of data points	% within WMO limits
PFR_N22	+0.001 ± 0.000	[+0.000, +0.002]	1.000	(0.994, 0.001)	3 194	100
PFR_N25	–0.001 ± 0.000	[–0.002, –0.000]	1.000	(1.008, –0.001)	3 169	100
PFR_N27	+0.000 ± 0.000	[–0.000, +0.001]	1.000	(0.996, 0.000)	3 108	100
PFR_ML_07	–0.001 ± 0.000	[–0.001, +0.000]	1.000	(1.015, –0.001)	3 137	100
PFR_CH_24	–0.002 ± 0.002	[–0.002, +0.003]	1.000	(1.001, –0.002)	3 089	100
PFR_CH_21	–0.000 ± 0.001	[–0.001, +0.001]	0.999	(1.011, –0.001)	2 911	100
PFR_CH_01	–0.001 ± 0.000	[–0.002, +0.000]	1.000	(1.008, –0.001)	3 187	100
PFR_IR_01	+0.004 ± 0.001	[+0.002, +0.005]	0.999	(1.020, 0.003)	3 220	100
PFR_NS_101	–0.001 ± 0.000	[–0.001, –0.000]	1.000	(1.001, –0.001)	3 003	100
PFR_NS_105	–0.001 ± 0.000	[0.002, –0.001]	1.000	(0.993, –0.001)	3 153	100
PFR_CA_08	–0.001 ± 0.001	[–0.002, +0.002]	0.999	(1.036, –0.002)	2 337	100
PFR_CA_57	–0.001 ± 0.001	[–0.002, +0.001]	0.999	(1.020, –0.001)	3 035	100
PFR_CA_58	+0.002 ± 0.001	[–0.001, +0.003]	0.999	(0.949, 0.004)	1 694	100
PFR_CA_35	+0.002 ± 0.000	[+0.002, +0.003]	1.000	(1.007, 0.002)	1 592	100
PFR_AT_N08	+0.002 ± 0.000	[+0.002, +0.003]	1.000	(1.005, 0.002)	453	100
PFR_DE_N57	–0.005 ± 0.001	[–0.007, –0.003]	0.999	(1.026, –0.006)	1 873	99
PFR_KO_N58	–0.001 ± 0.001	[–0.002, +0.000]	0.999	(1.005, –0.001)	2 823	100
PFR_SE_N35	+0.004 ± 0.002	[+0.000, +0.005]	0.998	(1.012, 0.003)	917	100
CIM_UL_1270	+0.000 ± 0.001	[–0.001, +0.002]	0.999	(1.033, –0.001)	413	100
CIM_IZ_1091	–0.002 ± 0.001	[–0.003, +0.001]	0.997	(1.013, –0.002)	2 333	100
CIM_CH_1	–0.004 ± 0.002	[–0.008, –0.001]	0.985	(0.968, –0.003)	1 507	100
CIM_UV_1219	–0.005 ± 0.002	[–0.008, –0.002]	0.994	(1.013, –0.006)	2 244	100
POM_DE_1	–0.010 ± 0.002	[–0.013, –0.004]	0.994	(0.981, –0.009)	1 202	46
POM_IT_1	–0.008 ± 0.003	[–0.011, –0.002]	0.993	(0.949, –0.005)	1 403	78
CW193_CN	+0.002 ± 0.003	[–0.006, +0.006]	0.991	(0.888, 0.011)	191	100
QASUME	+0.005 ± 0.003	[+0.001, +0.010]	0.937	(1.017, 0.005)	117	96
PSR_DE_4	–0.011 ± 0.003	[–0.015, –0.006]	0.991	(1.049, –0.013)	2 325	36
PSR_DE_6	–0.009 ± 0.012	[–0.038, –0.003]	0.994	(1.009, –0.009)	766	62
PSR_CH_8	+0.011 ± 0.006	[+0.005, +0.026]	0.990	(1.263, –0.000)	2 058	31
PSR_CH_9	–0.002 ± 0.003	[–0.004, +0.004]	0.983	(0.968, 0.001)	2 717	100
PSR_CH_0	+0.003 ± 0.003	[–0.004, +0.005]	0.995	(1.022, 0.002)	3 109	100

Wavelength: 500 ± 3 nm

Instrument	Median ± 1σ	Percentiles [5, 95]	Correlation coefficient	Linear fit (slope, intercept)	Number of data points	% within WMO limits
PFR_N22	+0.001 ± 0.000	[–0.000, +0.001]	1.000	(1.001, 0.000)	3 202	100
PFR_N25	–0.001 ± 0.000	[–0.002, –0.001]	1.000	(0.998, –0.001)	3 186	100
PFR_N27	+0.000 ± 0.000	[+0.000, +0.001]	1.000	(1.002, 0.000)	3 187	100
PFR_ML_07	–0.000 ± 0.000	[–0.001, +0.001]	1.000	(1.020, –0.001)	3 088	100
PFR_CH_24	–0.001 ± 0.000	[–0.001, +0.000]	1.000	(1.016, –0.001)	3 112	100
PFR_CH_21	+0.000 ± 0.001	[–0.001, +0.001]	0.999	(0.988, 0.000)	2 887	100
PFR_CH_01	–0.002 ± 0.000	[–0.003, –0.002]	1.000	(1.005, –0.003)	3 184	100
PFR_IR_01	–0.000 ± 0.001	[–0.001, +0.000]	0.999	(1.010, –0.001)	3 175	100
PFR_NS_101	–0.002 ± 0.001	[–0.004, –0.001]	0.998	(0.965, –0.001)	3 042	100
PFR_NS_105	–0.001 ± 0.001	[–0.002, –0.000]	0.999	(1.006, –0.001)	3 173	100
PFR_CA_08	–0.001 ± 0.001	[–0.002, +0.000]	0.999	(1.006, –0.001)	2 317	100
PFR_CA_57	–0.002 ± 0.001	[–0.003, –0.000]	0.999	(1.039, –0.003)	3 058	100
PFR_CA_58	–0.001 ± 0.001	[–0.002, –0.001]	1.000	(0.980, –0.001)	1 696	100
PFR_CA_35	–0.001 ± 0.001	[–0.002, +0.001]	0.999	(1.050, –0.003)	1 598	100
PFR_AT_N08	+0.000 ± 0.001	[–0.001, +0.001]	0.999	(1.016, –0.000)	454	100
PFR_DE_N57	–0.004 ± 0.001	[–0.005, –0.003]	0.999	(1.020, –0.005)	1 869	100
PFR_KO_N58	–0.001 ± 0.001	[–0.002, –0.000]	0.999	(1.002, –0.001)	2 856	100
PFR_SE_N35	+0.003 ± 0.002	[–0.001, +0.005]	0.995	(1.040, 0.001)	915	100
CIM_UL_1270	–0.001 ± 0.001	[–0.002, –0.000]	0.999	(1.014, –0.002)	415	100
CIM_IZ_1091	–0.005 ± 0.001	[–0.006, –0.003]	0.997	(0.984, –0.004)	2 327	100
CIM_CH_1	–0.006 ± 0.001	[–0.007, –0.004]	0.997	(0.975, –0.005)	1 505	100
CIM_UV_1219	–0.006 ± 0.002	[–0.007, –0.003]	0.998	(0.991, –0.005)	2 244	100
SPO_AU_2	–0.006 ± 0.002	[–0.009, –0.002]	0.990	(1.087, –0.010)	994	99
POM_DE_1	–0.010 ± 0.002	[–0.011, –0.006]	0.995	(1.004, –0.009)	1 200	53
POM_IT_1	–0.008 ± 0.001	[–0.010, –0.005]	0.996	(0.963, –0.006)	1 402	90
CW193_CN	–0.001 ± 0.005	[–0.008, +0.007]	0.932	(0.832, 0.010)	192	100
QASUME	–0.001 ± 0.002	[–0.003, +0.006]	0.977	(0.920, 0.002)	105	100
PSR_DE_4	–0.009 ± 0.002	[–0.010, –0.005]	0.993	(0.996, –0.008)	2 305	99
PSR_DE_6	–0.012 ± 0.003	[–0.015, –0.006]	0.987	(0.988, –0.011)	634	21
PSR_CH_8	–0.003 ± 0.003	[–0.004, +0.006]	0.996	(1.202, –0.009)	2 058	100
PSR_CH_9	–0.003 ± 0.001	[–0.004, –0.002]	0.998	(0.999, –0.003)	2 706	100
PSR_CH_0	–0.000 ± 0.001	[–0.002, +0.002]	0.997	(1.006, –0.000)	3 108	100

Wavelength: 675 nm

Instrument	Median ± 1σ	Percentiles [5, 95]	Correlation coefficient	Linear fit (slope, intercept)	Number of data points	% within WMO limits
PFR_N22	+0.000 ± 0.000	[+0.000 , +0.001]	1.000	(1.006, 0.000)	3 234	100
PFR_N25	–0.001 ± 0.000	[–0.002 , –0.001]	0.999	(0.983, –0.001)	3 218	100
PFR_N27	+0.001 ± 0.000	[+0.000, +0.001]	1.000	(1.010, 0.000)	3 202	100
PFR_ML_07	–0.000 ± 0.000	[–0.001, +0.000]	0.999	(1.027, –0.001)	3 175	100
PFR_CH_24	–0.001 ± 0.000	[–0.001, –0.000]	0.999	(1.002, –0.001)	3 132	100
PFR_CH_21	–0.000 ± 0.000	[–0.001, +0.001]	0.998	(0.976, 0.000)	2 951	100
PFR_CH_01	–0.001 ± 0.000	[–0.002, –0.001]	1.000	(1.005, –0.002)	3 182	100
PFR_IR_01	–0.003 ± 0.000	[–0.003, –0.002]	0.999	(1.001, –0.003)	3 217	100
CIM_UL_1270	–0.002 ± 0.001	[–0.002, –0.001]	0.998	(0.971, –0.001)	414	100
CIM_IZ_1091	–0.003 ± 0.001	[–0.005, –0.002]	0.996	(0.936, –0.002)	2 333	100
CIM_CH_1	–0.004 ± 0.001	[–0.006, –0.002]	0.991	(0.912, –0.002)	1 505	100
CIM_UV_1219	–0.004 ± 0.002	[–0.007, –0.003]	0.997	(0.930, –0.003)	2 244	100
POM_DE_1	–0.006 ± 0.001	[–0.007, –0.004]	0.996	(0.982, –0.005)	1 199	99
POM_IT_1	–0.004 ± 0.001	[–0.006, –0.003]	0.996	(0.916, –0.003)	1 396	100
CW193_CN	–0.001 ± 0.003	[–0.005, +0.003]	0.942	(0.839, 0.005)	192	100
IR-QASUME	–0.005 ± 0.004	[–0.008, +0.001]	0.879	(0.917, –0.002)	206	100
PSR_DE_4	–0.006 ± 0.003	[–0.015, –0.003]	0.988	(0.967, –0.005)	2 673	88
PSR_DE_6	–0.014 ± 0.004	[–0.015, –0.004]	0.994	(1.285, –0.019)	1 605	40
PSR_CH_8	+0.001 ± 0.002	[–0.001, +0.006]	0.994	(1.176, –0.003)	2 057	100
PSR_CH_9	–0.002 ± 0.001	[–0.003, +0.001]	0.988	(0.946, –0.000)	2 712	100
PSR_CH_0	–0.003 ± 0.001	[–0.005, –0.000]	0.995	(0.950, –0.002)	3 108	100

Wavelength: 862 / 870 nm

Instrument	Median ± 1σ	Percentiles [5, 95]	Correlation coefficient	Linear fit (slope, intercept)	Number of data points	% within WMO limits
PFR_N22	+0.000 ± 0.000	[–0.000, +0.001]	0.998	(1.012, 0.000)	3 092	100
PFR_N25	–0.001 ± 0.000	[–0.002, –0.000]	0.995	(0.981, –0.001)	3 220	100
PFR_N27	+0.000 ± 0.000	[+0.000, +0.001]	0.998	(1.012, 0.000)	3 191	100
PFR_ML_07	–0.001 ± 0.000	[–0.001, +0.000]	0.997	(1.039, –0.001)	3 156	100
PFR_CH_24	–0.001 ± 0.000	[–0.001, –0.000]	0.998	(1.009, –0.001)	3 130	100
PFR_CH_21	–0.000 ± 0.000	[–0.001, +0.000]	0.996	(0.982, –0.000)	2 903	100
PFR_CH_01	–0.000 ± 0.000	[–0.001, +0.000]	0.999	(1.014, –0.000)	3 063	100
PFR_IR_01	–0.003 ± 0.001	[–0.004, –0.002]	0.989	(0.992, –0.003)	3 221	100
PFR_NS_101	+0.001 ± 0.001	[–0.001, +0.002]	0.982	(0.866, 0.002)	3 040	100
PFR_NS_105	–0.000 ± 0.000	[–0.001, +0.000]	0.998	(1.002, –0.000)	3 071	100
PFR_CA_08	+0.000 ± 0.000	[–0.001, +0.001]	0.997	(0.957, 0.001)	2 309	100
PFR_CA_57	–0.001 ± 0.001	[–0.001, +0.001]	0.997	(1.092, –0.002)	3 061	100
PFR_CA_58	+0.000 ± 0.001	[–0.001, +0.001]	0.998	(0.907, 0.001)	1 689	100
PFR_CA_35	+0.000 ± 0.000	[–0.001, +0.001]	0.998	(0.967, 0.001)	1 577	100
PFR_AT_N08	–0.000 ± 0.000	[–0.001, +0.000]	0.999	(1.042, –0.001)	445	100
PFR_DE_N57	–0.000 ± 0.000	[–0.001, +0.000]	0.997	(1.018, –0.001)	1 857	100
PFR_KO_N58	–0.001 ± 0.000	[–0.002, –0.001]	0.998	(1.008, –0.001)	2 846	100
PFR_SE_N35	–0.001 ± 0.000	[–0.002, –0.001]	0.998	(1.004, –0.001)	917	100
CIM_UL_1270	+0.000 ± 0.000	[–0.001, +0.001]	0.996	(1.009, –0.000)	411	100
CIM_IZ_1091	–0.001 ± 0.000	[–0.002, –0.000]	0.997	(0.965, –0.000)	2 336	100
CIM_CH_1	–0.002 ± 0.001	[–0.003, –0.000]	0.973	(0.931, –0.001)	1 507	100
CIM_UV_1219	–0.003 ± 0.001	[–0.004, –0.001]	0.998	(0.955, –0.002)	2 244	100
SPO_AU_2	+0.003 ± 0.004	[–0.003, +0.007]	0.975	(1.707, –0.010)	994	100
POM_DE_1	–0.007 ± 0.001	[–0.008, –0.005]	0.978	(0.964, –0.006)	1 201	100
POM_IT_1	–0.004 ± 0.002	[–0.007, –0.001]	0.935	(0.808, –0.001)	1 403	100

Instrument	Median ± 1σ	Percentiles [5, 95]	Correlation coefficient	Linear fit (slope, intercept)	Number of data points	% within WMO limits
CW193_CN	+0.002 ± 0.003	[–0.002, +0.008]	0.788	(0.779, 0.007)	192	100
IR-QASUME	–0.002 ± 0.004	[–0.005, +0.005]	0.735	(0.970, –0.000)	207	100
PSR_DE_4	–0.005 ± 0.002	[–0.009, –0.003]	0.924	(0.933, –0.004)	2 673	99
PSR_DE_6	–0.005 ± 0.002	[–0.007, –0.002]	0.984	(1.139, –0.007)	1 700	100
PSR_CH_8	+0.002 ± 0.002	[+0.001, +0.006]	0.990	(1.225, –0.000)	2 054	100
PSR_CH_9	+0.002 ± 0.002	[–0.001, +0.005]	0.949	(1.019, 0.002)	2 715	100
PSR_CH_0	+0.002 ± 0.002	[–0.000, +0.006]	0.910	(0.934, 0.003)	3 107	100

Wavelength: 1 020 nm

Instrument	Median ± 1σ	Percentiles [5, 95]	Correlation coefficient	Linear fit (slope, intercept)	Number of data points	% within WMO limits
PFR_N22	+0.000 ± 0.000	[–0.000, +0.001]	0.997	(1.013, 0.000)	3 194	100
PFR_N25	–0.001 ± 0.000	[–0.002, –0.000]	0.993	(0.976, –0.000)	3 220	100
PFR_N27	+0.000 ± 0.000	[+0.000, +0.001]	0.998	(1.016, 0.000)	3 203	100
PFR_ML_07	–0.001 ± 0.000	[–0.001, +0.000]	0.996	(1.043, –0.001)	3 182	100
PFR_CH_24	–0.001 ± 0.000	[–0.001, –0.000]	0.997	(1.003, –0.001)	3 132	100
PFR_CH_21	–0.000 ± 0.000	[–0.001, +0.000]	0.995	(0.977, –0.000)	2 953	100
PFR_CH_01	–0.000 ± 0.000	[–0.000, +0.000]	0.999	(1.016, –0.000)	3 180	100
PFR_IR_01	–0.003 ± 0.001	[0.003, –0.002]	0.984	(0.983, –0.002)	3 221	100
CIM_UL_1270	–0.001 ± 0.001	[–0.001, +0.001]	0.992	(1.045, –0.001)	412	100
CIM_IZ_1091	+0.000 ± 0.001	[–0.000, +0.001]	0.994	(0.997, 0.000)	2 327	100
CIM_CH_1	–0.000 ± 0.001	[–0.002, +0.001]	0.963	(0.977, –0.000)	1 505	100
CIM_UV_1219	–0.001 ± 0.002	[–0.002, +0.001]	0.997	(0.992, –0.001)	2 244	100
POM_IT_1	+0.002 ± 0.004	[–0.004, +0.007]	0.869	(1.433, –0.003)	1 404	100
CW193_CN	+0.001 ± 0.003	[–0.003, +0.006]	0.905	(1.316, –0.005)	192	100
IR-QASUME	+0.005 ± 0.003	[+0.002, +0.010]	0.889	(1.304, 0.002)	210	96
PSR_DE_4	–0.006 ± 0.002	[–0.012, –0.004]	0.890	(0.474, –0.001)	1 941	91
PSR_DE_6	+0.014 ± 0.005	[+0.005, +0.022]	0.785	(1.441, 0.009)	1 701	18
PSR_CH_8	+0.009 ± 0.003	[+0.005, +0.015]	0.936	(1.379, 0.005)	2 058	76
PSR_CH_9	+0.004 ± 0.003	[–0.001, +0.008]	0.854	(1.195, 0.002)	2 715	100
PSR_CH_0	–0.005 ± 0.002	[–0.008, –0.001]	0.990	(0.681, –0.002)	3 108	100

Appendix 4. Individual instrument performance

The following figures show the differences between individual instruments and the WORCC PFR reference triad for each of the comparison days (with different colours, as per the legend) and for each of their measuring wavelengths. Grey lines represent the WMO U95 criterion (see Formula 1 in the Introduction). The ± 2 nm or ± 10 nm prefix next to the wavelength indicates the range of the nominal wavelengths of the two instruments compared.

PFR_ML_07

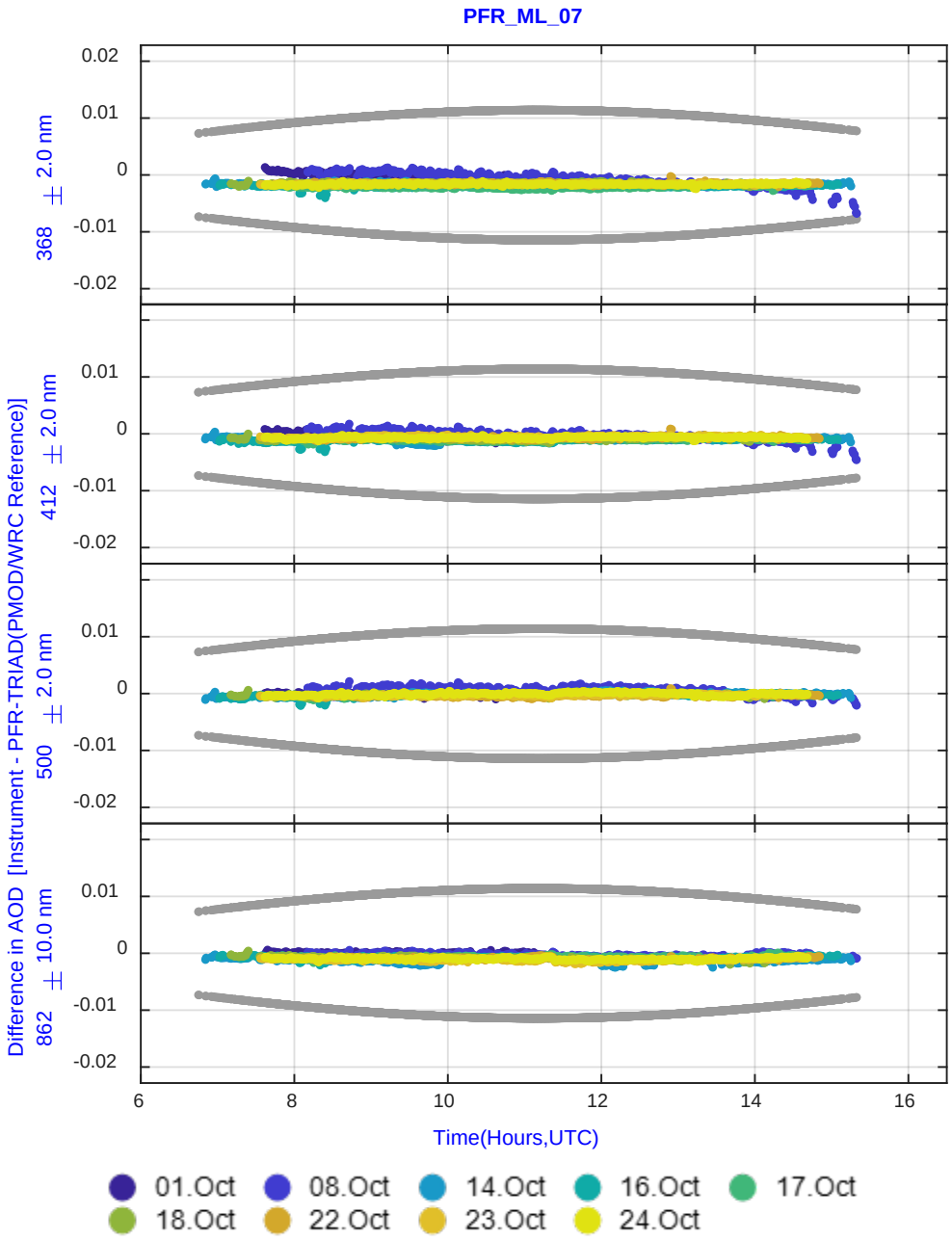

PFR_ML_07 – Extrapolated wavelengths using AE

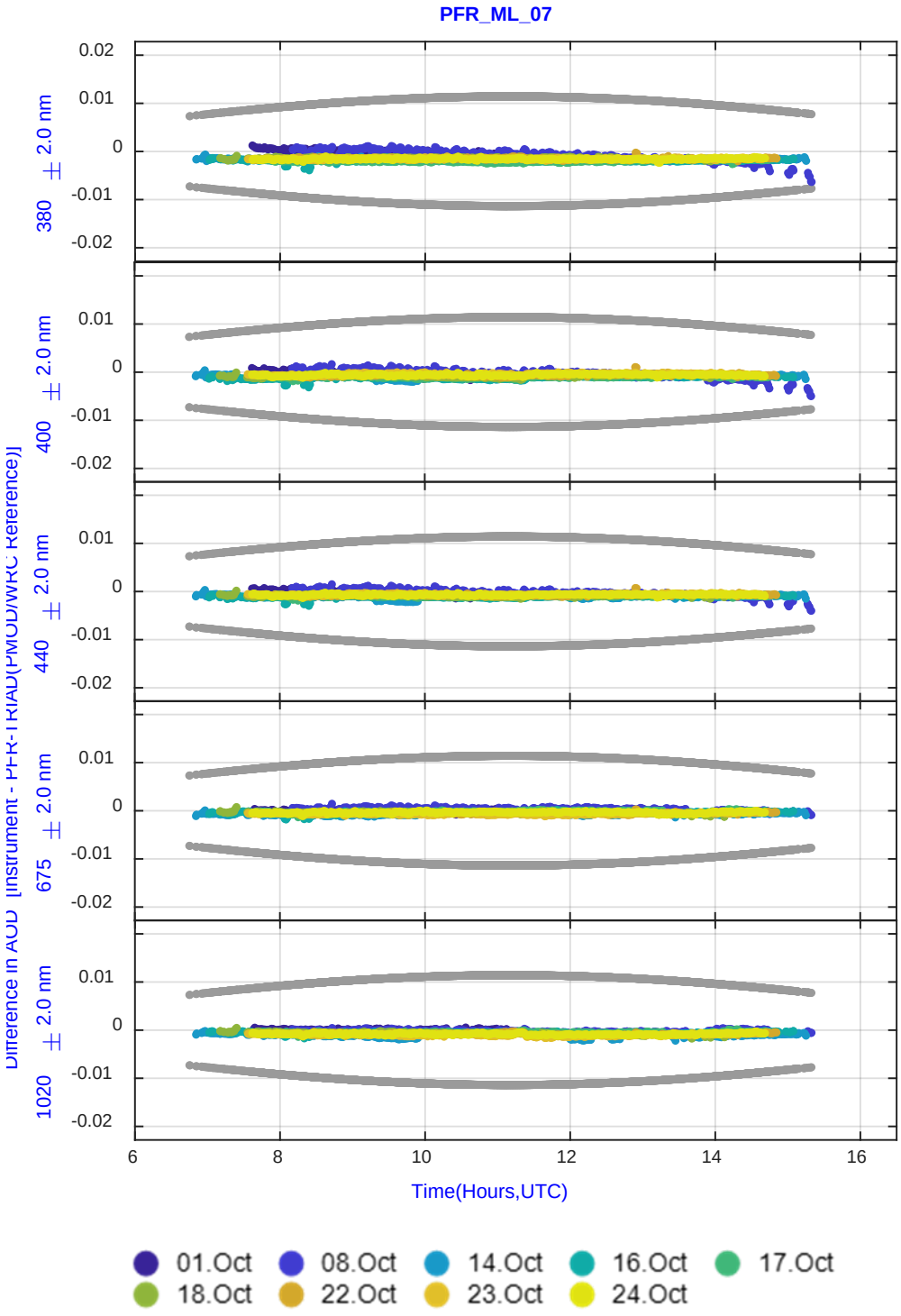

PFR_CH_24

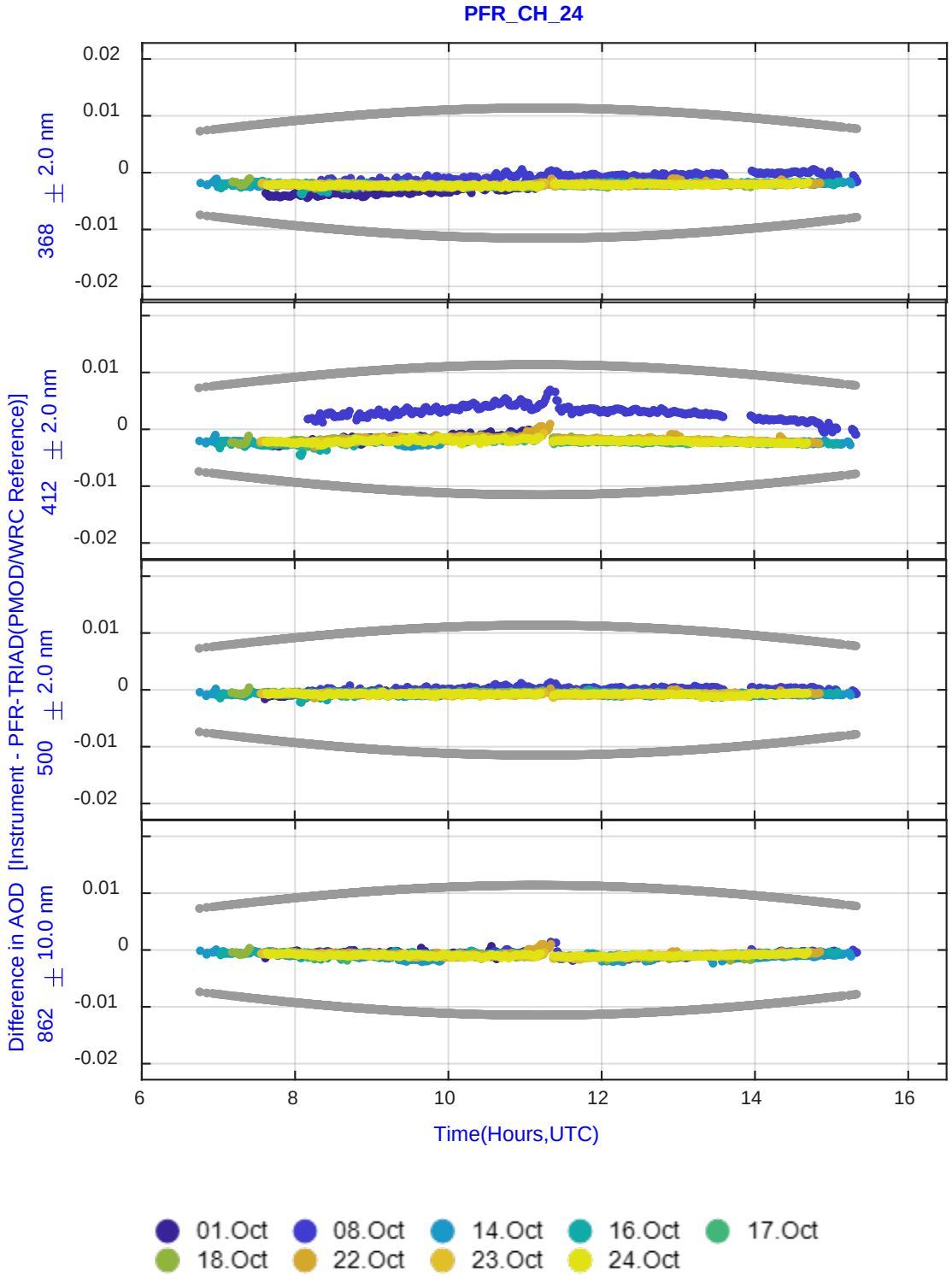
PFR_CH_24
Difference in AOD [Instrument - PFR-TRIAD(PMOD/WRC Reference)]
368 ± 2.0 nm
412 ± 2.0 nm
500 ± 2.0 nm
862 ± 10.0 nm
0.02
0.01
0
-0.01
-0.02
6
8
10
12
14
16
Time(Hours,UTC)
01.Oct
08.Oct
14.Oct
16.Oct
17.Oct
18.Oct
22.Oct
23.Oct
24.Oct

PFR_CH_24 – Extrapolated wavelengths using AE

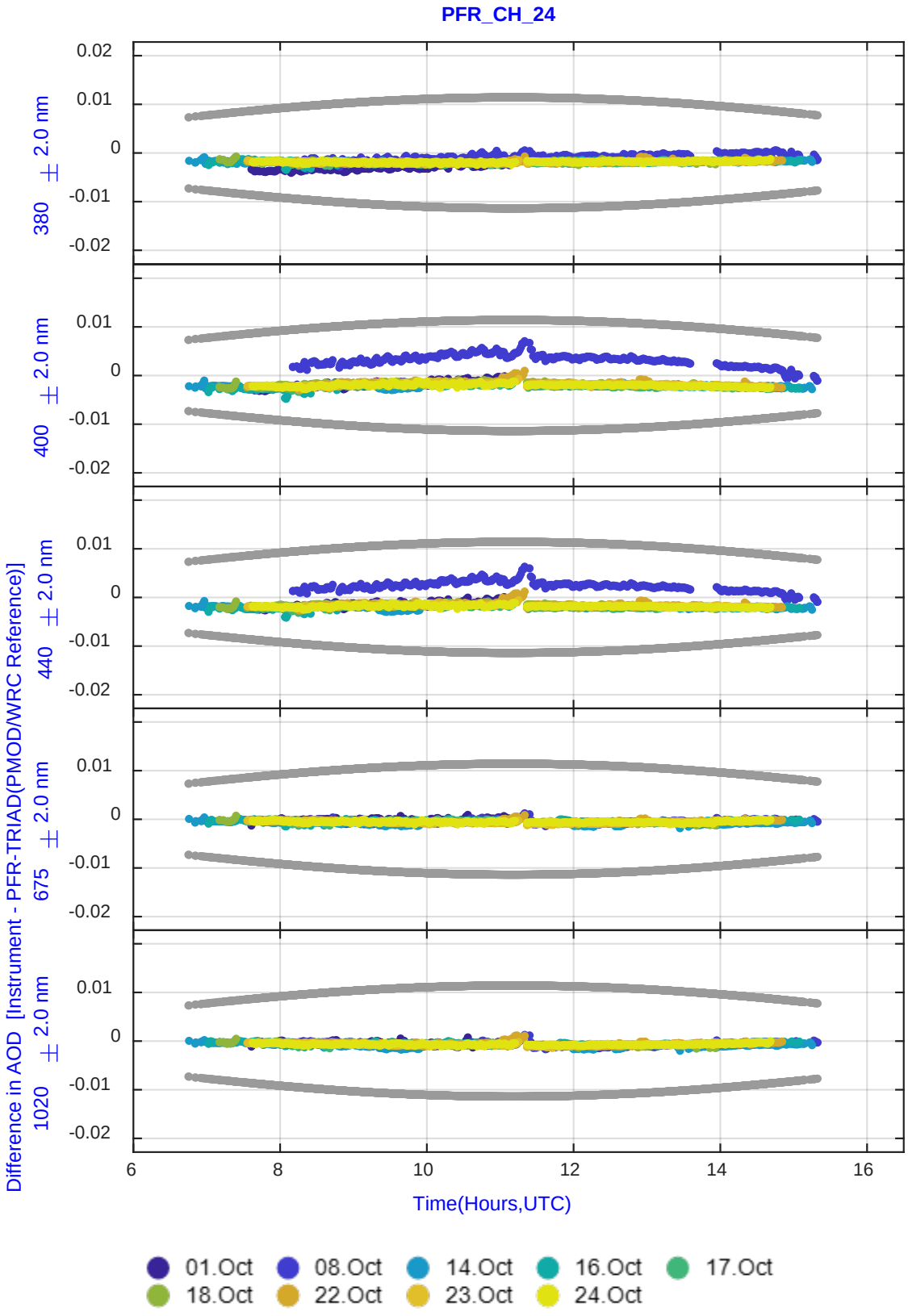

PFR_CH_21

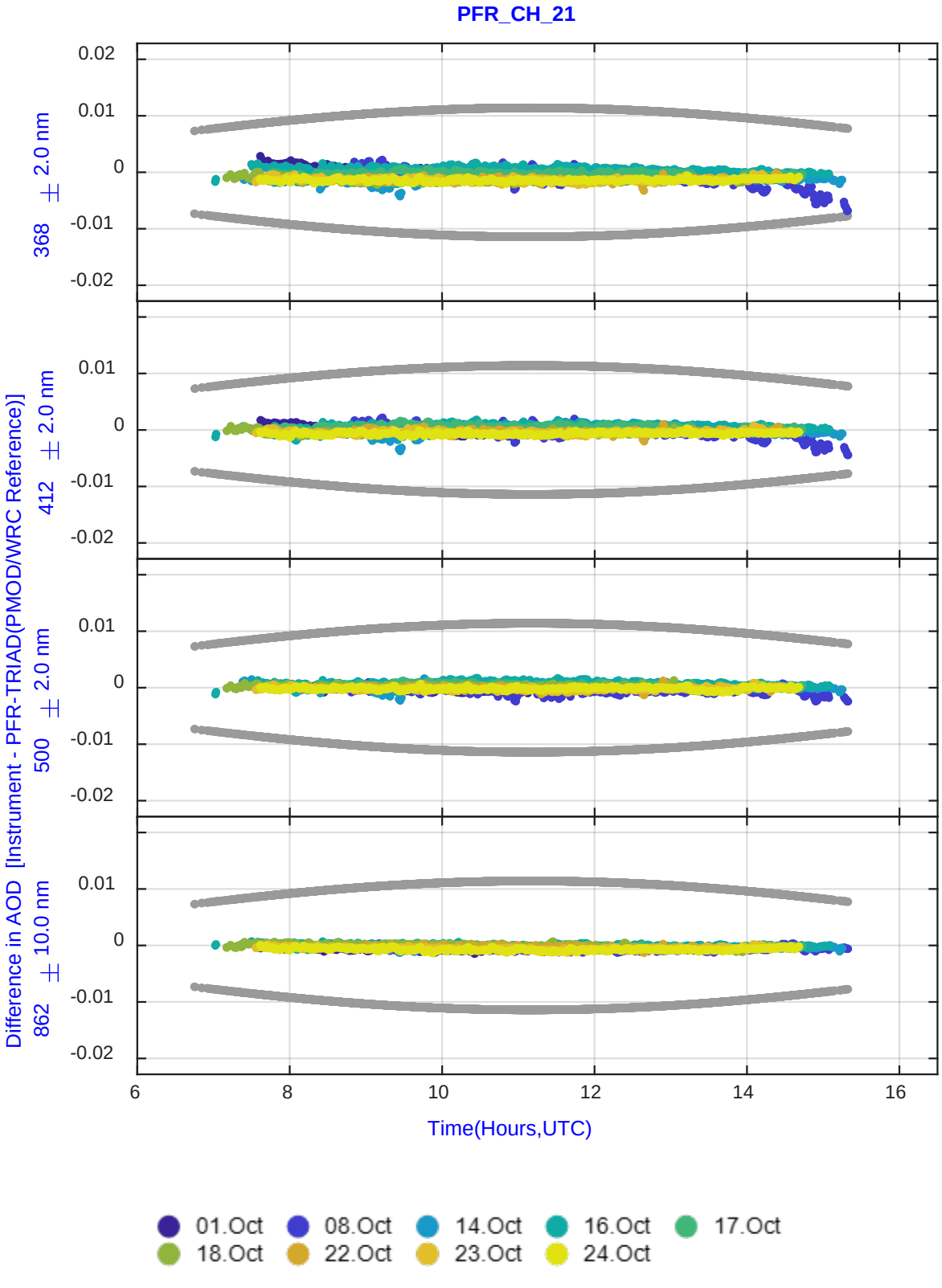
PFR_CH_21
Difference in AOD [Instrument - PFR-TRIAD(PMOD/WRC Reference)]
368 ± 2.0 nm
412 ± 2.0 nm
500 ± 2.0 nm
862 ± 10.0 nm
0.02
0.01
0
-0.01
-0.02
6
8
10
12
14
16
Time(Hours,UTC)
01.Oct
08.Oct
14.Oct
16.Oct
17.Oct
18.Oct
22.Oct
23.Oct
24.Oct

PFR_CH_21 – Extrapolated wavelengths using AE

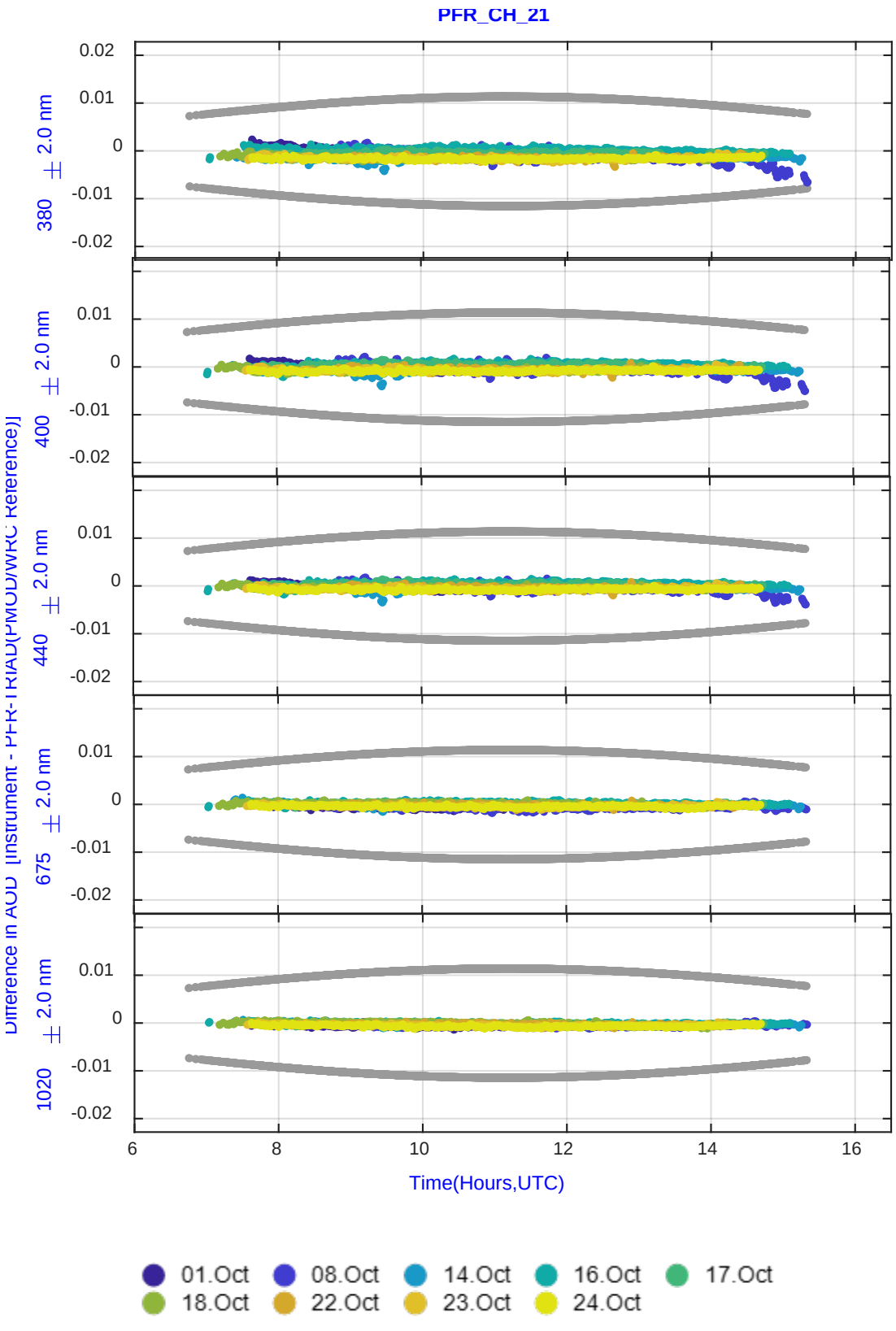

PFR_NS_101

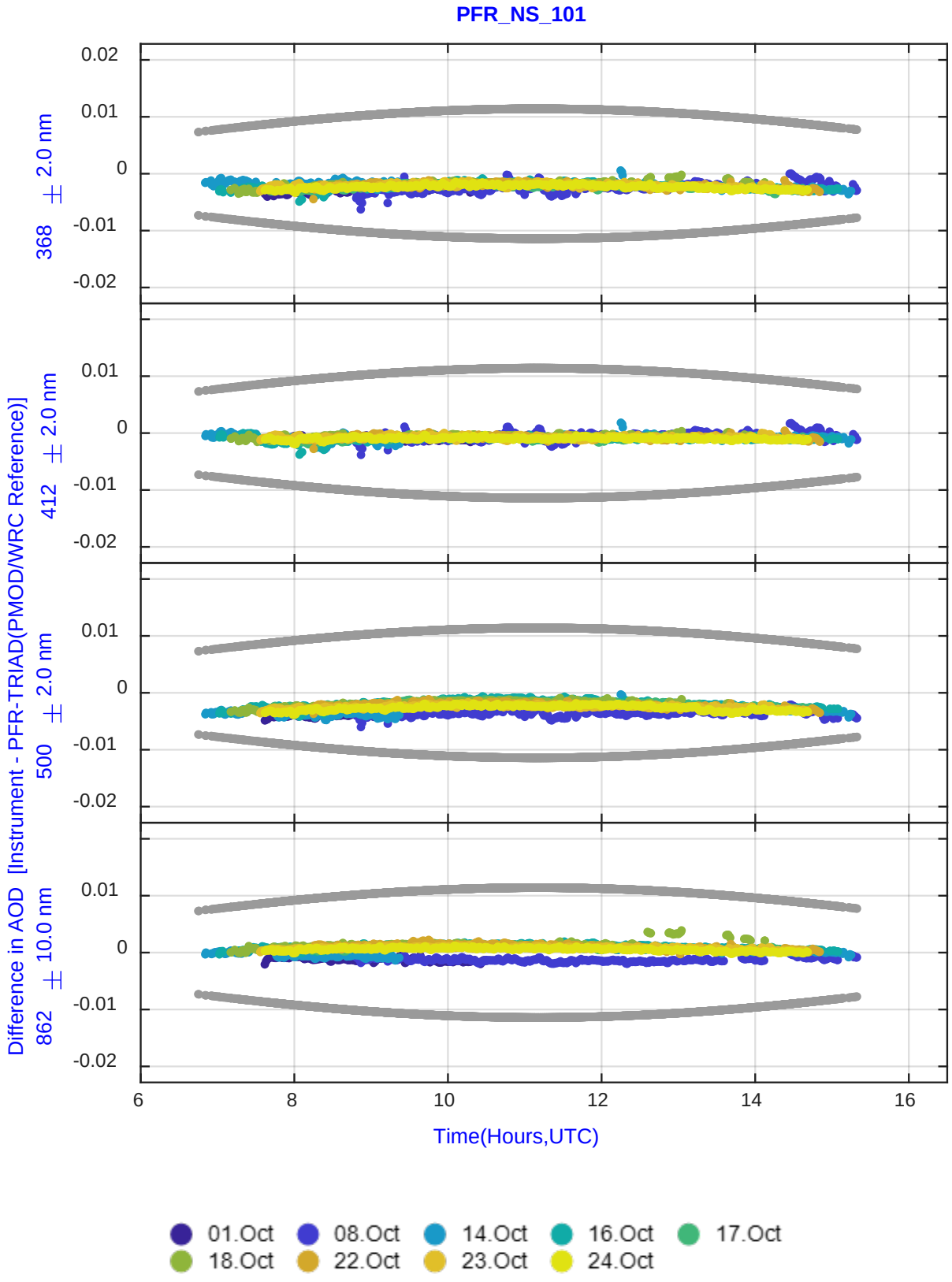
PFR_NS_101
Difference in AOD [Instrument - PFR-TRIAD(PMOD/WRC Reference)]
368 ± 2.0 nm
412 ± 2.0 nm
500 ± 2.0 nm
862 ± 10.0 nm
0.02
0.01
0
-0.01
-0.02
6
8
10
12
14
16
Time(Hours,UTC)
01.Oct
08.Oct
14.Oct
16.Oct
17.Oct
18.Oct
22.Oct
23.Oct
24.Oct

PFR_NS_105

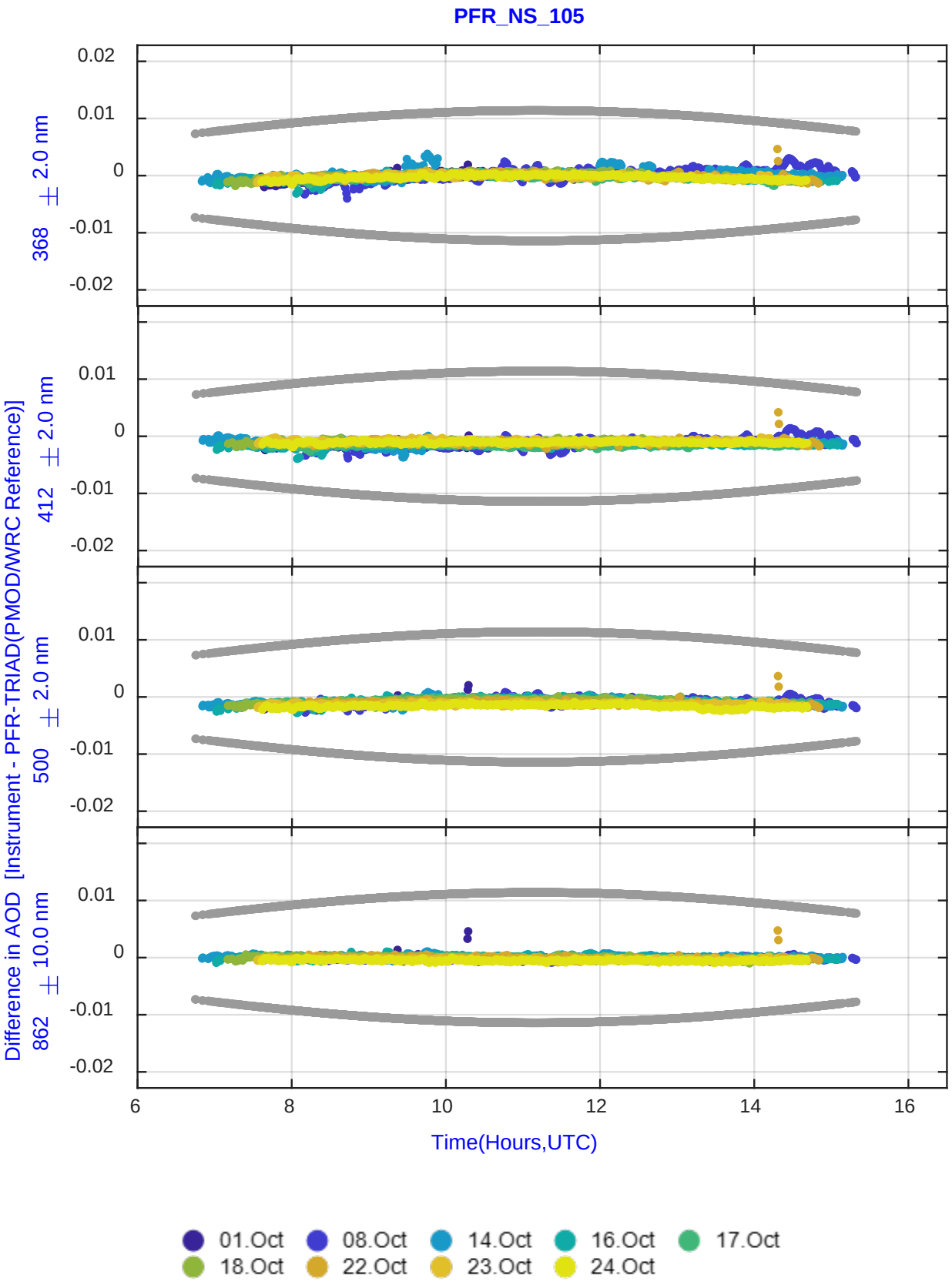
PFR_NS_105
Difference in AOD [Instrument - PFR-TRIAD(PMOD/WRC Reference)]
368 ± 2.0 nm
412 ± 2.0 nm
500 ± 2.0 nm
862 ± 10.0 nm
0.02
0.01
0
-0.01
-0.02
6
8
10
12
14
16
Time(Hours,UTC)
01.Oct
08.Oct
14.Oct
16.Oct
17.Oct
18.Oct
22.Oct
23.Oct
24.Oct

PFR_SE_35 – Initial calibration

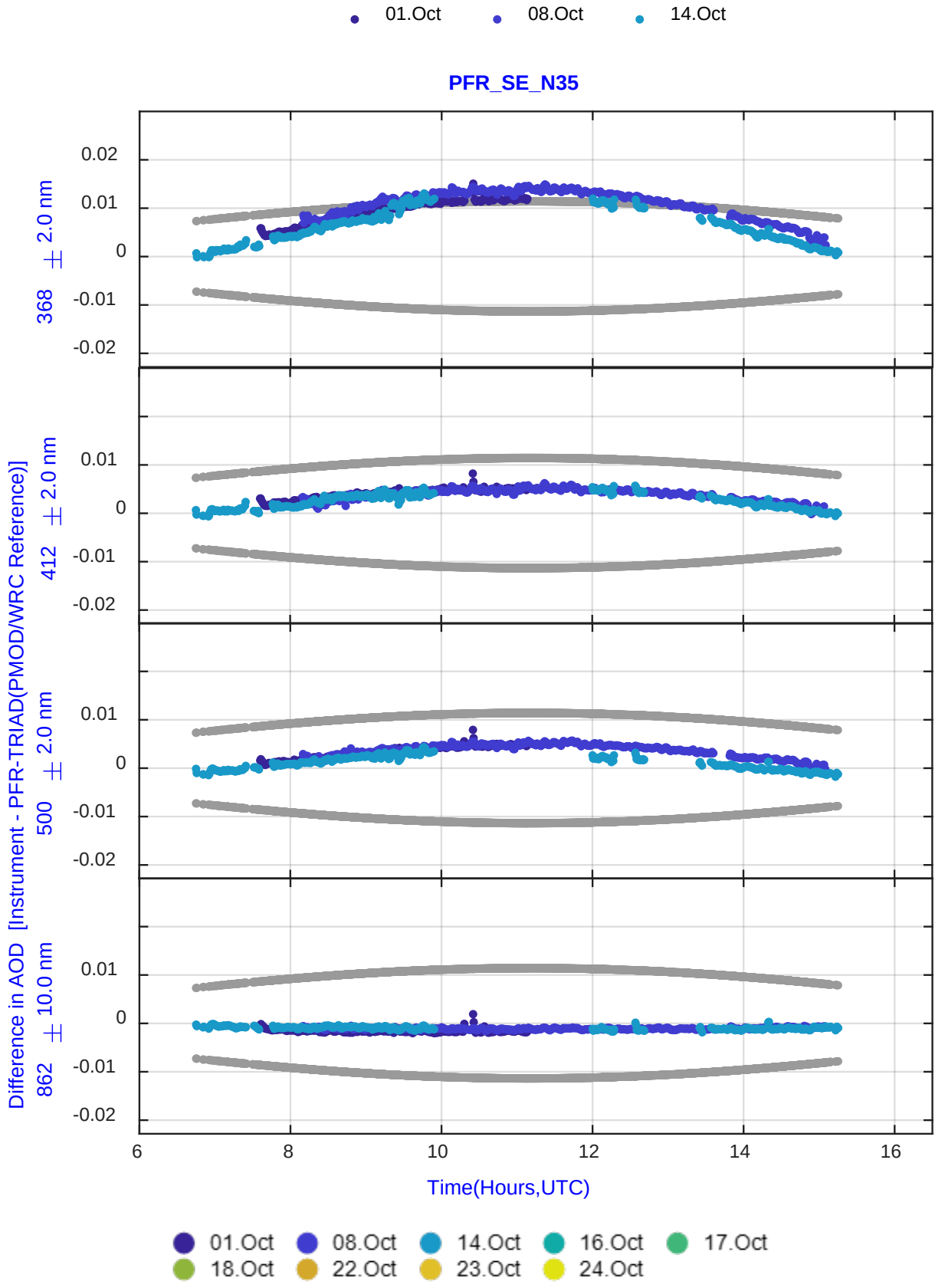

PFR_CA_35 – Calibration at WORCC, 2021

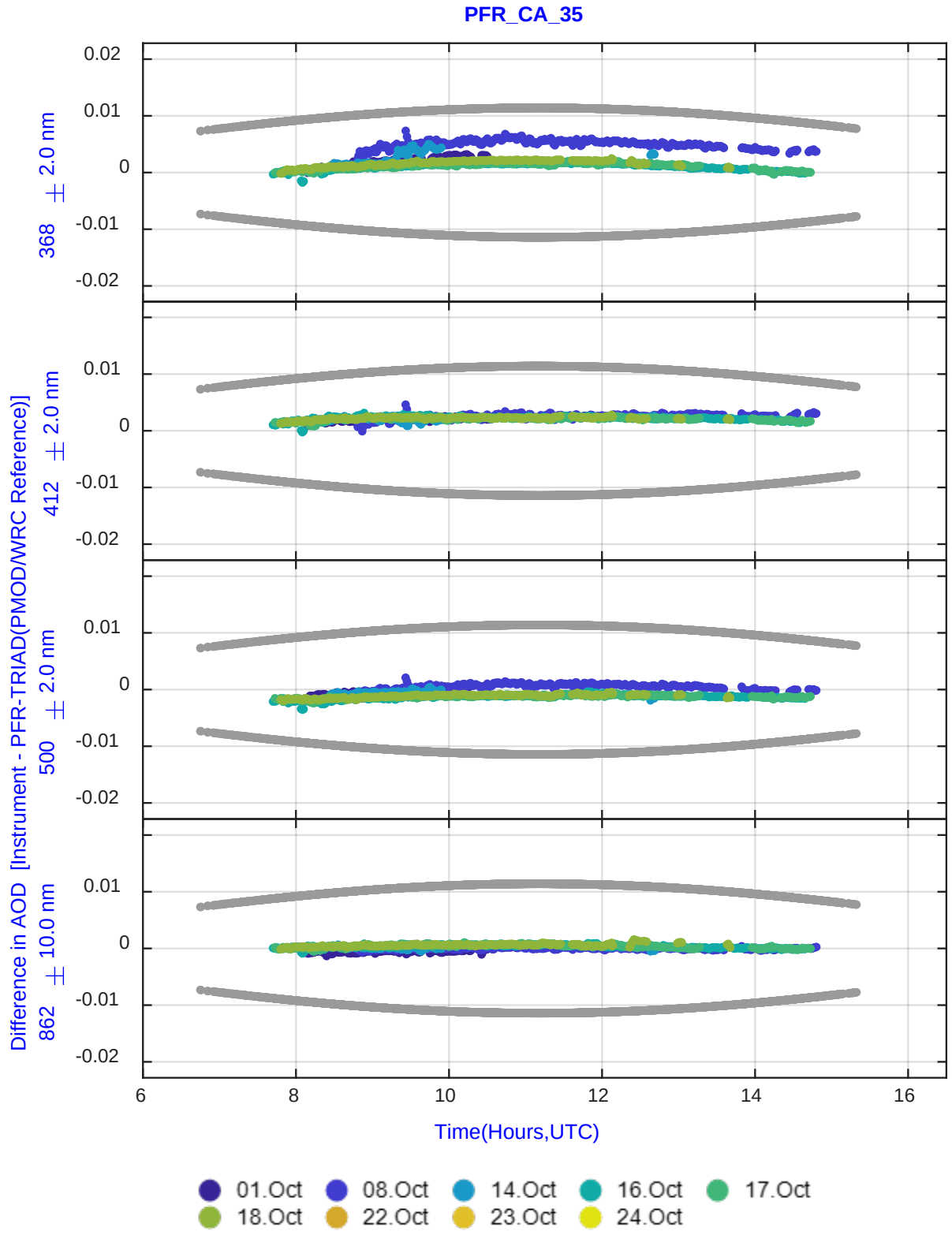

PFR_DE_N57 – Initial calibration

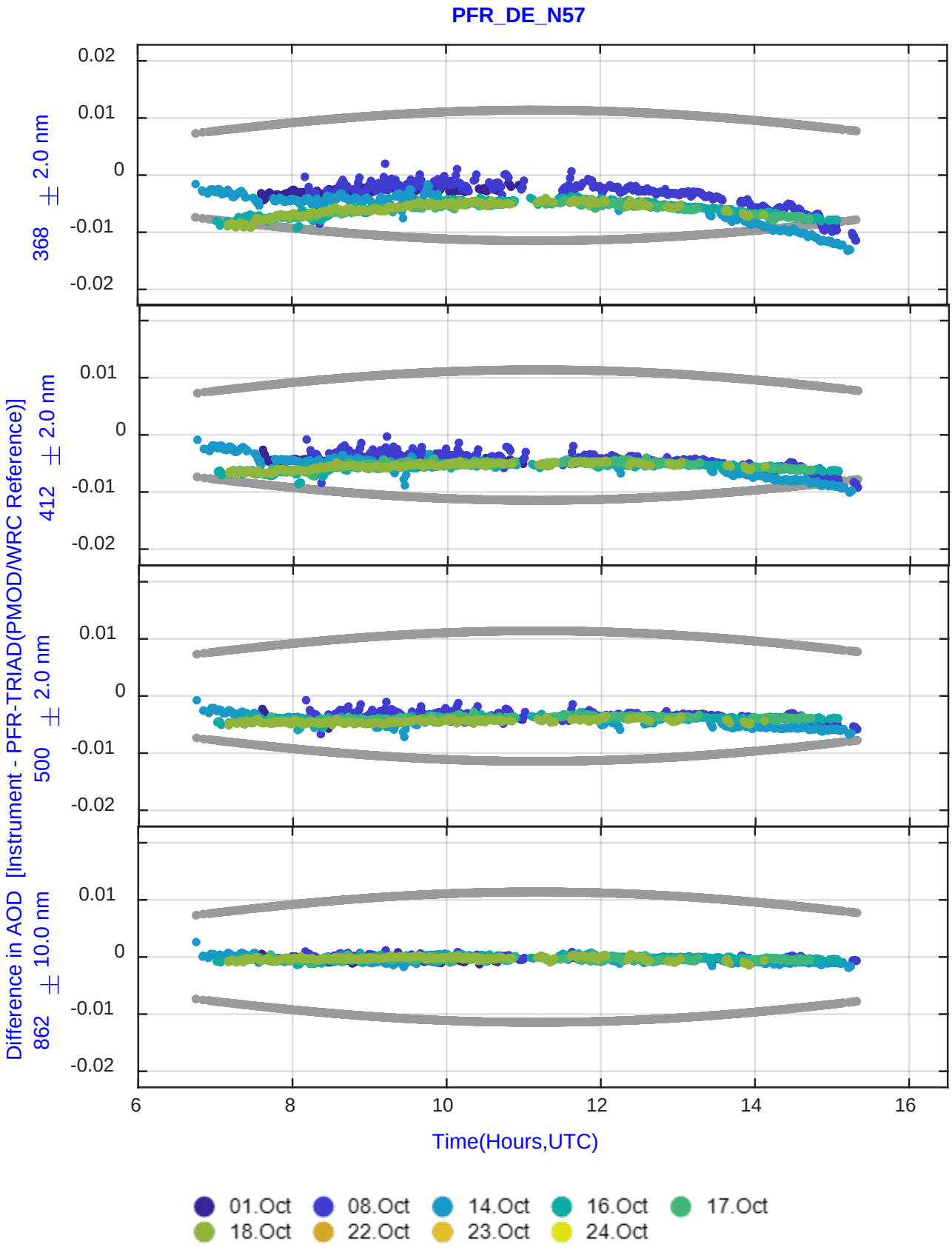

PFR_CA_57 – Data processed by PMOD / WRC WORCC, 2021 calibration

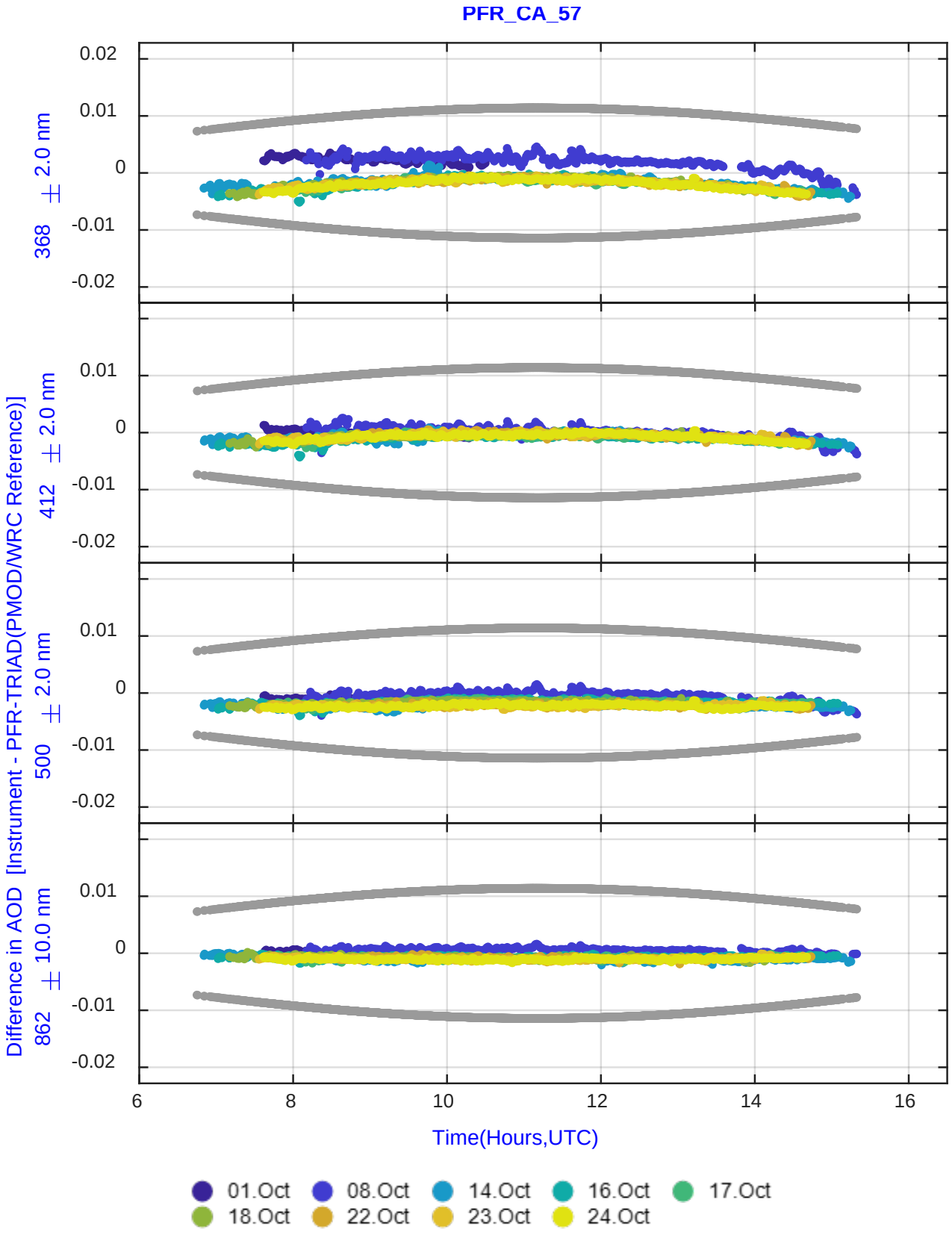

PFR_KO_N58 – Data submission from owners

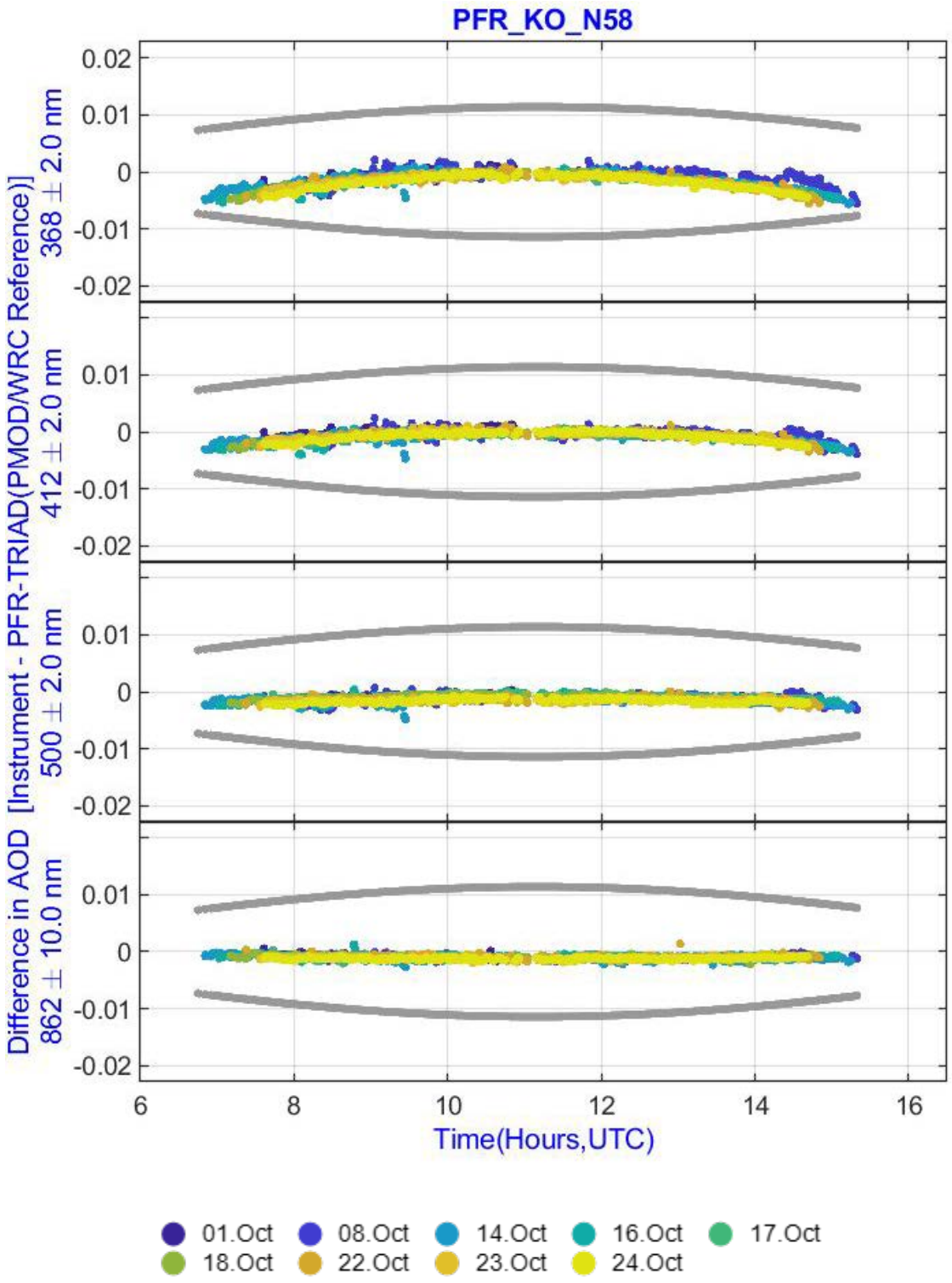

PFR_CA_58 – Data processed by PMOD / WRC, WORCC, 2021 calibration

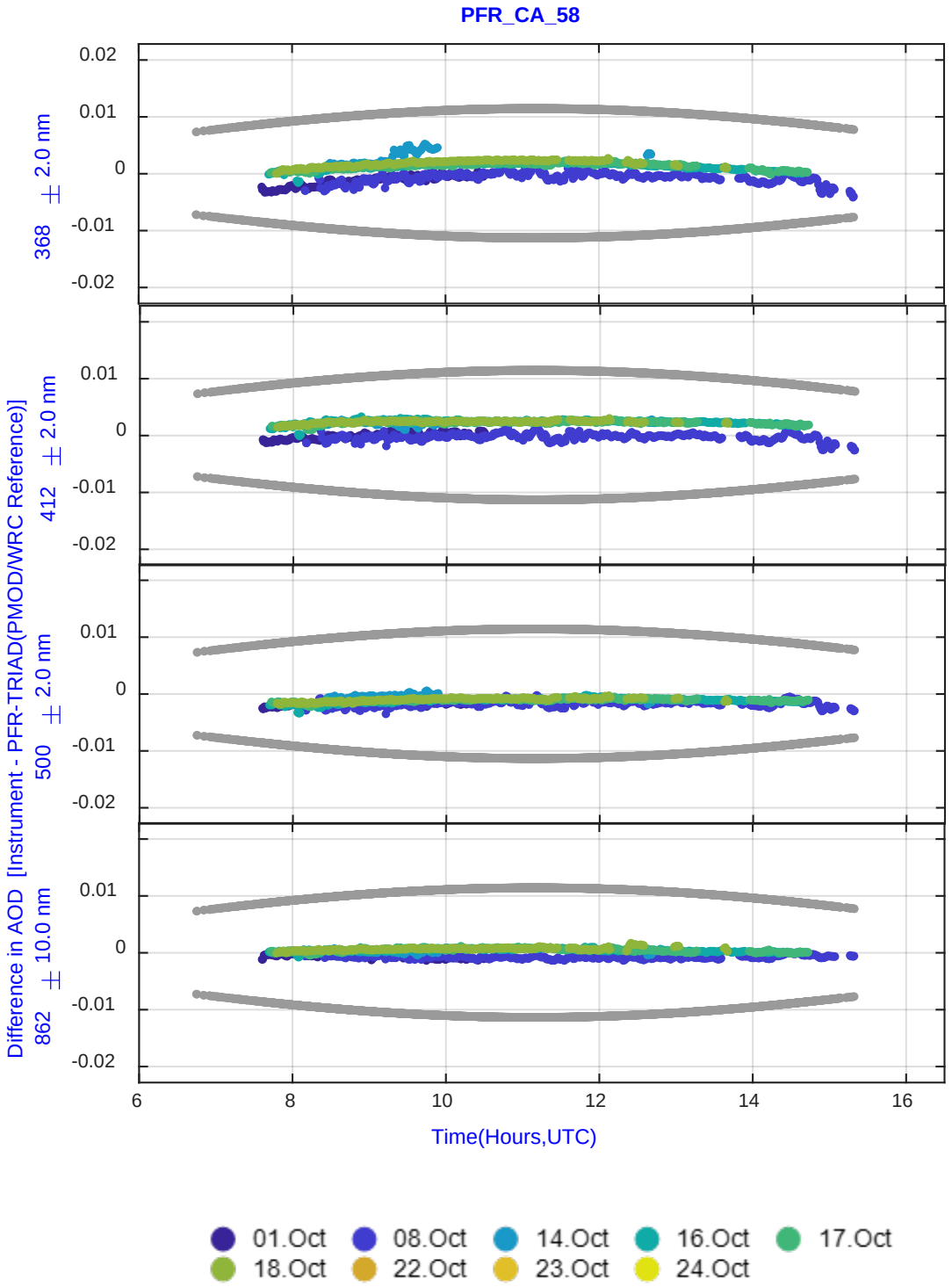

PFR_AT_N08 – Initial calibration

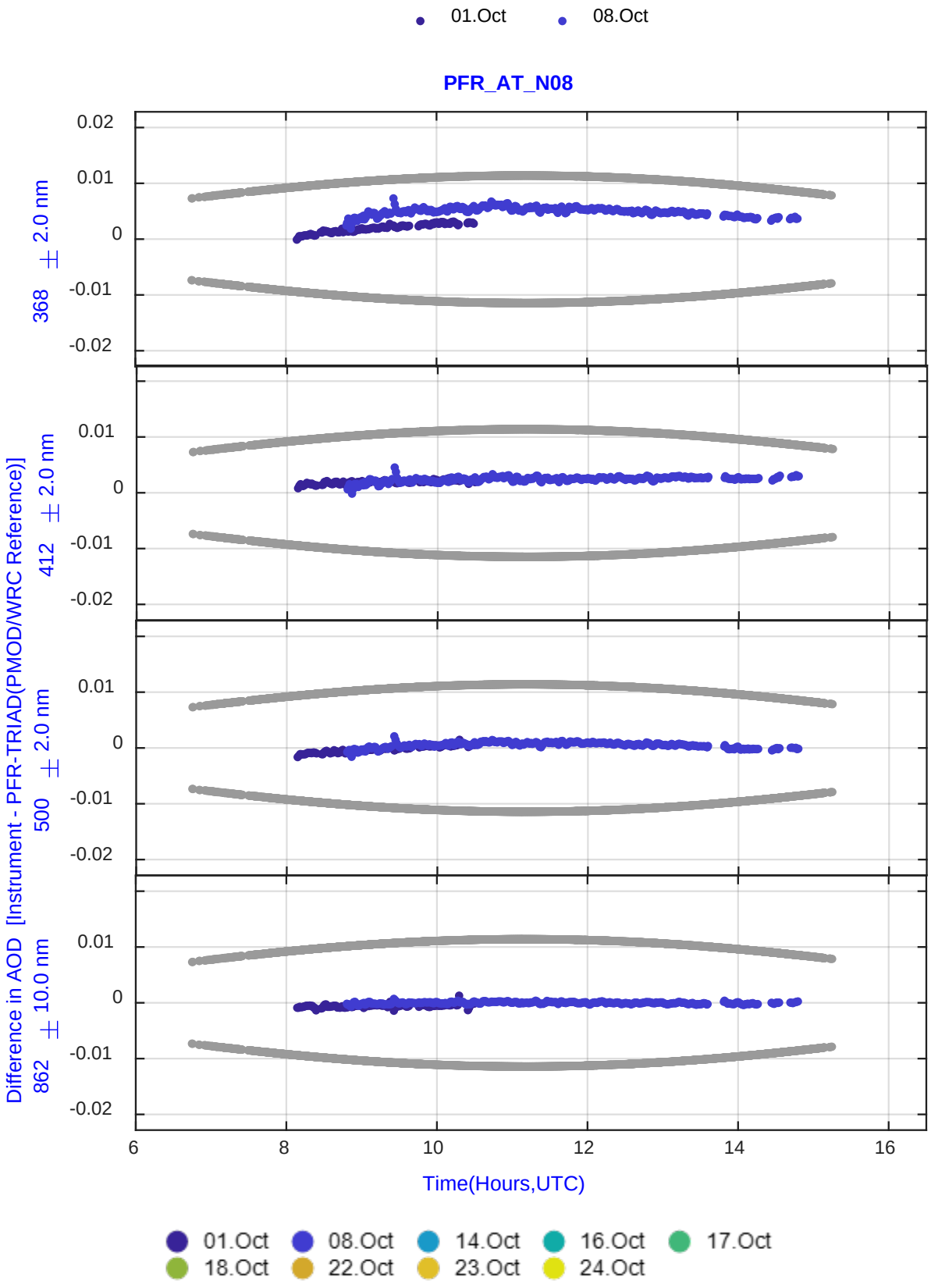

PFR_CA_08 – Data processed by PMOD / WRC, WORCC, 2021 calibration

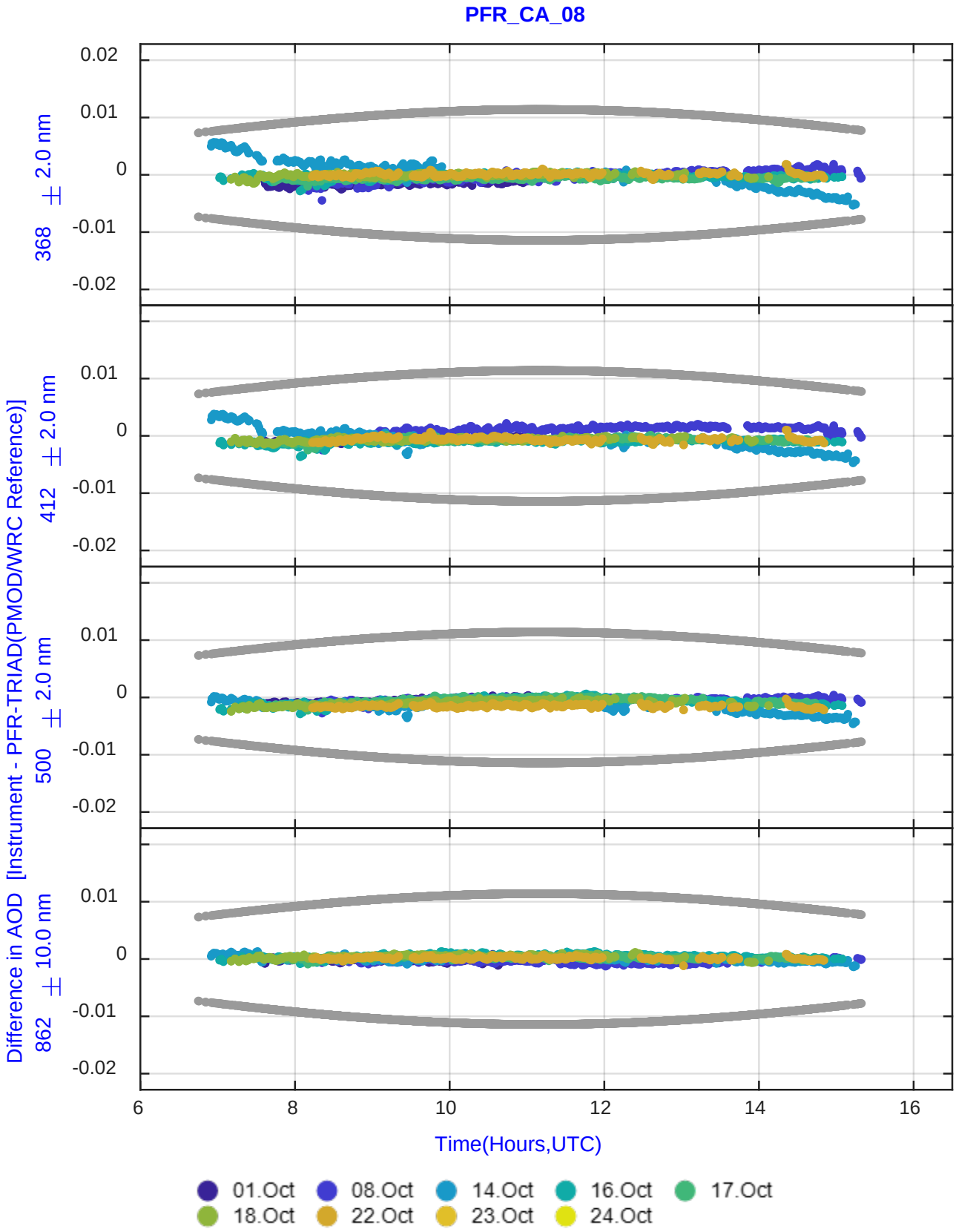

CIM_IZ_1091

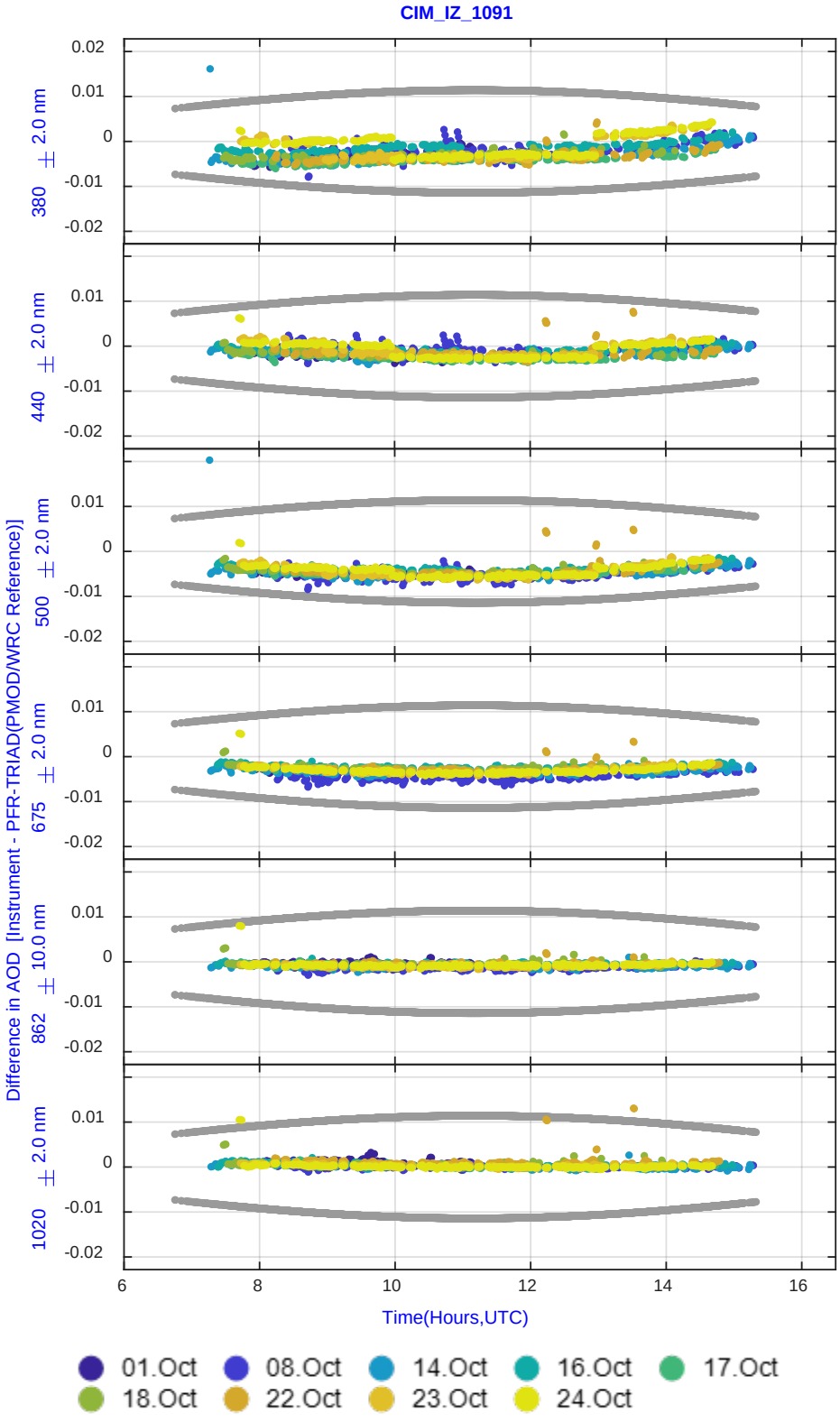
CIM_IZ_1091
Difference in AOD [Instrument - PFR-TRIAD(PMOD/WRC Reference)]
380 ± 2.0 nm
440 ± 2.0 nm
500 ± 2.0 nm
675 ± 2.0 nm
862 ± 10.0 nm
1020 ± 2.0 nm
0.02
0.01
0
-0.01
-0.02
6
8
10
12
14
16
Time(Hours,UTC)
01.Oct
08.Oct
14.Oct
16.Oct
17.Oct
18.Oct
22.Oct
23.Oct
24.Oct

CIM_CH_1

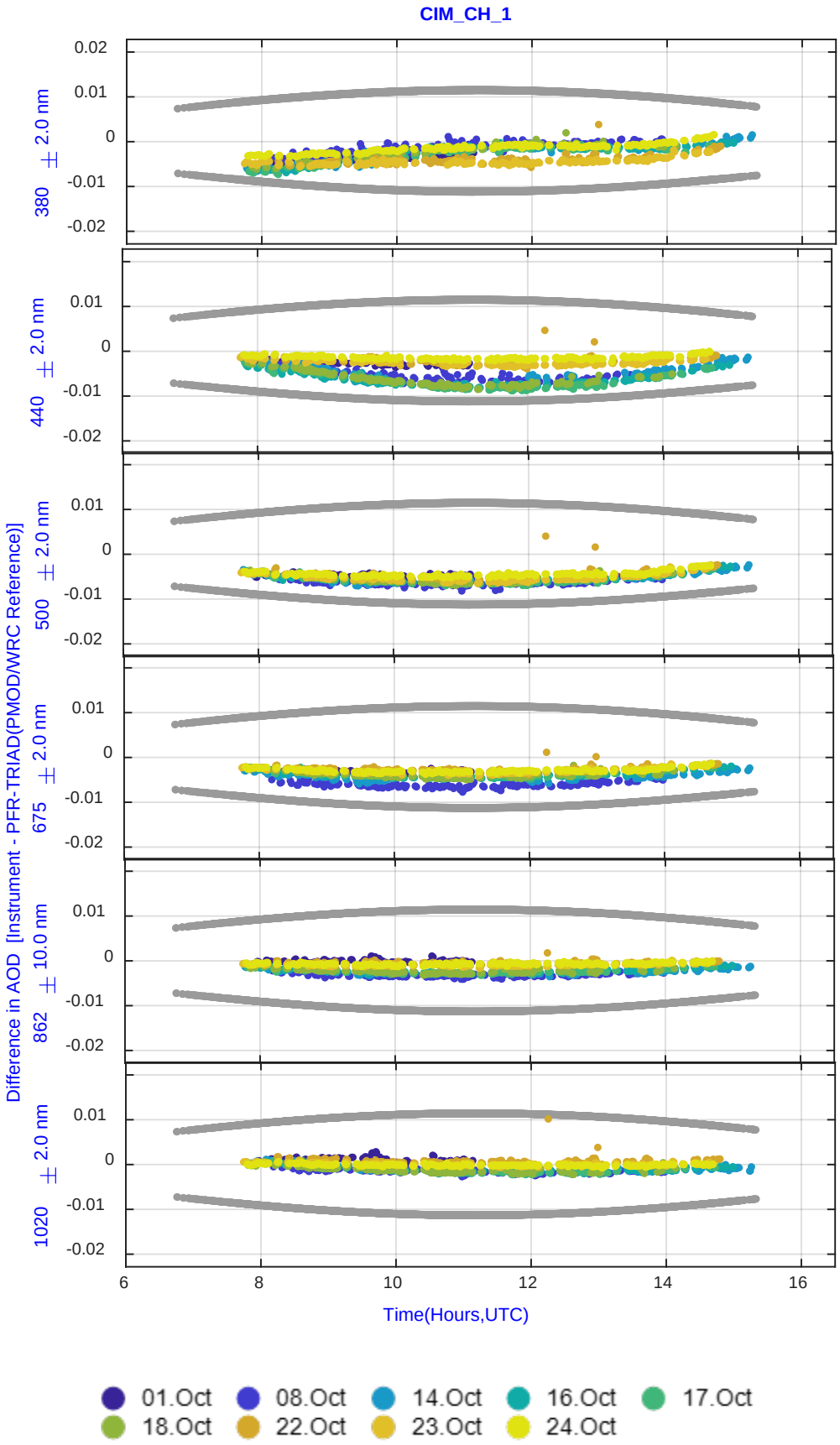
CIM_CH_1
Difference in AOD [Instrument - PFR-TRIAD(PMOD/WRC Reference)]
380 ± 2.0 nm
440 ± 2.0 nm
500 ± 2.0 nm
675 ± 2.0 nm
862 ± 10.0 nm
1020 ± 2.0 nm
0.02
0.01
0
-0.01
-0.02
6
8
10
12
14
16
Time(Hours,UTC)
01.Oct
08.Oct
14.Oct
16.Oct
17.Oct
18.Oct
22.Oct
23.Oct
24.Oct

CIM_UV_1219

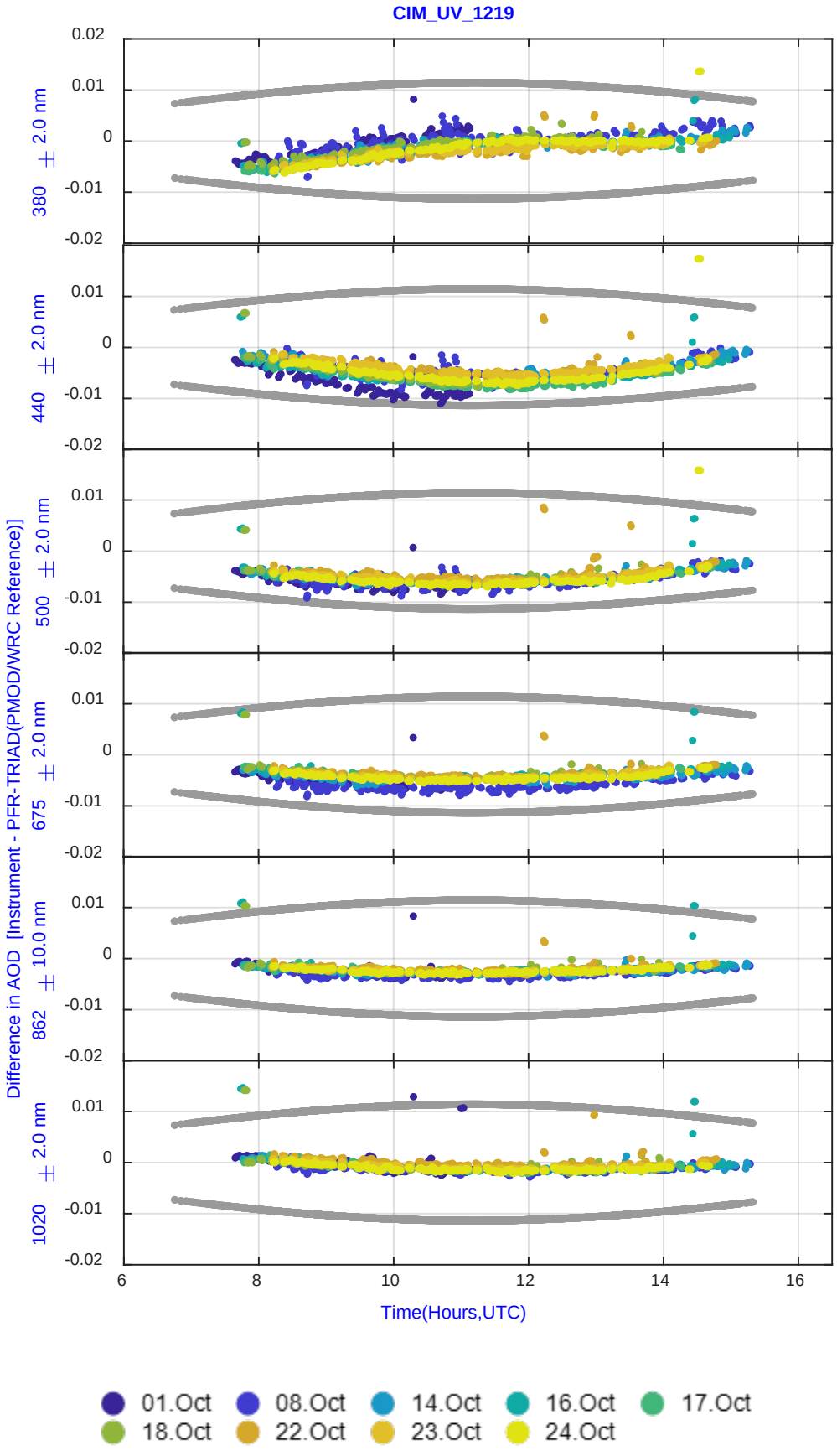
CIM_UV_1219
Difference in AOD [Instrument - PFR-TRIAD(PMOD/WRC Reference)]
380 ± 2.0 nm
440 ± 2.0 nm
500 ± 2.0 nm
675 ± 2.0 nm
862 ± 10.0 nm
1020 ± 2.0 nm
0.02
0.01
0
-0.01
-0.02
6
8
10
12
14
16
Time(Hours,UTC)
01.Oct
08.Oct
14.Oct
16.Oct
17.Oct
18.Oct
22.Oct
23.Oct
24.Oct

CIM_UL_1270

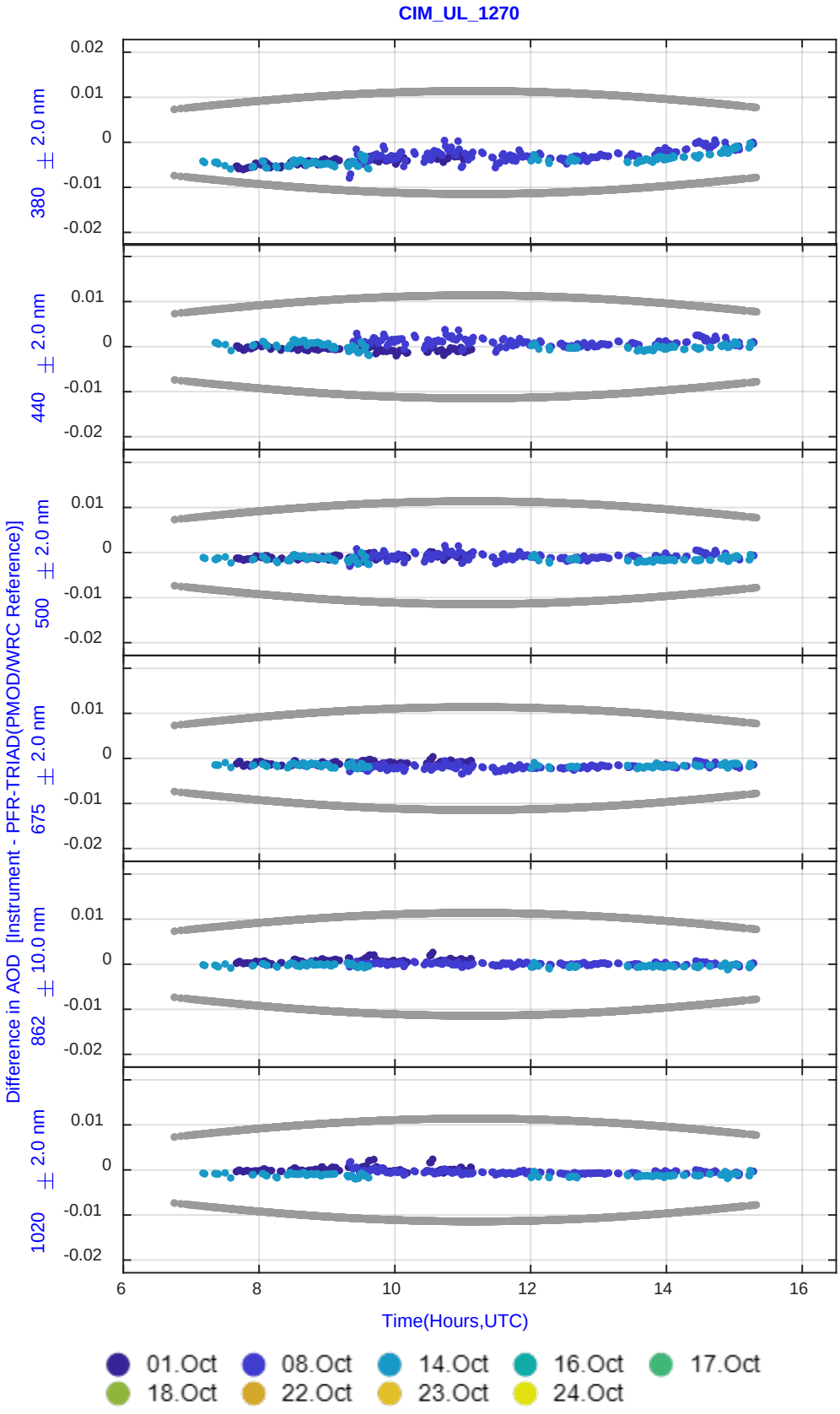
CIM_UL_1270
Difference in AOD [Instrument - PFR-TRIAD(PMOD/WRC Reference)]
380 ± 2.0 nm
440 ± 2.0 nm
500 ± 2.0 nm
675 ± 2.0 nm
862 ± 10.0 nm
1020 ± 2.0 nm
0.02
0.01
0
-0.01
-0.02
6
8
10
12
14
16
Time(Hours,UTC)
01.Oct
08.Oct
14.Oct
16.Oct
17.Oct
18.Oct
22.Oct
23.Oct
24.Oct

SPO_AU_2

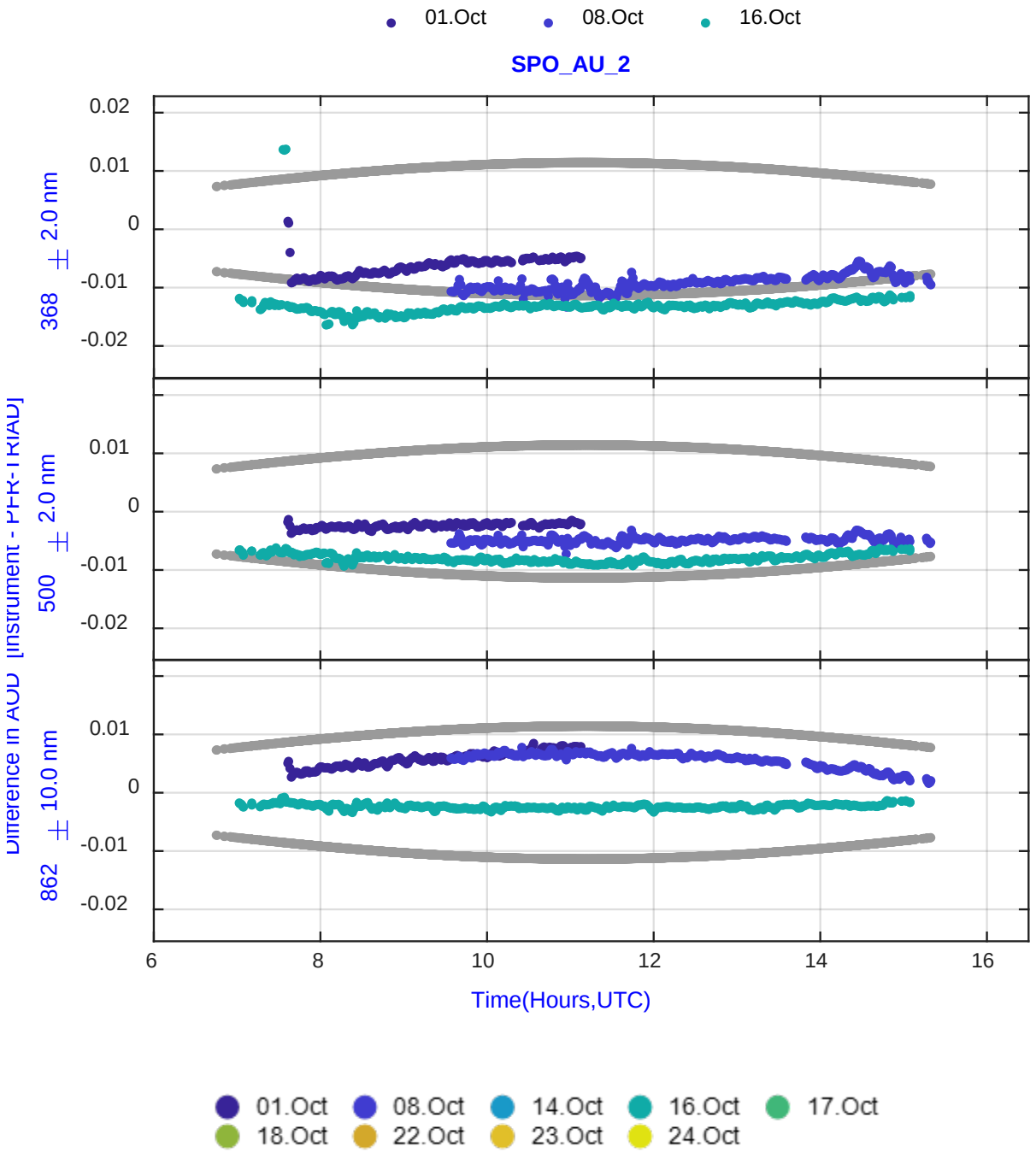
01.Oct
08.Oct
16.Oct
SPO_AU_2
Difference in AOD [Instrument - PHR-PRIAD]
368 ± 2.0 nm
500 ± 2.0 nm
862 ± 10.0 nm
0.02
0.01
0
-0.01
-0.02
6
8
10
12
14
16
Time(Hours,UTC)
01.Oct
08.Oct
14.Oct
16.Oct
17.Oct
18.Oct
22.Oct
23.Oct
24.Oct

POM_IT_1

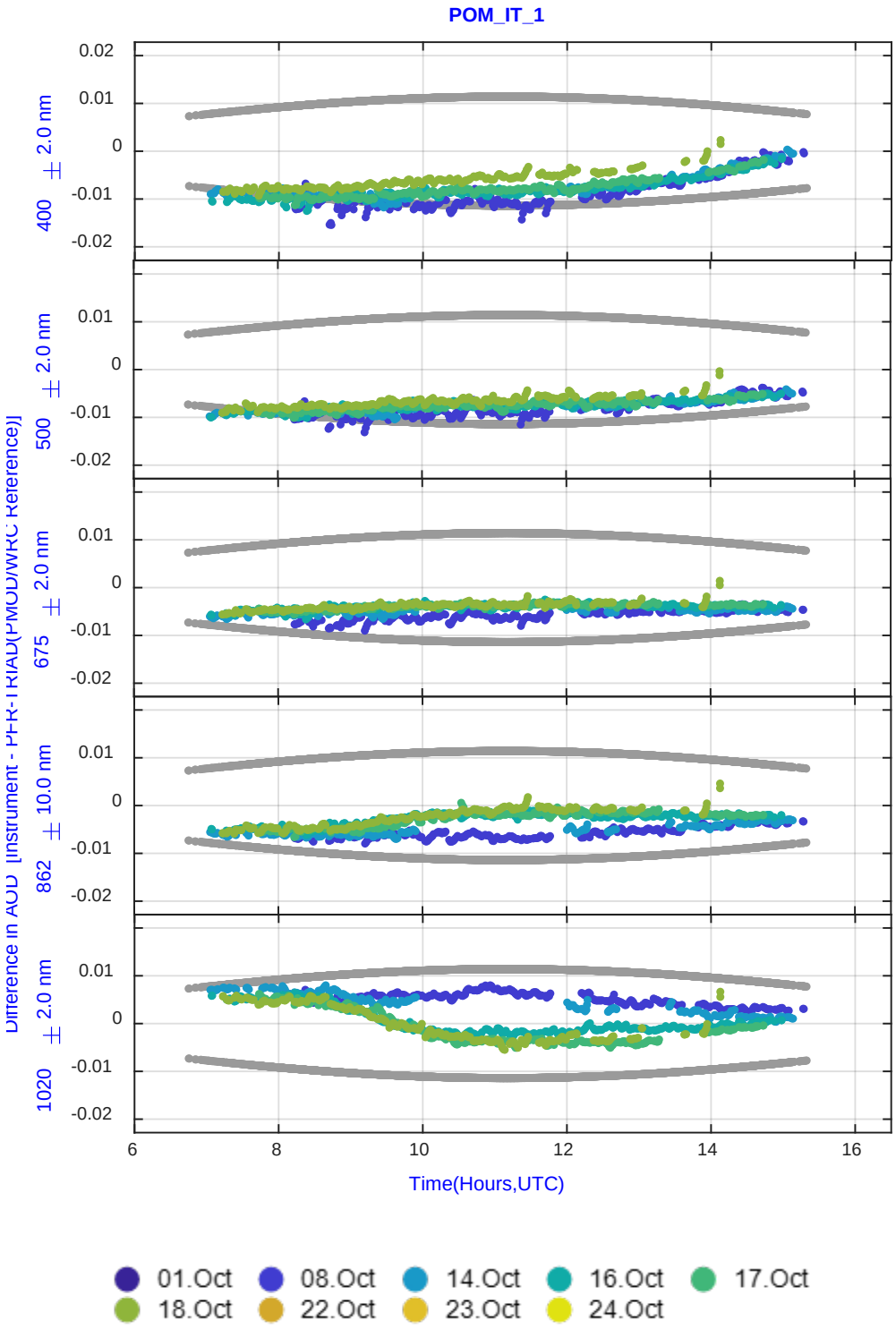
POM_IT_1
0.02
0.01
0
-0.01
-0.02
400 ± 2.0 nm
500 ± 2.0 nm
675 ± 2.0 nm
862 ± 10.0 nm
1020 ± 2.0 nm
6
8
10
12
14
16
Time(Hours,UTC)
01.Oct
08.Oct
14.Oct
16.Oct
17.Oct
18.Oct
22.Oct
23.Oct
24.Oct

POM_DE_1

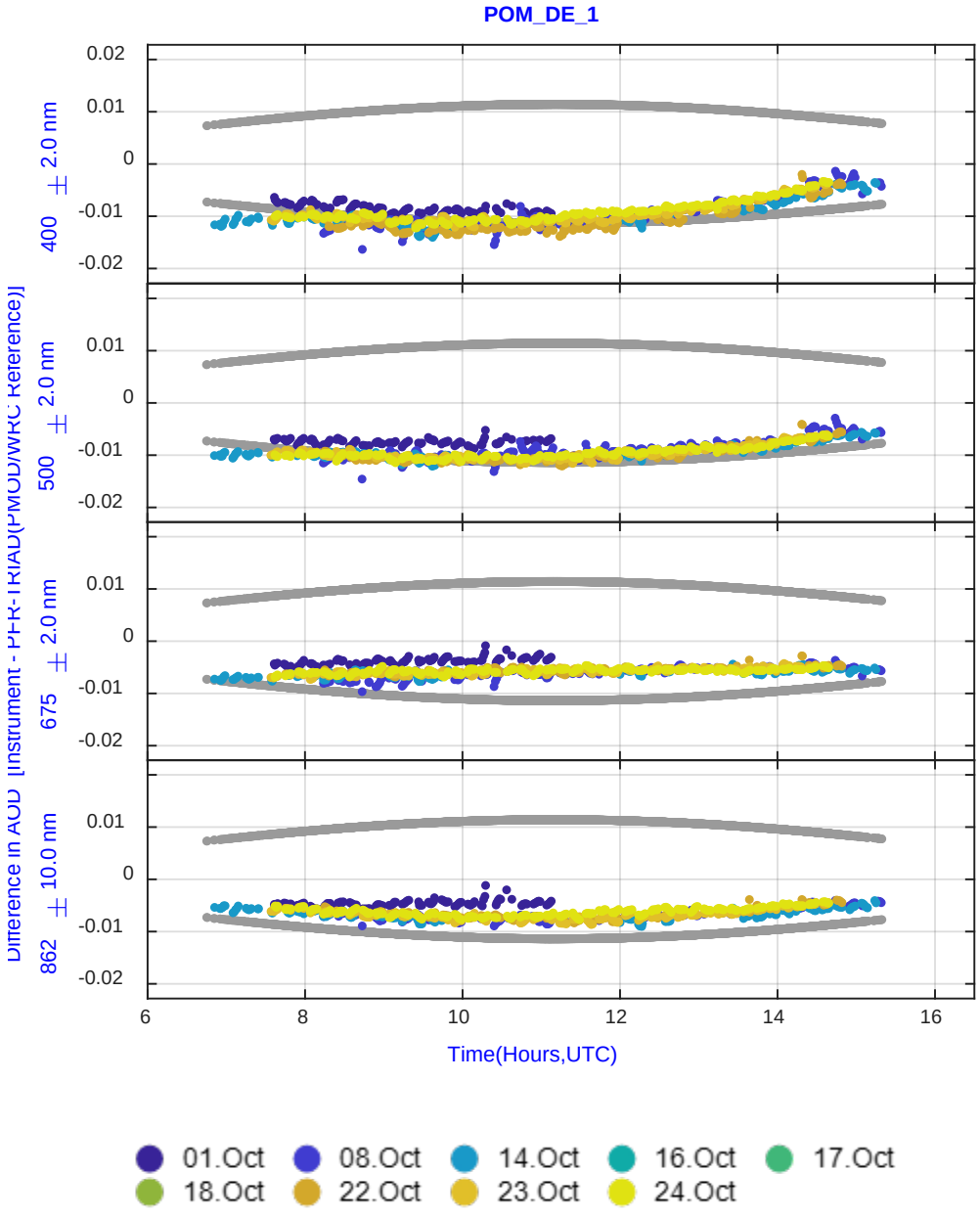
POM_DE_1
Difference in AOD [Instrument - PHR-1 RAD(PMOD/WRC Reference)]
400 ± 2.0 nm
500 ± 2.0 nm
675 ± 2.0 nm
862 ± 10.0 nm
0.02
0.01
0
-0.01
-0.02
6
8
10
12
14
16
Time(Hours,UTC)
01.Oct
08.Oct
14.Oct
16.Oct
17.Oct
18.Oct
22.Oct
23.Oct
24.Oct

CW193_CN

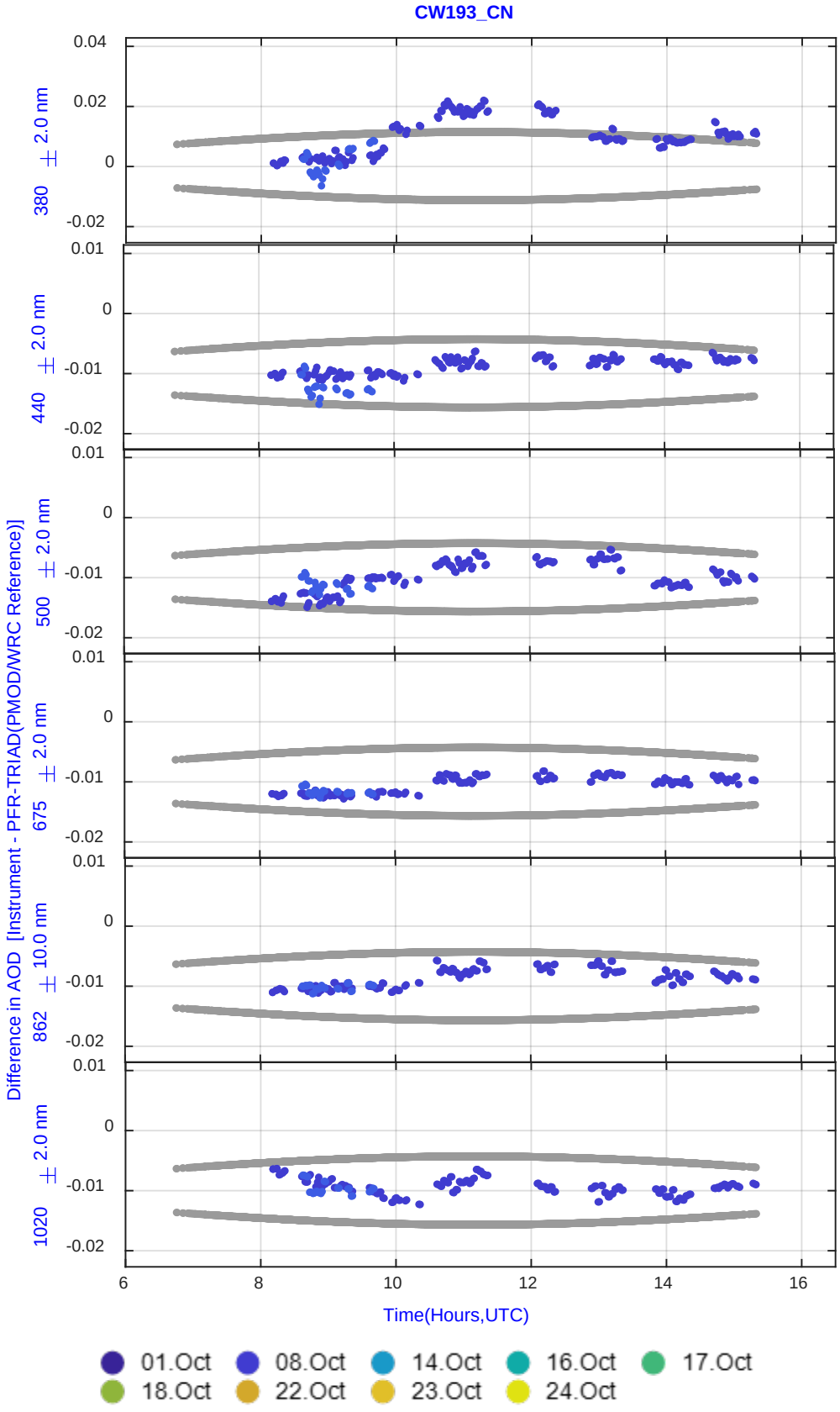
CW193_CN
Difference in AOD [Instrument - PFR-TRIAD(PMOD/WRC Reference)]
380 ± 2.0 nm
440 ± 2.0 nm
500 ± 2.0 nm
675 ± 2.0 nm
862 ± 10.0 nm
1020 ± 2.0 nm
0.04
0.02
0
-0.02
0.01
-0.01
6
8
10
12
14
16
Time(Hours,UTC)
01.Oct
08.Oct
14.Oct
16.Oct
17.Oct
18.Oct
22.Oct
23.Oct
24.Oct

PFR_CH_01

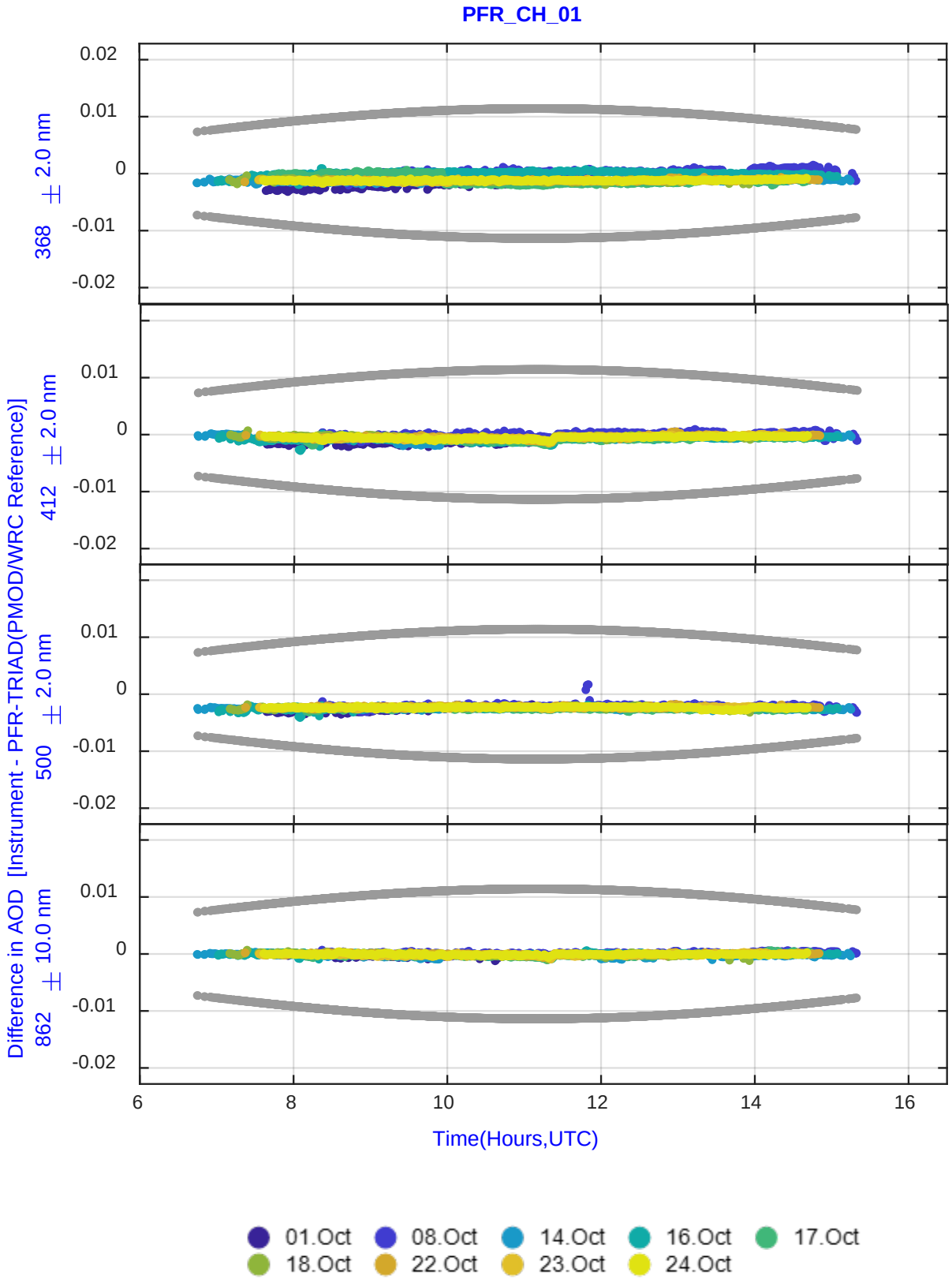
PFR_CH_01
Difference in AOD [Instrument - PFR-TRIAD(PMOD/WRC Reference)]
368 ± 2.0 nm
412 ± 2.0 nm
500 ± 2.0 nm
862 ± 10.0 nm
0.02
0.01
0
-0.01
-0.02
6
8
10
12
14
16
Time(Hours,UTC)
01.Oct
08.Oct
14.Oct
16.Oct
17.Oct
18.Oct
22.Oct
23.Oct
24.Oct

PFR_CH_1 – Extrapolated wavelengths using AE

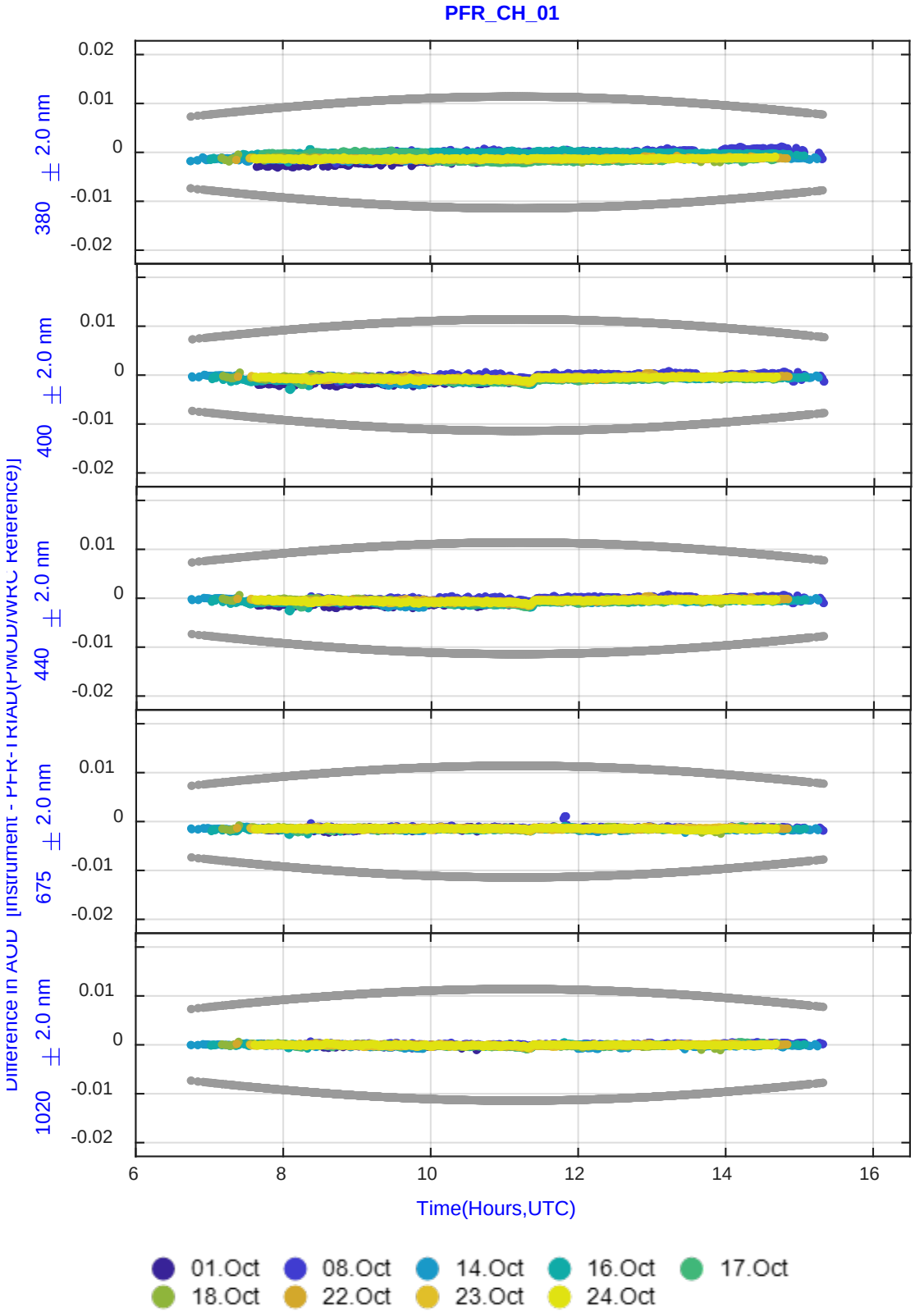

PFR_IR_01 (PFR_CH_1 using irradiance calibration)

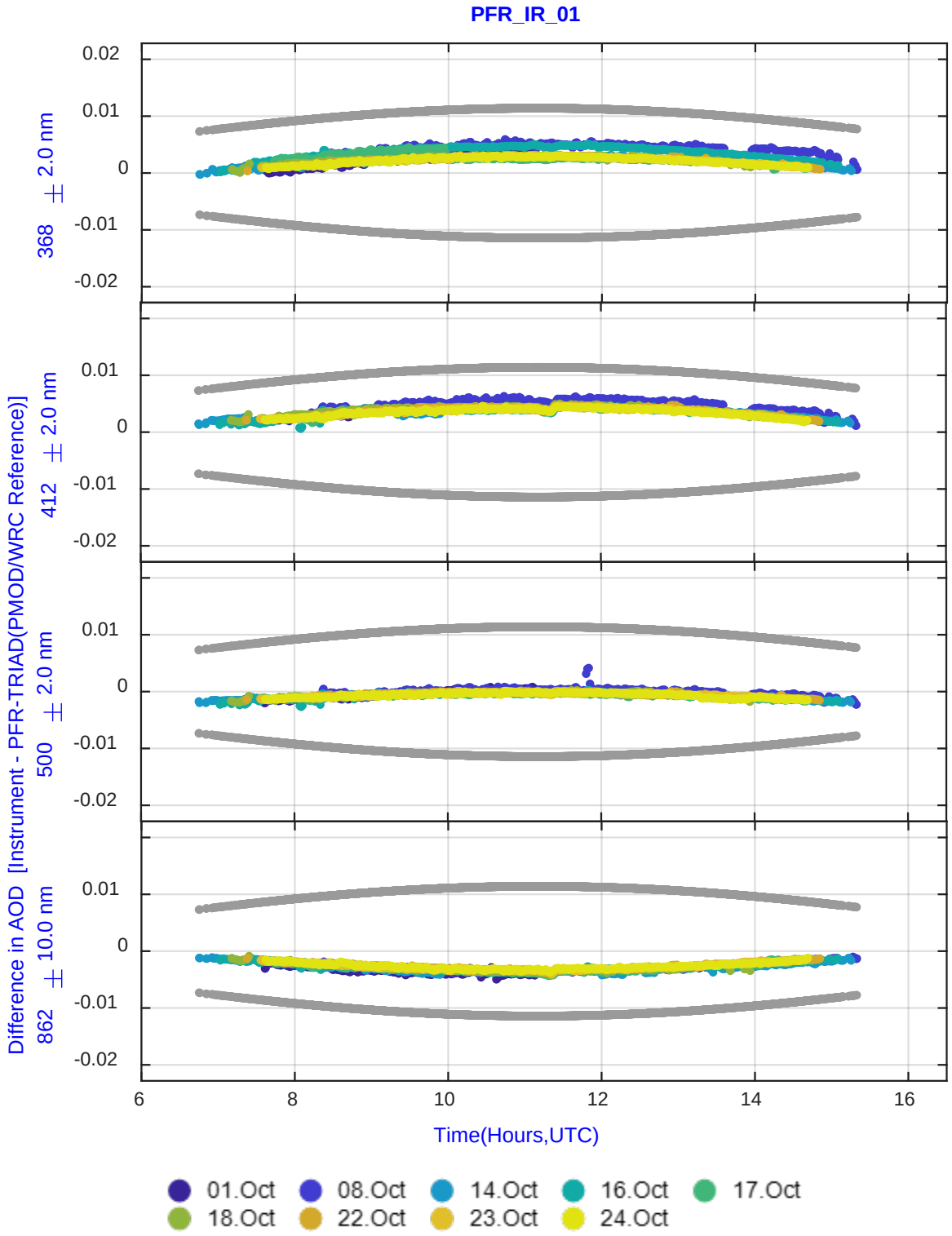

PFR_IR_01 (PFR_CH_1 using irradiance calibration) – Extrapolated wavelengths using AE

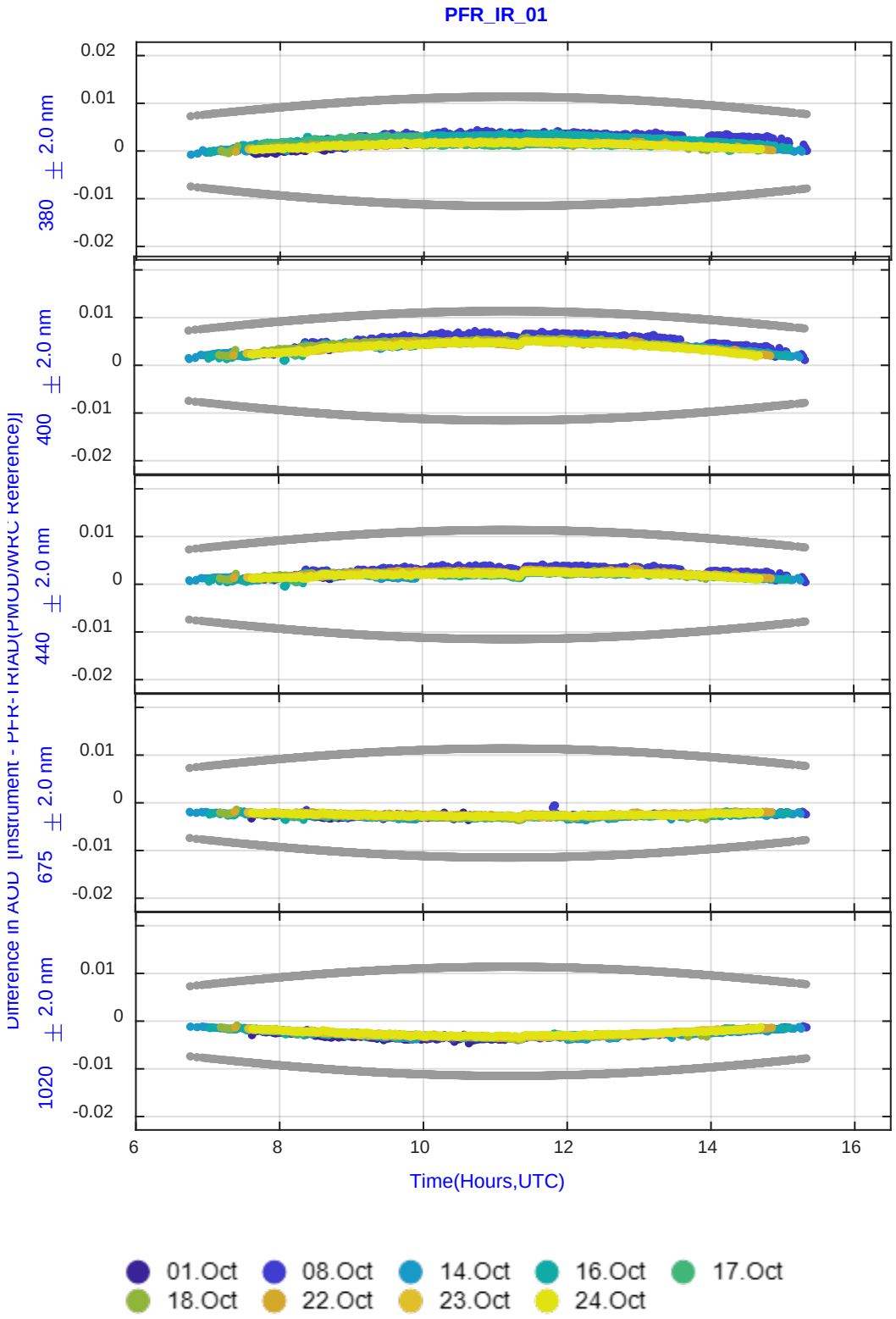

QASUME

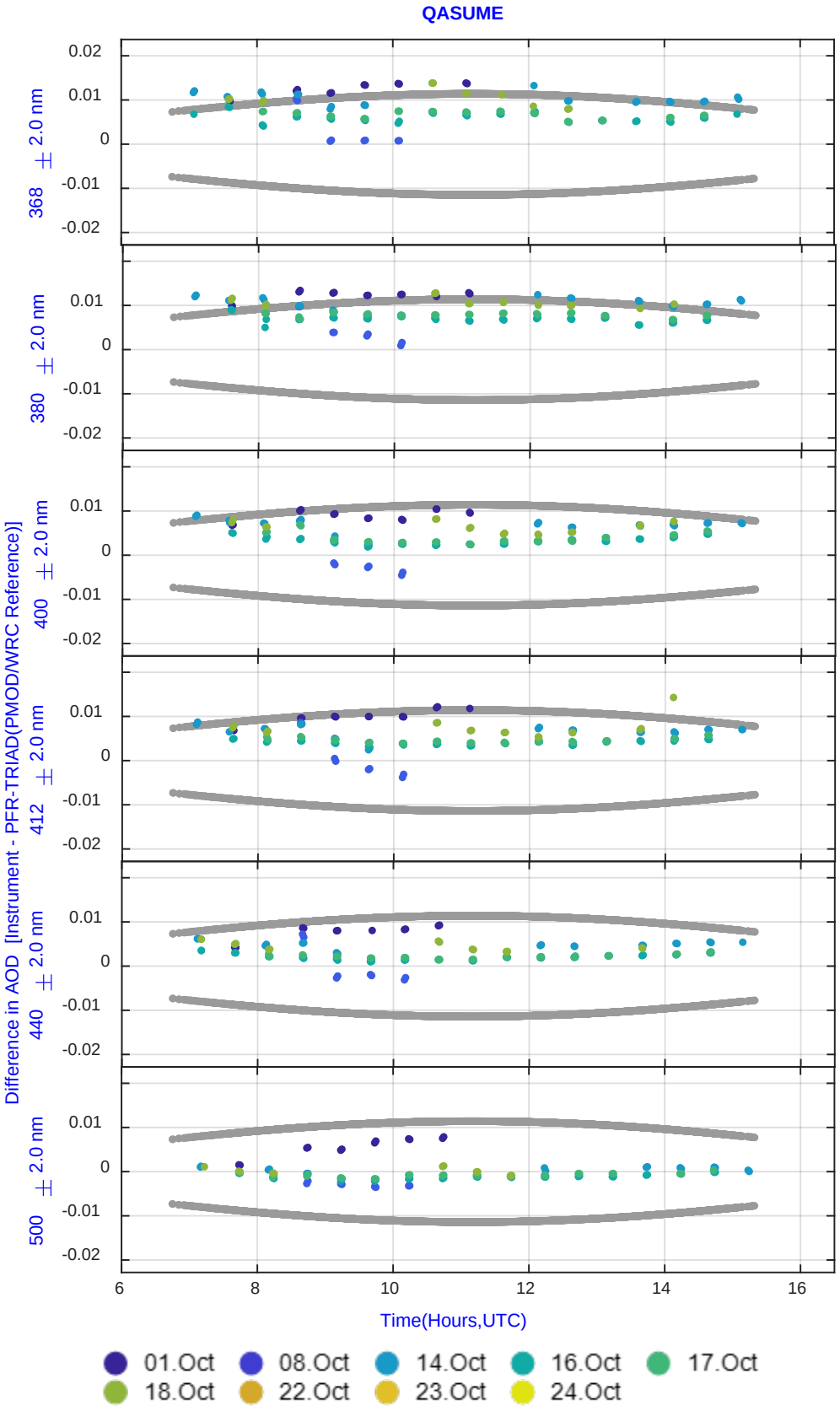
QASUME
Difference in AOD [Instrument - PFR-TRIAD(PMOD/WRC Reference)]
368 ± 2.0 nm
380 ± 2.0 nm
400 ± 2.0 nm
412 ± 2.0 nm
440 ± 2.0 nm
500 ± 2.0 nm
0.02
0.01
0
-0.01
-0.02
6
8
10
12
14
16
Time(Hours,UTC)
01.Oct
08.Oct
14.Oct
16.Oct
17.Oct
18.Oct
22.Oct
23.Oct
24.Oct

IR-QASUME

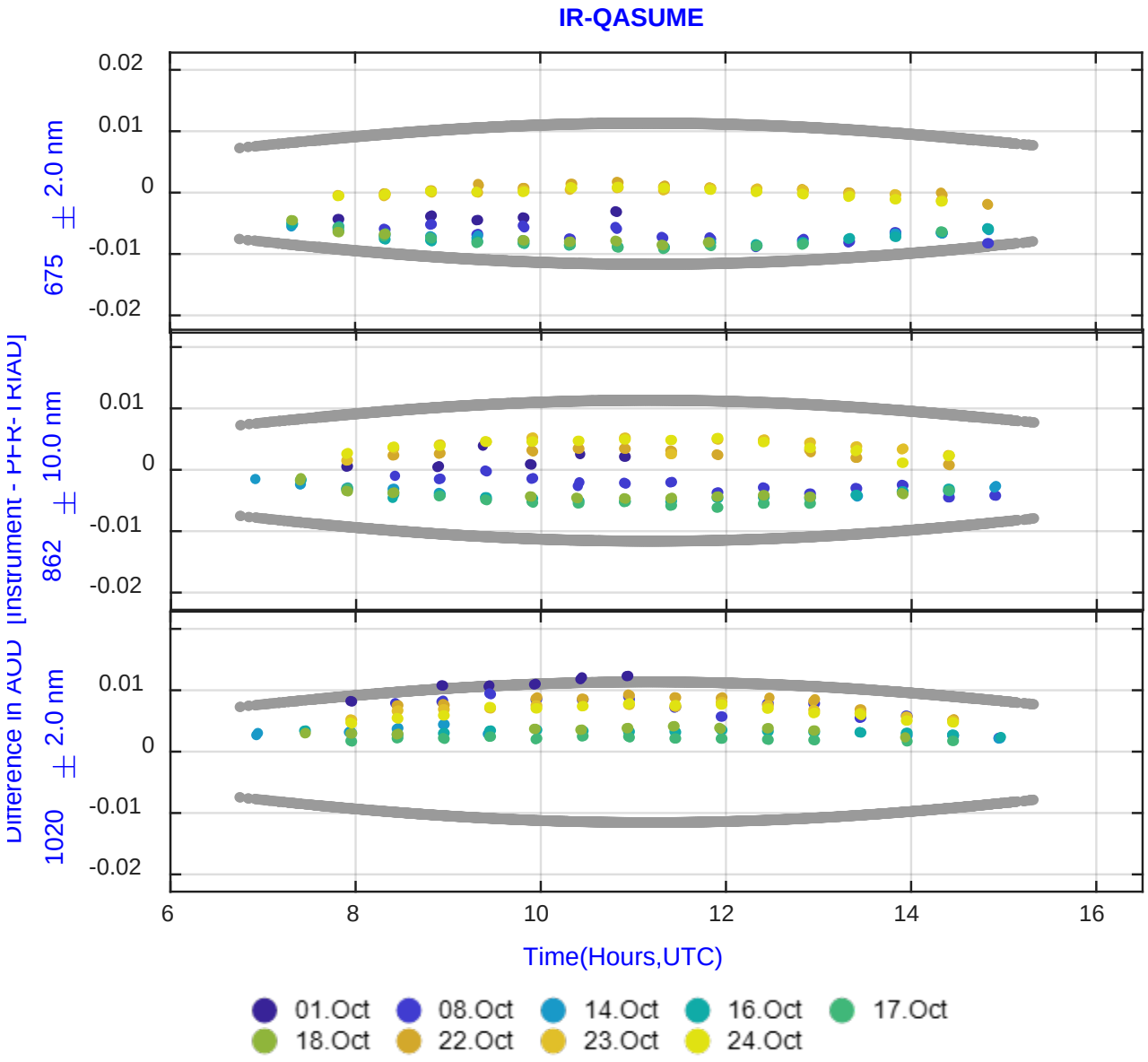
IR-QASUME
Difference in AOD [Instrument - PHR-PRIAD]
675 ± 2.0 nm
862 ± 10.0 nm
1020 ± 2.0 nm
0.02
0.01
0
-0.01
-0.02
6
8
10
12
14
16
Time(Hours,UTC)
01.Oct
08.Oct
14.Oct
16.Oct
17.Oct
18.Oct
22.Oct
23.Oct
24.Oct

PSR_DE_4 (PSR_004)

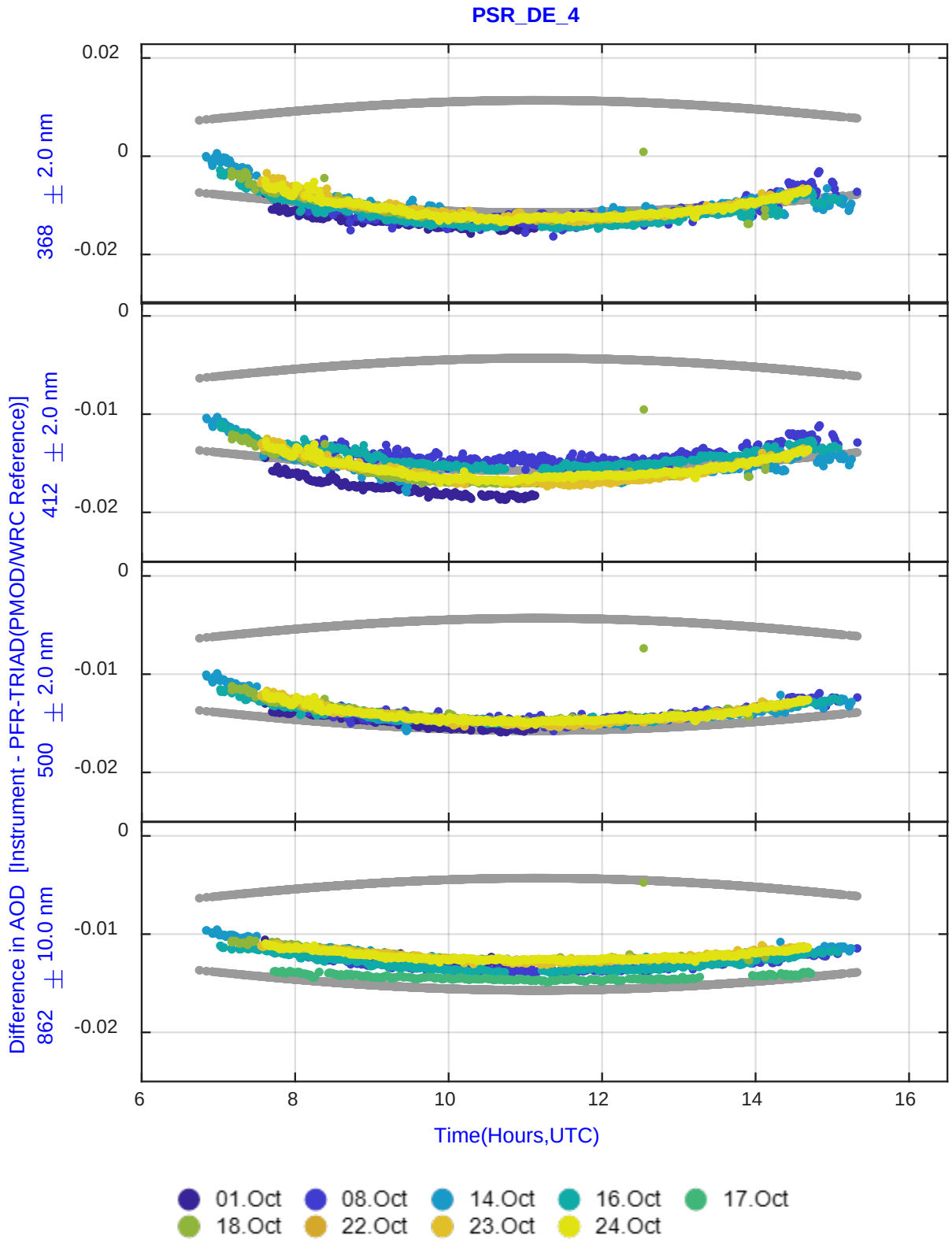

PSR_DE_4 (PSR_004) *continued*

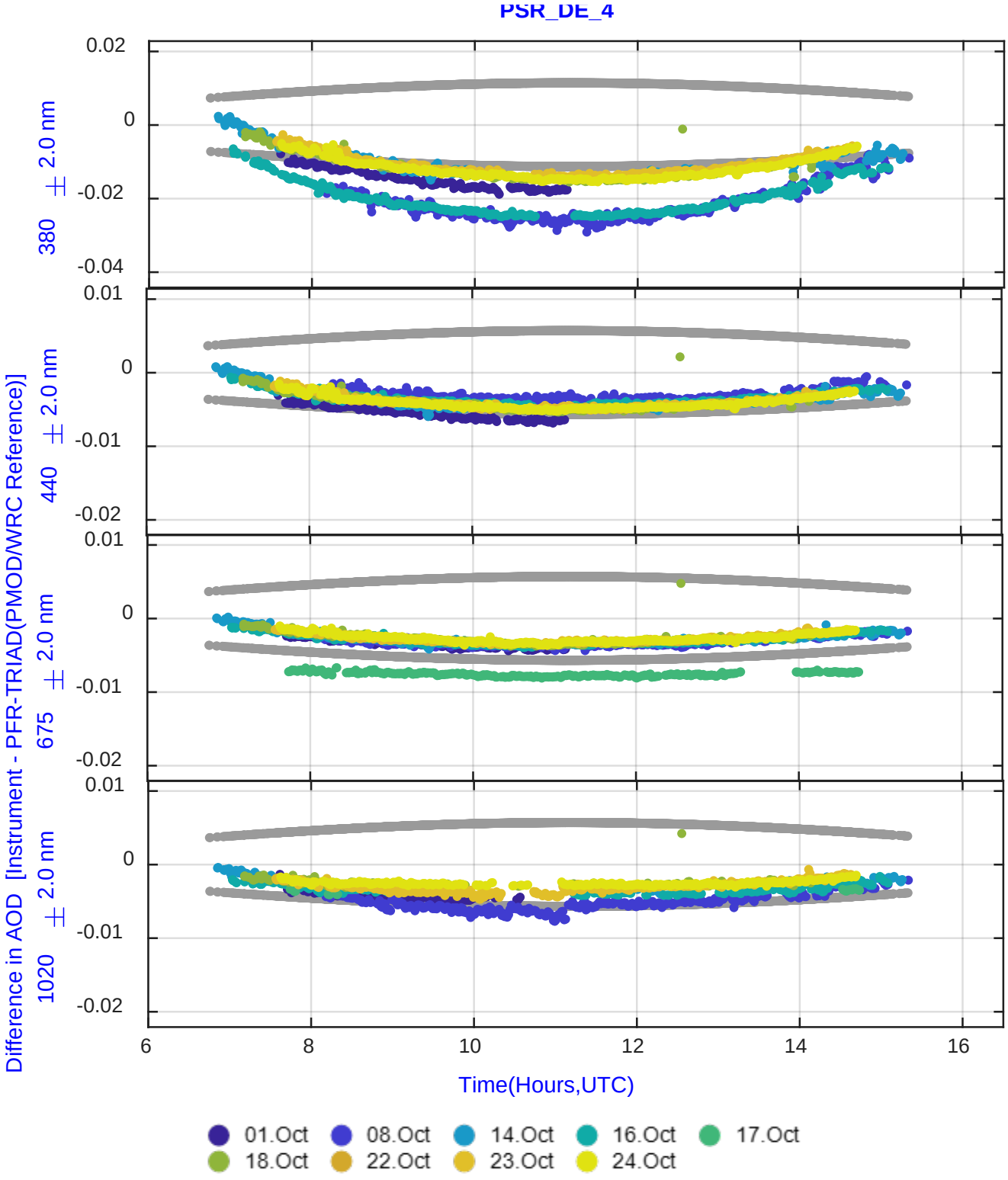

PSR_DE_6 (PSR_006)

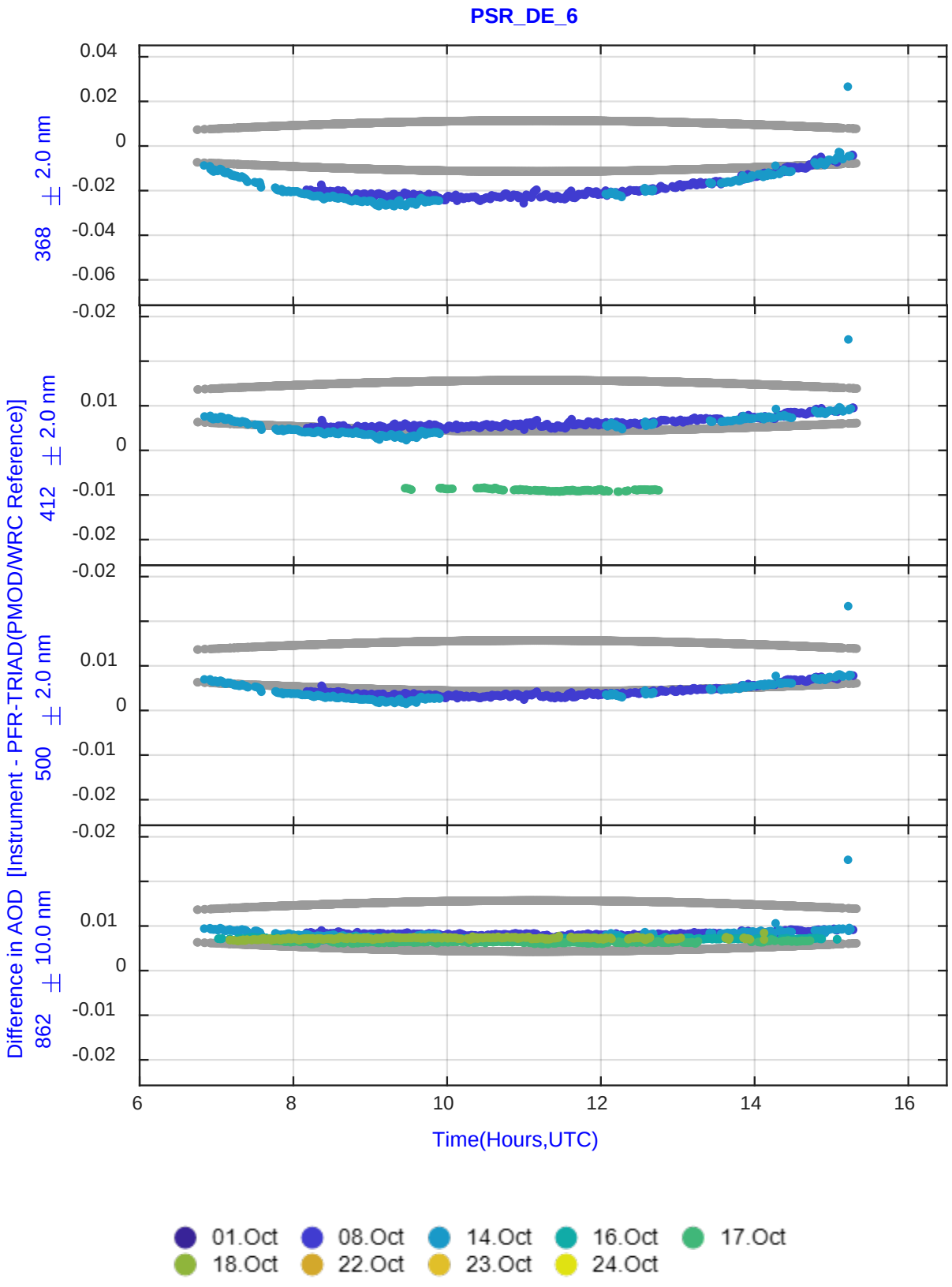

PSR_DE_6 (PSR_006) *continued*

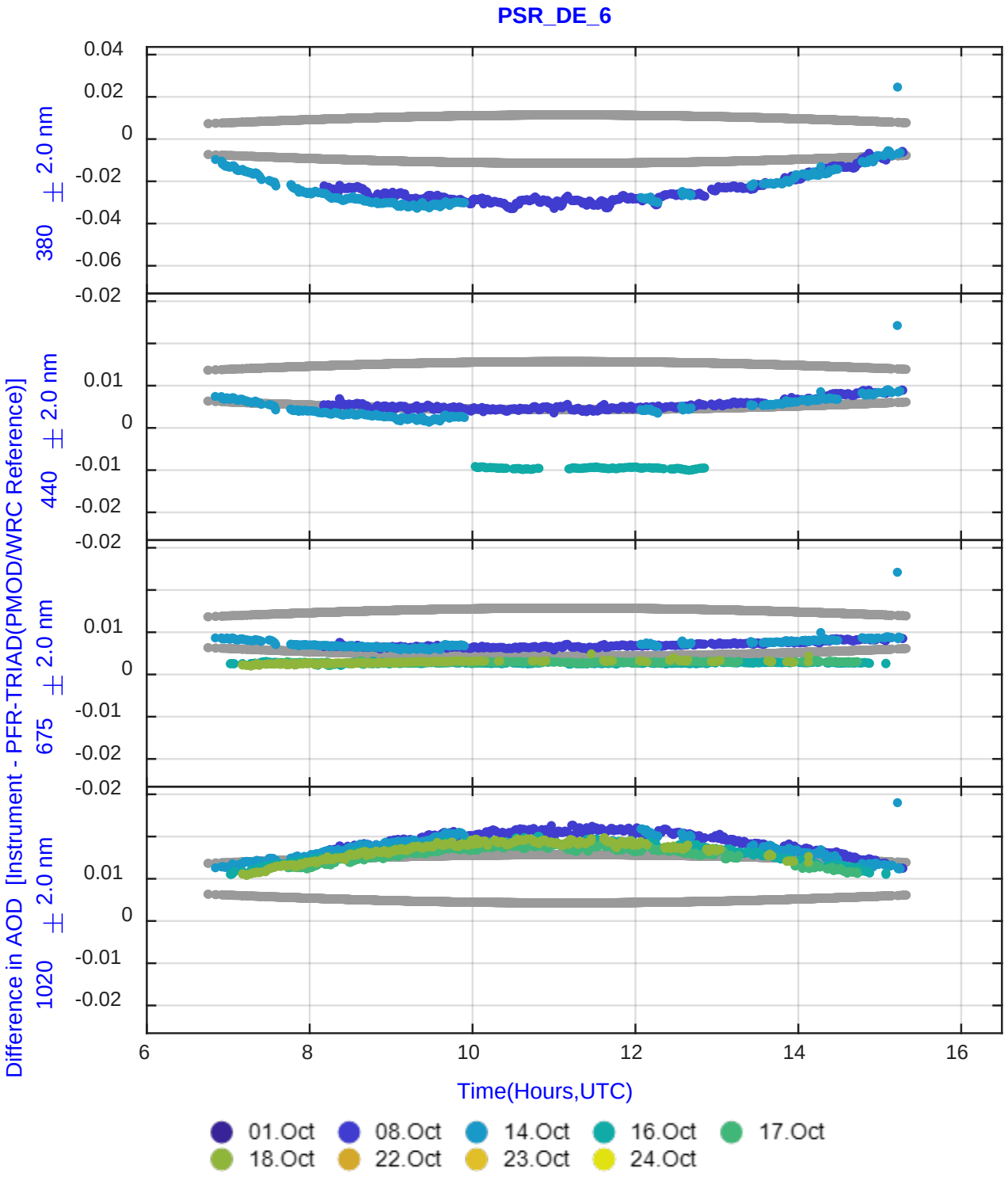

PSR_CH_8 (PSR_008)

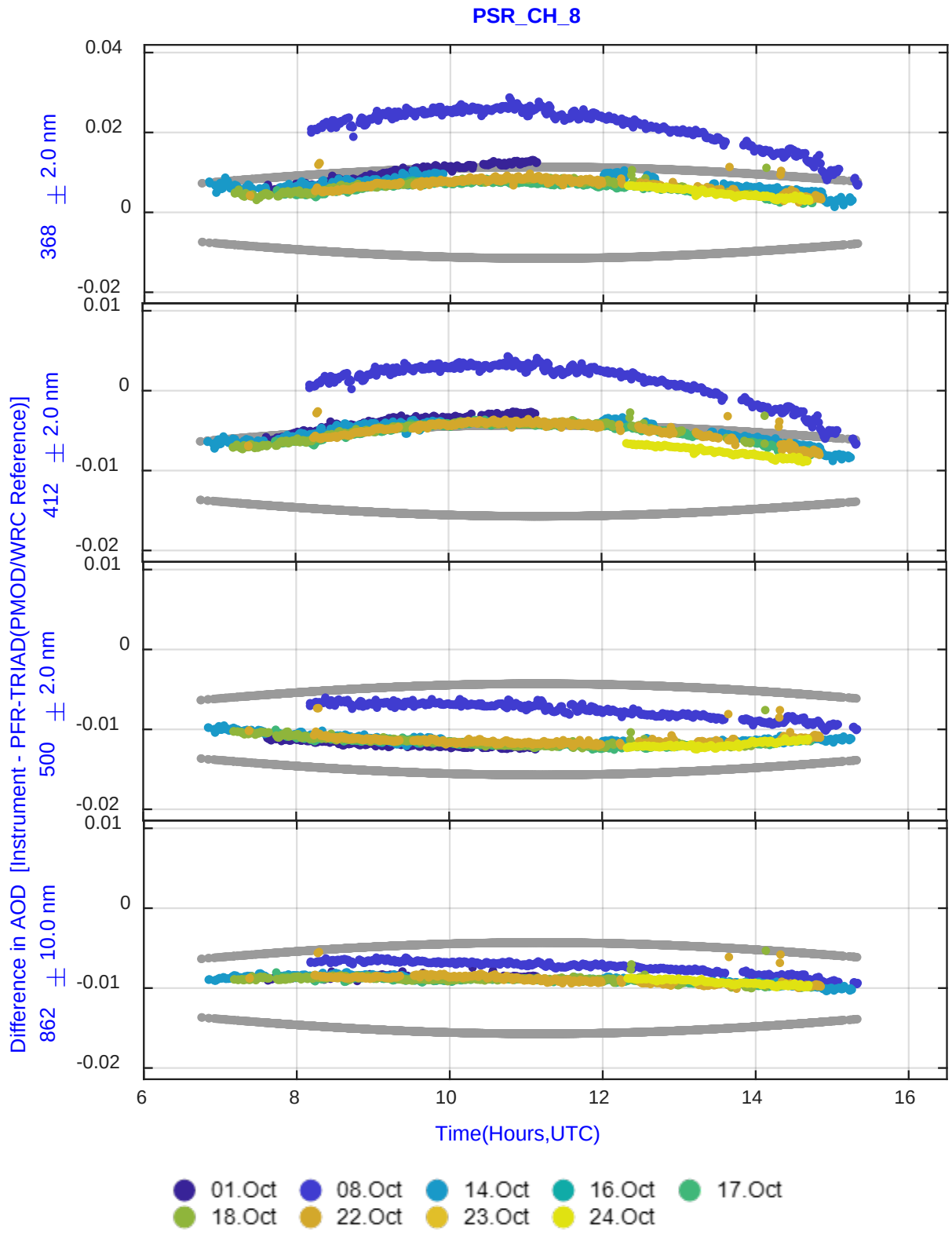

PSR_CH_8 (PSR_008) *continued*

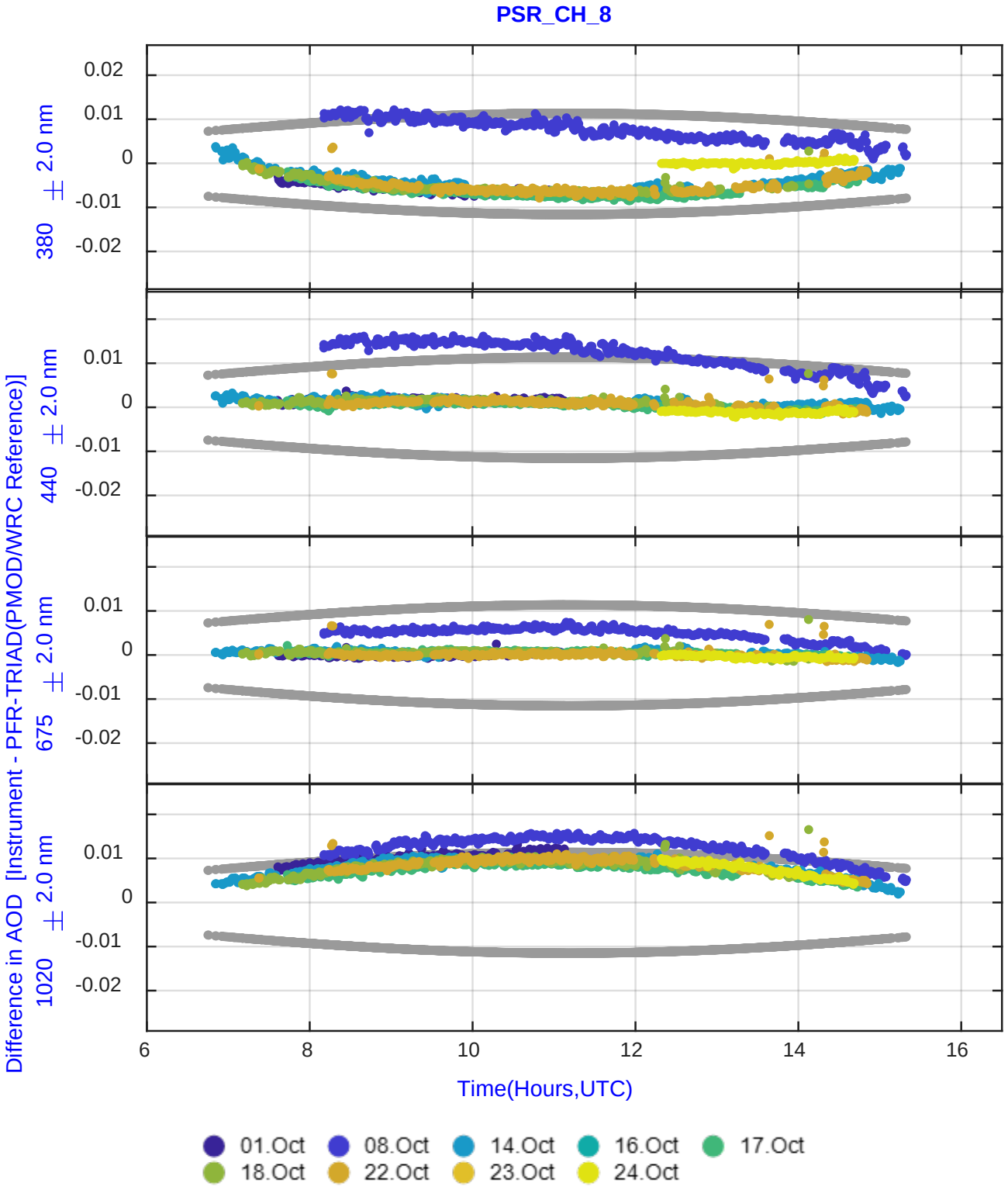

PSR_CH_9 (PSR_009)

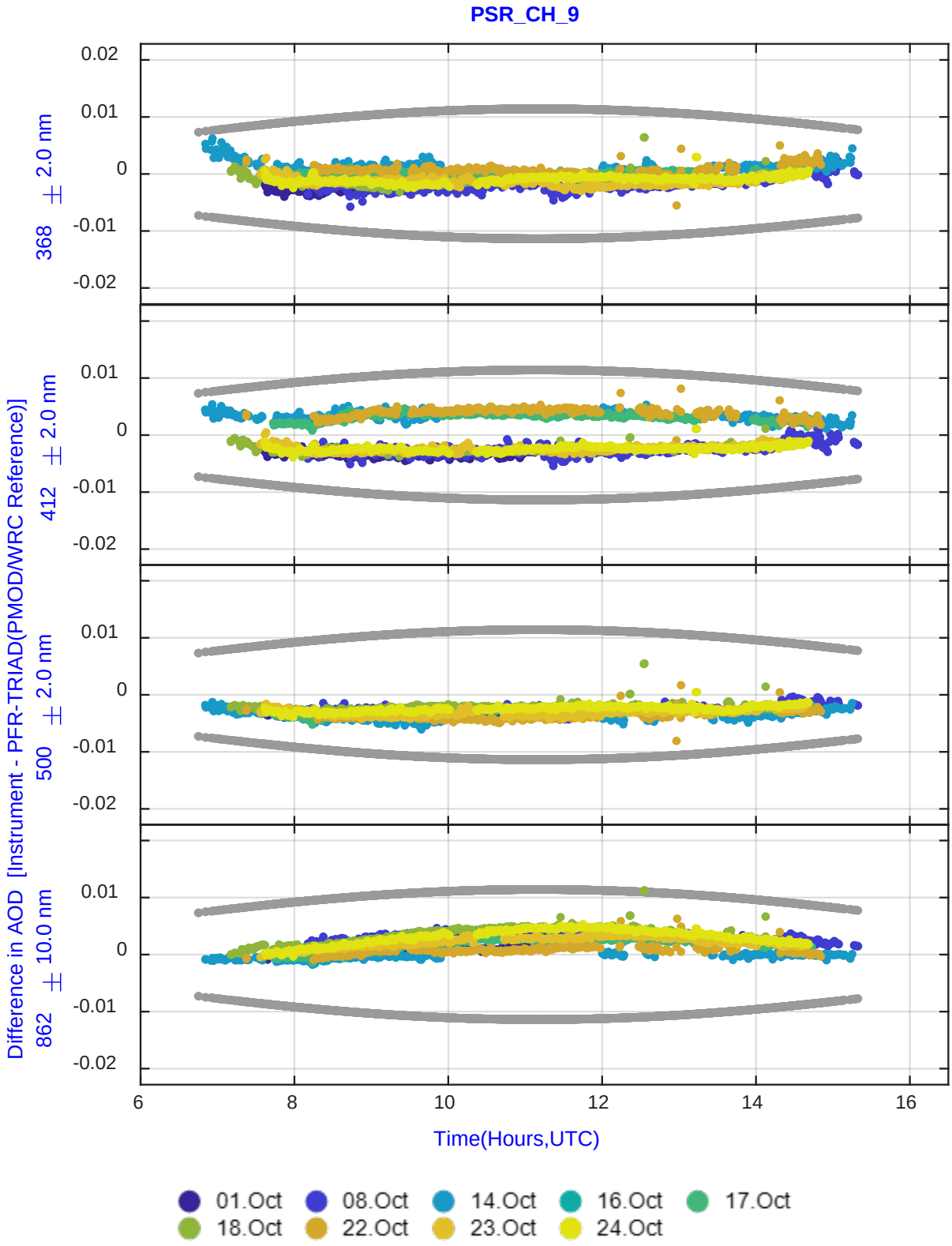

PSR_CH_9 (PSR_009) *continued*

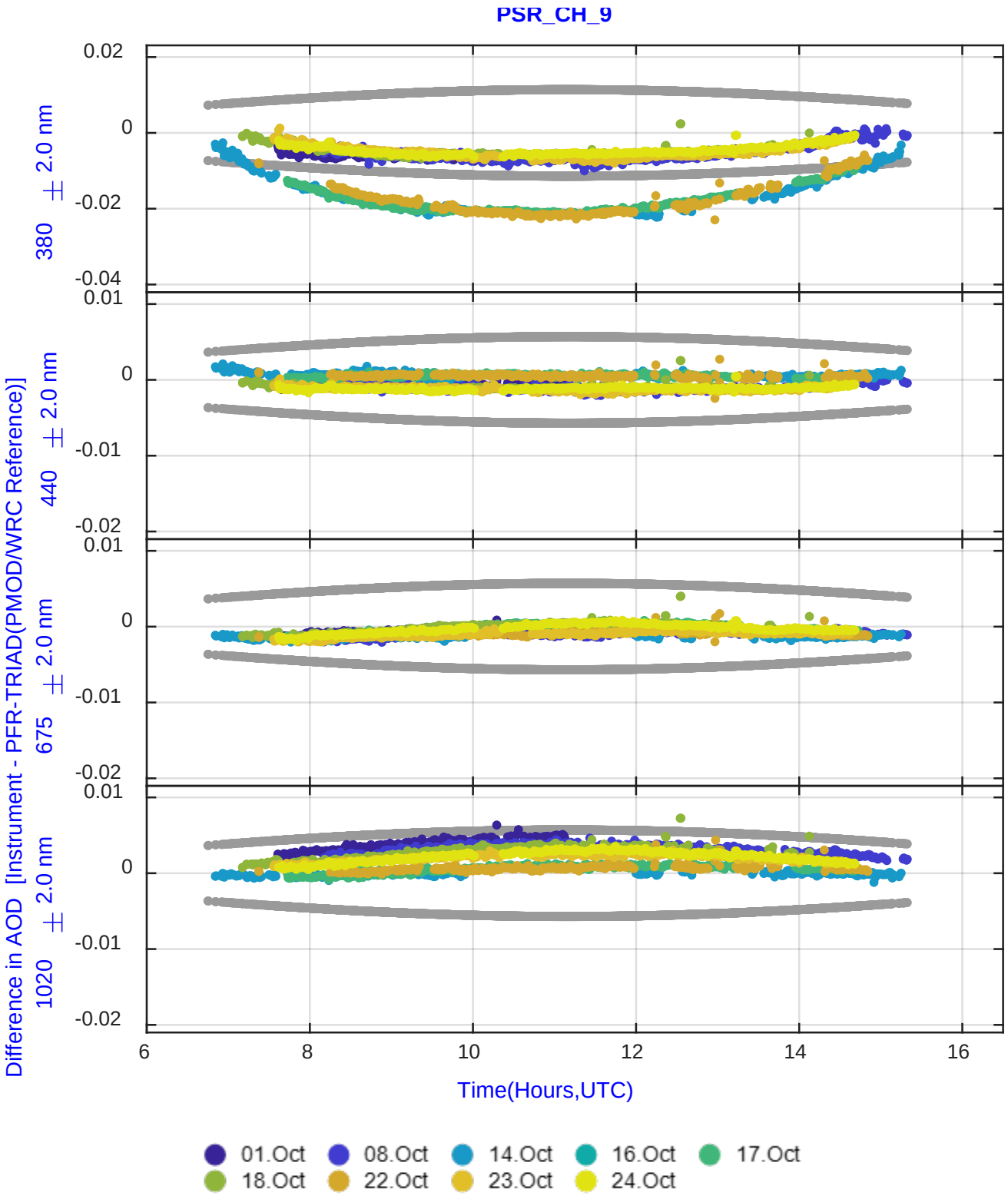

PSR_CH_0 (PSR_010)

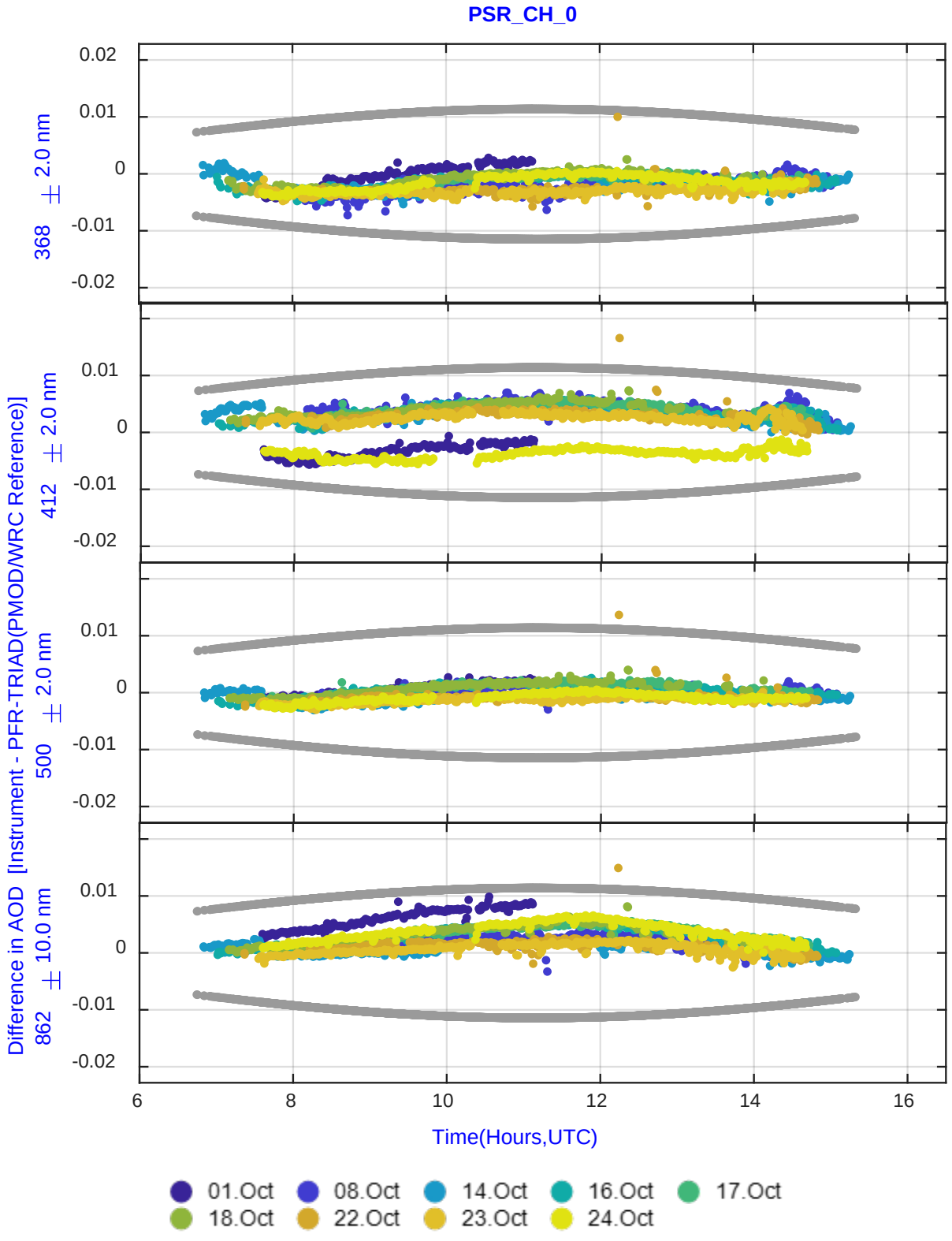

PSR_CH_0 (PSR_010) *continued*

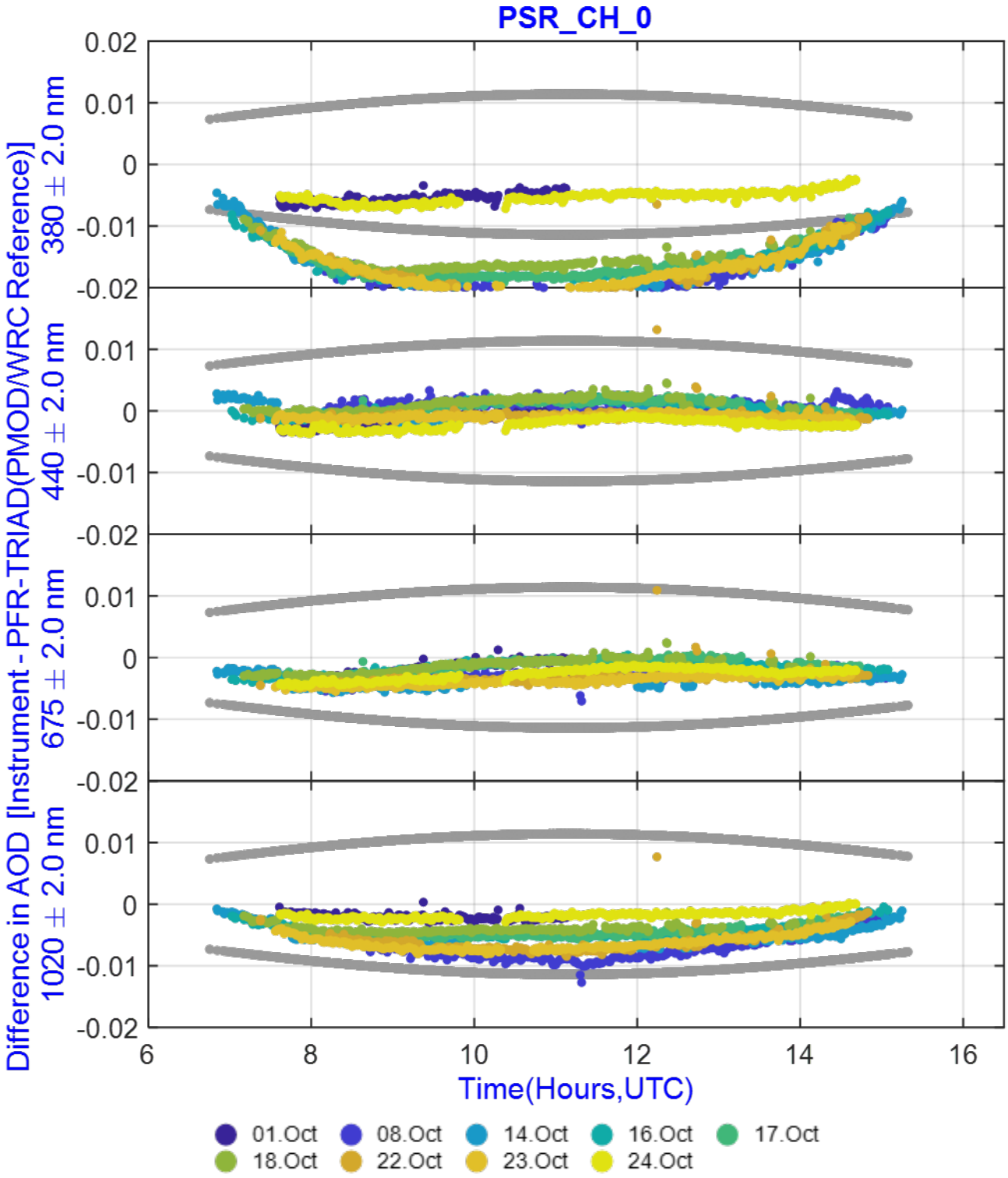

Appendix 5. List of abbreviations

AE	Ångström exponent
AEMET	Spanish State Meteorological Agency
AERONET	Aerosol Robotic Network
AOD	Aerosol optical depth
ARPA	Regional Environmental Protection Agency
BOM	Bureau of Meteorology
CARS	Centre for Aerosol Remote Sensing
CARSNET	China Aerosol Remote Sensing Network
DWD-MOL	German Weather Service-Meteorological Observatory Lindenberg
FEL	Fielde emission lamp
FOV	Field of view
FRC	Filter Radiometer Comparison
WORCC	World Optical Depth Research and Calibration Centre
FTS	Fourier transform spectroradiometer
FWHM	Full width at half maximum
GAW	Global Atmosphere Watch
GAW-PFR	Global Atmospheric Watch Precision Filter Radiometer network
GCOS	Global Climate Observing System
IR	Infrared
IR-QASUME	Infrared Quality Assurance of Spectral Ultraviolet Measurements in Europe
LOA	Laboratoire d'Optique Atmosphérique
METAS	Swiss Federal Institute of Metrology
NIMS-KMA	National Institute of Meteorological Sciences-Korea Meteorological Administration
NOAA/ESRL	National Oceanic and Atmospheric Administration/Earth System Research Laboratory
PFR	Precision Filter Radiometer
PMOD/WRC	Physikalisch-Meteorologisches Observatorium Davos, World Radiation Centre
PSR	Precision Solar Radiometer

PTB	Physikalisch-Technische Bundesanstalt (German national metrology institute)
QASUME	Quality Assurance of Spectral Ultraviolet Measurements in Europe
SI	International System of Units
SKYNET	Sky radiometer network
SMHI	Swedish Meteorological and Hydrological Institute
SURFRAD	Surface Radiation Budget network
TSIS-1 HSRS	Total and Spectral Solar Irradiance Sensor-1 Hybrid Solar Reference Spectrum
UTC	Coordinated Universal Time
UV	Ultraviolet
WMO	World Meteorological Organization

For more information, please contact:

World Meteorological Organization

Science and Innovation Department

7 bis, avenue de la Paix – P.O. Box 2300 – CH 1211 Geneva 2 – Switzerland

Tel.: +41 (0) 22 730 81 11 – Fax: +41 (0) 22 730 81 81

Email: GAW@wmo.int

Website: https://public.wmo.int/en/programmes/global-atmosphere-watch-programme

JN 2337